INFORMATION TO USERS

The most advanced technology has been used to photograph and reproduce this manuscript from the microfilm master. UMI films the text directly from the original or copy submitted. Thus, some thesis and dissertation copies are in typewriter face, while others may be from any type of computer printer.

The quality of this reproduction is dependent upon the quality of the copy submitted. Broken or indistinct print, colored or poor quality illustrations and photographs, print bleedthrough, substandard margins, and improper alignment can adversely affect reproduction.

In the unlikely event that the author did not send UMI a complete manuscript and there are missing pages, these will be noted. Also, if unauthorized copyright material had to be removed, a note will indicate the deletion.

Oversize materials (e.g., maps, drawings, charts) are reproduced by sectioning the original, beginning at the upper left-hand corner and continuing from left to right in equal sections with small overlaps. Each original is also photographed in one exposure and is included in reduced form at the back of the book.

Photographs included in the original manuscript have been reproduced xerographically in this copy. Higher quality 6" x 9" black and white photographic prints are available for any photographs or illustrations appearing in this copy for an additional charge. Contact UMI directly to order.

U·M·I

University Microfilms International
A Bell & Howell Information Company
300 North Zeeb Road, Ann Arbor, MI 48106-1346 USA
313/761-4700 800/521-0600

Order Number 9111462

Stabilization and degradation of acetal copolymers

Pesce, Rose Ann, Ph.D.

City University of New York, 1988

U·M·I
300 N. Zeeb Rd.
Ann Arbor, MI 48106

A

STABILIZATION AND DEGRADATION OF ACETAL COPOLYMERS

by

ROSE ANN PESCE

A dissertation submitted to the Graduate Faculty in Chemistry in partial fulfillment of the requirements for the degree of Doctor of Philosophy, The City University of New York.

1988

This manuscript has been read and accepted for the Graduate Faculty in Chemistry in satisfaction of the dissertation requirement for the Degree of Doctor of Philosophy.

9/13/88
date

Chairman of Examining Committee

9/14/88
date

Executive Officer

David C. Lorenz

Supervisory Committee

The City University of New York

Abstract

Stabilization and Degradation
of Acetal Copolymers

by

Rose Ann Pesce

Adviser : Professor Nan-Loh Yang

Polyacetal copolymers are technically important macromolecules that are competitive with metals, ceramics and nylons in many applications. As the simplest form of aliphatic polyethers, they are of fundamental interest. The present investigation involves detailed studies aimed at the improvement of polyacetal stability.

Radical and acidolytic degradation of a model trioxane-ethylene oxide copolymer in solution were examined. Degradation products, identified by NMR spectroscopy, have been confirmed to be formaldehyde, formic acid and cyclic acetals (1,3-dioxolane, 1,3,5-trioxepane, 1,3,5-trioxane and 1,3,5,7-tetraoxane). The formation of these cyclic acetals is attributed to backbiting of the depolymerizing chain end.

A method for evaluating formaldehyde-accepting stabilizers for use in polyacetal systems has been developed. Based on acceptor-adduct equilibrium studies, conducted by titration, NMR spectroscopy and

thermal analysis, the relative efficiencies of a series of acceptors was determined.

The need for polyacetals capable of binding stabilizers led to the synthesis of three new functionalized acetal copolymers. The first, a copolymer of trioxane and 1,3-dioxep-5-ene, yields a *cis*-2-butene stopper unit. This thermally stable copolymer has been found to have crystallinity comparable to trioxane-ethylene oxide copolymers. Examples of copolymer modification are reported. Resistance to bromine degradation has also been demonstrated. M_n and M_v have been found to be as high as 6×10^4 and 8×10^4 respectively.

The second, a copolymer of trioxane and glycerol formal, is thermally stable and has pendant hydroxy and methylol groups. M_v is estimated to be less than 5×10^3. Equilibrium studies of the glycerol formal comonomer are also discussed.

The third, a copolymer of trioxane and glycidyl acrylate, is a thermally stable, crosslinked copolymer with pendant acrylate groups. DSC analysis of copolymers with glycidyl acrylate feeds ranging from 4 to 24 weight percent shows crystallinities ranging from 36 to 11%.

Each of the new copolymers has a functionalized comonomer unit which serves as both a stopper against unzipping and a site for further modification.

Acknowledgements

I would like to express my sincere gratitude to my mentor and friend, Professor Nan-Loh Yang, for his support, encouragement and patience.

Special thanks are extended to Professors David Locke and Carol Steiner, members of my thesis committee, for their interest and the generosity of their time. Thanks also to Andy Auerbach and Jim Paul, of Hoechst-Celanese Engineering Plastics Division, for their valuable discussions.

Acknowledgement is gratefully made to the following sources of financial support: (a) the Chemistry Department of the College of Staten Island for teaching appointments from 1984 to 1988 an (b) Hoechst-Celanese Engineering Plastics Division for partial support.

I especially wish to thank my parents and all of my family, including the Udale family, the Rodriguez family and Libaniel, for their continuous faith, support and love.

Table of Contents

List of Tables

List of Figures

1. BACKGROUND SURVEY

Polyacetal copolymers are technically important macromolecules, competitive with metals, ceramics and nylons in many applications. As the simplest form of aliphatic polyethers, they are of fundamental interest. The present investigation involves detailed studies aimed at the improvement of polyacetal copolymer stability.

Acetal copolymers were first reported by Butlerov in 1859 (1), but were not studied in depth until the 1920's (2). Formaldehyde polymers with commercially useful molecular weights were not prepared until the late 1950's. At that time end-capped, thermally stable formaldehyde polymers went into production by DuPont. The stabilization method involved the reaction of unstable methylol, $-CH_2OH$, endgroups with acetic anhydride to yield an acetate end-capped homopolymer (Delrin) (3). Soon after, a thermally stable copolymer was developed by Celanese (Celcon) (4). The product was the result of the copolymerization of trioxane and ethylene oxide. Today, acetal resins are widely used as replacements for metals in areas such as machinery, appliances, hardware and plumbing. For a detailed review of polyacetal history see reference 5.

One important class of acetal copolymers is typically synthesized by the cationic ring-opening polymerization of trioxane and a cyclic ether such as ethylene oxide or 1,3-dioxolane.

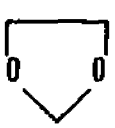

The relatively brief induction period for trioxane homopolymerization, in which monomeric formaldehyde reaches an equilibrium concentration, is lengthened to varying degrees depending on the comonomer.

For the copolymerization of trioxane and ethylene oxide, it has been shown that all comonomer reacts before any trioxane is polymerized (6,7). During this period, the comonomer reacts with formaldehyde generated from the ring-opening of trioxane to form larger cyclic ethers, primarily 1,3-dioxolane and 1,3,5-trioxepane. The concentration of these species increase until the ethylene oxide is completely consumed and the trioxane polymerization begins (8).

It would appear that polymerization by such a process would yield a product consisting of blocks of comonomer. However, due to the process of transacetalization (see Figure 1.1), block copolymers do not result. In the homogeneous cationic polymerization of cyclic acetals, chain transfer to polymer proceeds efficiently because polymer is more basic than monomer.

Repeated attack by growing chain ends on acetal units of completed chains result in randomization of comonomer units. This efficient chain transfer reaction also has the consequence of affecting chain length, such that segments of long and short chains are shuffled to yield typical polyacetals with a MWD of two. The key factor in transforming unstable homopolymer into such a successful engineering resin was the understanding of the degradation processes to which acetal polymers are subjected.

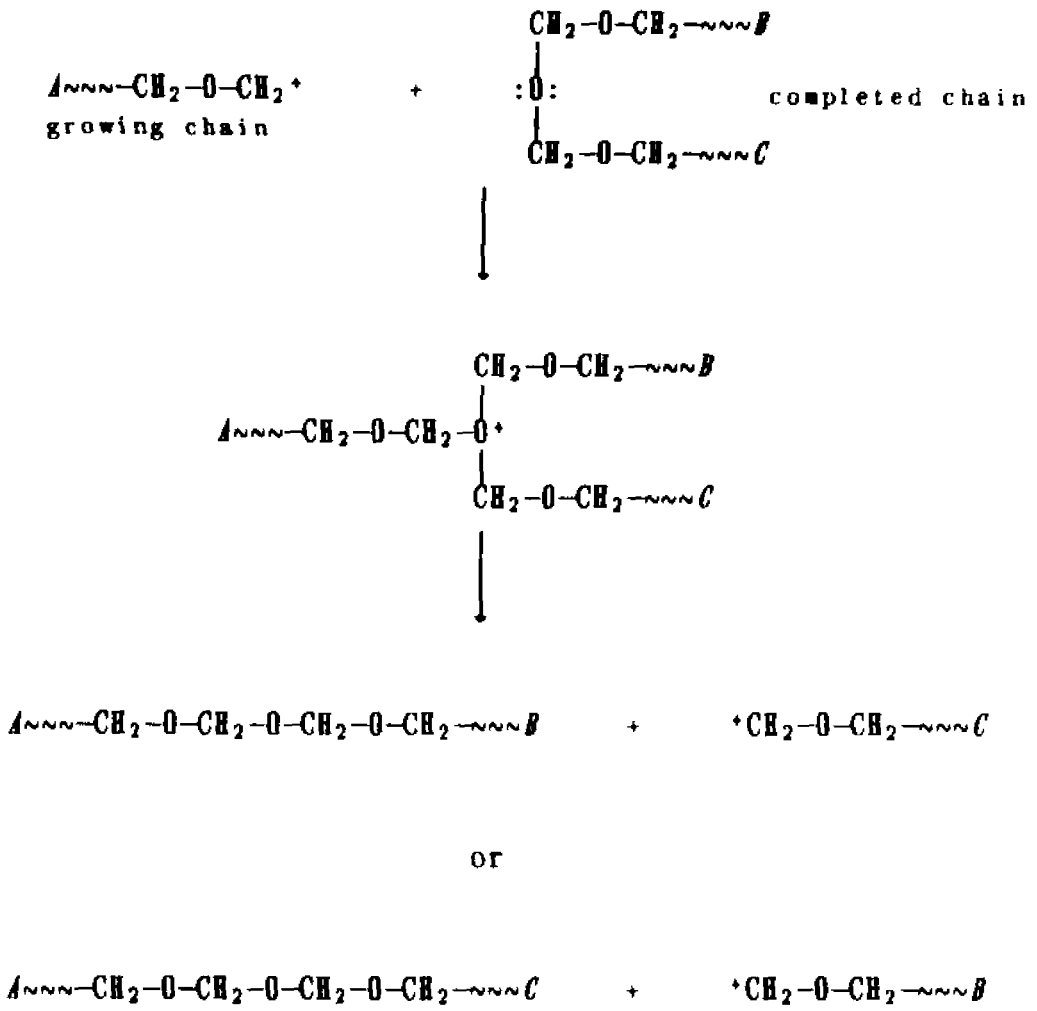

Figure 1.1 : Transacetalization scheme

At elevated temperatures, even high molecular-weight polyoxymethylenes readily depolymerize to monomeric formaldehyde. Degradation begins at chain ends and molecular weight rapidly decreases as a result of unzipping. The rate of depolymerization can be reduced substantially by end-capping or by incorporation of comonomer.

The scheme in Figure 1.2 outlines the fundamental degradation processes of the acetal copolymer system (9). Acetal copolymers are susceptible to both radical and acidolytic degradation. Acetal units possess labile methylenic hydrogens susceptible to radical abstraction. The unshared electron pairs of the oxygen atom of the acetal unit may be attacked by acid. In both cases, β-elimination will occur; polymer degradation will result in "unzipping" and the generation of formaldehyde. It is clear that an unstabilized polyacetal, such as polyoxymethylene, is readily degraded by both acid and radicals. Formaldehyde, as shown in the scheme above, plays an interesting role in the degradation process. In the presence of heat and light, formaldehyde can produce radicals. Hydroperoxide produced during the degradation process can oxidize formaldehyde to formic acid. When this occurs, the degradation of the polyacetal is observed to autoaccelerate.

Successful stablization formulations should stabilize the acetal polymer against both short-term thermal degradation during processing and long-term oxidative degradation at service temperature. An ideal stabilization system should also inhibit the propagation of peroxide radicals and thus limit autoacceleration of the unzipping process.

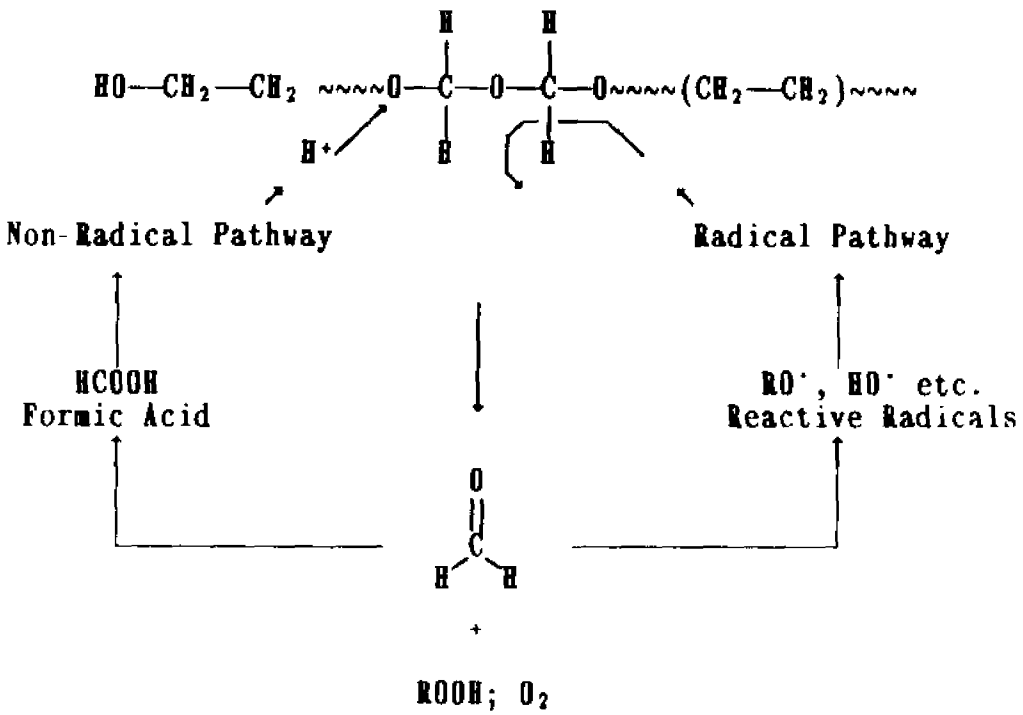

Figure 1.2 : Degradation Scheme

In general, effective stabilization of acetal copolymers consists of a combination of the use of: 1) comonomer stopper units; 2) formaldehyde acceptors; 3) acid scavengers and 4) radical inhibitors. Stopper units such as oxyethylene terminate polymer unzipping and thereby limit the extent of degradation. As stated earlier, methylenic hydrogens are subject to radical abstraction. Oxyethylene units are not acetals, and their protons are not readily abstracted by radicals. Hence unzipping proceeds only as far as an oxyethylene unit and results in a stable hydroxyethylene endgroup.

$$\sim\sim\sim CH_2-CH_2-O-CH_2CH_2-O-(CH_2-O)_n\sim\sim\sim \xrightarrow{H^+ \text{ or } R^\cdot}$$

$$\sim\sim\sim CH_2-OCH_2-O-CH_2CH_2-OH \; + \; n\, CH_2O$$

By means of an hydrolysis process, unstable hemiacetal groups, $-OCH_2OH$, can be intentionally removed, again resulting in stable endgroups. Attack by either acid or radical at any point within the chain will result in unzipping only up to the point of the next stopper unit, thereby limiting degradation.

An additional consideration for acetal copolymer stabilization is the dispersion of stabilizing agents. Concern about stabilizer dispersion has led to interest in polymer-bound stabilizers for several polymeric systems (10).

While the copolymers of trioxane and ethylene oxide are superior in stability, they do not carry functional groups, except at chain ends, for stabilizer binding. The literature reveals that a significant amount of work has been done to synthesize new trioxane

copolymers (11). For example, copolymerizations with comonomers having the general structure:

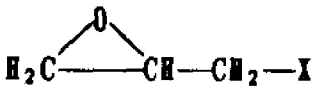

have been explored. Using this approach, polyoxymethylene ionomers were prepared by reaction of thioglycolate anions with trioxane-epichlorohydrin copolymers (12).

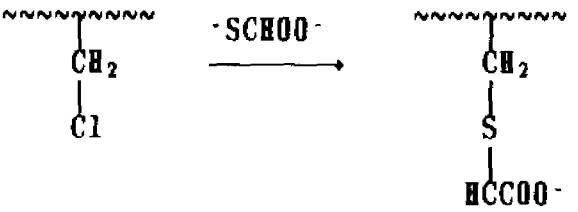

A similar reaction is (13):

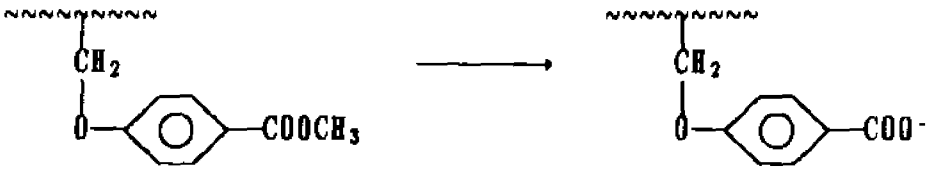

Trioxane-ethyl glycidate copolymers and modified copolymers have also been reported (14,15). Copolymerization with phenyl glycidyl ether has been reported (16), but does not yield a functional copolymer for ready modification.

Three copolymerization systems were explored in the present work. For the copolymerization of trioxane with another glycidyl comonomer,

i.e. glycidyl acrylate,

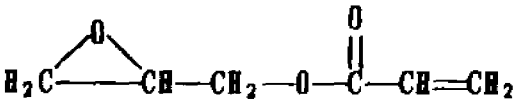

we report the synthesis and characterization of both the copolymer and the glycidyl acrylate homopolymer. Work on the copolymerization of glycidyl acrylate with 1,3-butadiene (17) and N-vinyl pyrrolidone (18) have been documented.

Also presented here is the copolymerization of trioxane and glycerol formal.

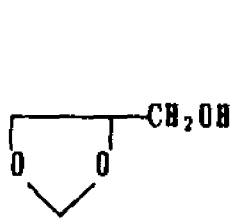

α,α-form

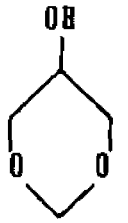

α,β-form

This copolymerization has not been reported to date, although a patent (19) referring to the copolymerization of the *α,α*-isomer of the glycerol formal ester has been issued.

This dissertation also describes the first detailed investigation of the copolymer of trioxane and 1,3-dioxep-5-ene. The

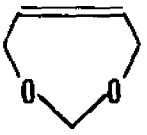

synthesis of this copolymer was accomplished by Schulz *et al* (20,21,22), however detailed studies on copolymerization, characterization and properties have not yet been published.

2 INTRODUCTION AND OBJECTIVES

The development of commercially useful acetal resins was possible only through understanding of the degradation mechanism. Based on a thorough understanding of the unique combination of chemical processes which acetal polymers undergo, intelligent decisions about stablilization can be made. Investigations towards the achievement of polyacetal-bound stabilizers have been carried out and are presented here. The scheme shown in Figure 2.1 illustrates the approach taken in this study of polyacetal stabilization and degradation. The ultimate goal of these investigations is the synthesis of a "super stable" polyacetal which could be obtained by the binding of optimum stabilizers to polyacetals via functionalized stopper units.

Two routes have been taken to identify "ideal" stabilizers. In the first, the radical and acidolytic solution degradation of a model trioxane-ethylene oxide copolymer was examined. Among the primary objectives of this study were the determination of relative stabilities of different comonomer sequences and the determination of sites of attack. More importantly, it was expected that identification of previously unknown degradation products or processes would lead to new stabilizers or stabilization methods. This investigation focuses on these two processes for a model trioxane-ethylene oxide copolymer in a DMSO solution. The model sample differs from commercial samples in that it contains an unusually high comonomer incorporation. This model compound was synthesized so that ^{13}C NMR pentad sequences and ^{1}H NMR triad sequences could be observed. This would not be possible with

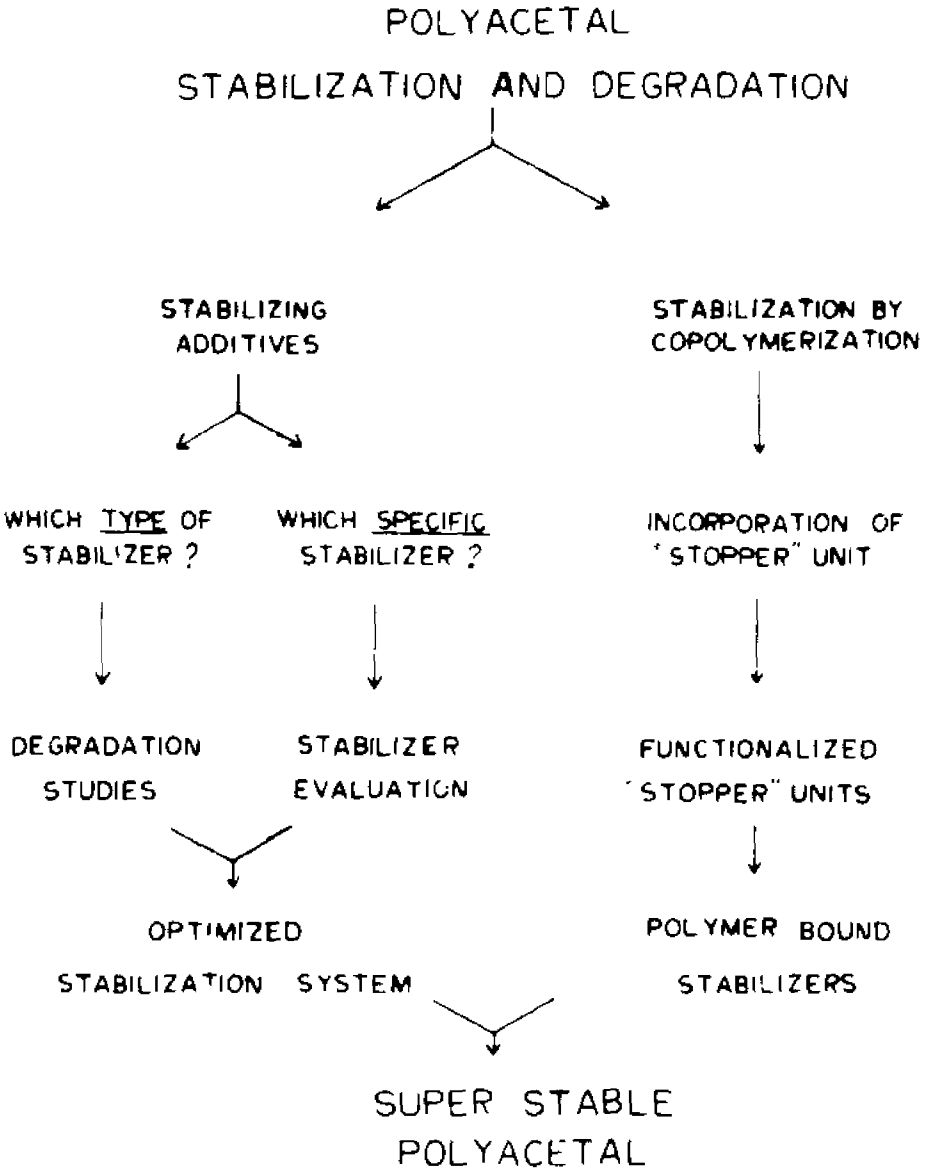

Figure 2.1
Outline of approach to polyacetal stabilization

samples having a low comonomer incorporation because various absorptions would be too small to observe. The degradation of the model polyacetal, performed *in situ* inside the probe of the NMR spectrometer, was followed by obtaining spectra at specific time intervals. Using this experimental design it was possible to monitor the appearance and disappearance of signals so that conclusions about the degradation process could be made. Identification of degradation products was accomplished by the use of both one- and two-dimensional NMR spectroscopy. Confirmation of the identities of these products was made by comparison with known compounds. Aside from formaldehyde and formic acid, all degradation products were found to be cyclic acetals generated by backbiting during depolymerization.

In the second phase of this study of polyacetal stabilization and degradation, the relative efficiency of a family of formaldehyde acceptors was examined. This class of compounds is used effectively to remove formaldehyde, a potentially harmful degradation product. The purpose of this investigation was to determine the effect of substituents on the formaldehyde accepting ability of amino triazines. The "parent" molecule, melamine, eight melamine derivatives and cyanoguanamine, a precursor in the synthesis of melamine, were each evaluated with respect to their inherent ability to react with formaldehyde. Removal of formaldehyde from degrading polyacetal copolymer systems by these compounds may be accomplished through the following reactions:

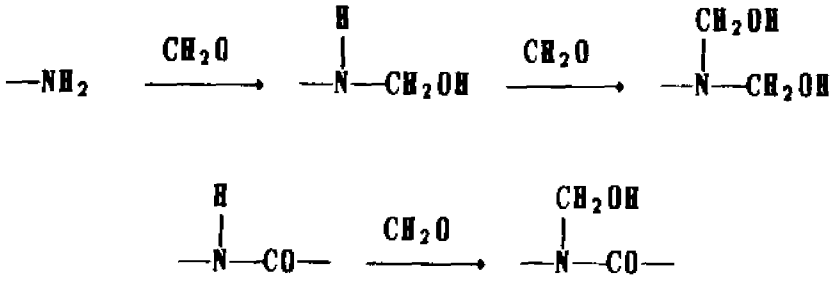

Together with the relative thermal stabilities of the stabilizer/CH_2O adducts, stabilizers' reactivities were used to assess suitability for polyacetal stabilization.

The determination of stabilizer reactivity towards formaldehyde was determined by two equivalent methods. In the first method, water soluble stabilizers were reacted with an aqueous formaldehyde solution of known concentration. The amount of formaldehyde reacted with each compound was calculated from the difference in formaldehyde concentration before and after reaction with each stabilizer. In the second method, water insoluble stabilizers and paraformaldehyde were dissolved in hexafluoroisopropanol (HFIP) and allowed to react. Semiquantification of the amount of formaldehyde with which each stabilizer reacted was performed by ^1H NMR. To insure that both methods are consistent with each other, two water soluble samples (that are also soluble in HFIP) were also evaluated by the method developed for the water insoluble samples.

The thermal stability of adducts obtained by both methods was then examined by thermogravimetric analysis, a technique in which the mass of the sample is measured continuously as a function of temperature.

A third, but less successful approach to the determination of stabilizer efficiency was also taken. This method involved the reaction of stabilizers and formaldehyde at the processing temperature of polyacetals (i.e. 220°C). Experiments were performed in a modified Parr bomb. Formaldehyde gas was generated by decomposition of paraformaldehyde. It was expected that the experimental design would be more consistent with the somewhat severe processing conditions. Unfortunately, due to several difficulties encountered, including temperature control, this method of analysis was suspended in favor of solution state analysis.

The ultimate goal of the studies described above was to learn more about the fundamental chemistry of several processes involved in polyacetal degradation stabilization, and thereby lay the groundwork for evaluation of optimum polyacetal stabilizers. In the quest for polyacetals capable of binding such stabilizers, three new functionalized acetal copolymers were synthesized and characterized.

The first was synthesized by the cationic ring-opening copolymerization of trioxane (TX) and 1,3-dioxep-5-ene (DXPE). The copolymers were characterized by ^{1}H and ^{13}C NMR spectroscopy as well as by thermal analysis (TGA, DSC). It was found that incorporation of the functionalized stopper unit, ~~~O-CH_2-CH=CH-CH_2-O~~~, provides greater thermal stability and chemical resistance than does the ethylene oxide stopper unit.

NMR and viscosity measurements reveal the TX-DXPE copolymers to be of reasonable molecular weights, i.e. M_n = 6 X 10^4 and M_v = 8 X 10^4.

Analysis by DSC indicates that crystallinity is not adversely affected by the incorporation of the *cis*-2-butene unit.

Modification of surface stopper units was demonstrated by the grafting of sodium acrylate. A colored copolymer results when the graft copolymer is stained with a cationic dye. Copolymers have also been modified by epoxidation and by incorporation of a urea moiety.

The second functionalized acetal copolymers was produced by copolymerization of trioxane and glycerol formal (GF). Two different stopper units, one with a pendant hydroxy group and the other with a pendant methylol group, have been identified by ^{13}C NMR spectroscopy.

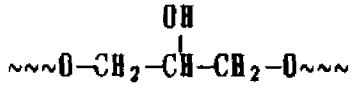

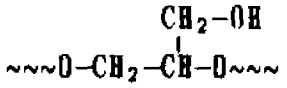

These copolymers also demonstrate superior thermal stability as compared to trioxane-ethylene oxide copolymers. Yields and molecular weights (M_v = 4 X 10^3) are notably lower than those of both trioxane-dioxepene and trioxane-ethylene oxide copolymers.

The third copolymer was synthesized by the copolymerization of trioxane and glycidyl acrylate (GA). The primary comonomer unit in this copolymer has a pendant acrylate group.

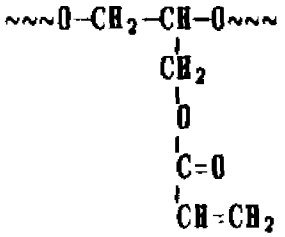

Secondary units are believed to result from reaction of the acrylate group, yielding crosslinked copolymers.

Samples with comonomer feeds ranging from 1.1 to 6.9 mole percent were found to have excellent thermal stability. Crystallinity for these copolymers fall between 11% and 35%. All copolymer are insoluble in hexafluoroisopropanol, HFIP, at room temperature as well as in DMSO and DMF at 170°C. Swelling was observed to vary with comonomer feeds, i.e. lower feed copolymers swell more than ones with higher feeds.

Each of the copolymers described above have functionalized comonomer units which serves as both stoppers against unzipping and as sites for further modification.

3 A STUDY OF POLYACETAL DEGRADATION AND STABILIZATION

3-1 Degradation Processes of Polyacetal Copolymers

3-1a Summary

The degradation products obtained by the radical and acidolytic degradation of a model acetal copolymer in solution have been identified by ^{1}H and ^{13}C NMR spectroscopy. These products have been confirmed to be formaldehyde, formic acid and the cyclic acetals 1,3-dioxolane, 1,3,5-trioxepane, 1,3,5-trioxane and 1,3,5,7-tetraoxane. The formation of these cyclic acetals is due to the depolymerizing chain end backbiting on an oxygen on its own chain.

3-1b Experimental

3-1b-1 Sample preparation

DMSO-d_6 solutions of the model polyacetal, which was kindly supplied by Hoechst-Celanese Engineering Plastics Division, were prepared by dissolving approximately 25 mg of the model compound in 0.3 mL of DMSO-d_6. To this solution was added either 2 mg of Luperox (2,5-dihydroxy-2,5-dimethylhexane) (Penwalt Corp.) or 5 μL trifluoroacetic acid, for radical and acid catalyzed degradation experiments, respectively. All samples were prepared directly in 5 mm NMR tubes. Prior to the addition of either peroxide or acid, samples were gently heated and mixed in a Vortex Genie to dissolve the polymer. On addition of degrading agent, samples were again mixed.

3-1b-2 NMR analysis

Both ^{1}H and ^{13}C NMR degradation spectra were obtained at 126°C, i.e. at the minimum temperature for complete polymer dissolution in DMSO. For purposes of comparison, model compounds for degradation products were also run at 126°C. All spectra were obtained on an IBM 200-SY NMR spectrometer using Bruker software.

Inversion recovery experiments (9) show that all carbons exhibit a T_1 value of approximately one second. For the observation of degradation processes, proper parameters e.g. pulse angle and relaxation delay, were selected to permit semi-quantitative comparison among absorption peaks. The delay times and the number of scans collected are indicated in the caption for each of the degradation spectra.

3-1c Results

The progress of the degradation of the model polyacetal was monitored by obtaining NMR spectra alternatively between ^{1}H and ^{13}C observation on the same sample with predetermined waiting times. ^{13}C NMR spectra obtained from the acid and hydroperoxide catalyzed degradation are presented in Figures 3.1 and 3.2 respectively. ^{1}H NMR spectra of the same samples are presented in Figures 3.3 and 3.4. Spectra are presented chronologically in ascending order. In ^{13}C NMR spectra, pentad sequences are identified. Triad sequences are identified for ^{1}H spectra. Original sequence identification was done by Fleischer and Schulz (23,24). In some instances, signals due to formaldehyde (196 ppm) and formic acid (164 ppm) were observed in ^{13}C

degradation spectra.

To assist in the assignment of the proton spectra, a two-dimentional NMR experiment was performed. The experiment, COSY (homonuclear shift-correlated spectroscopy), is commonly used to separate chemical shifts and spin coupling effects by displaying them in two orthogonal frequency dimensions ω_1, ω_2 (25). Figure 3.5 gives the COSY spectrum for the model compound degraded by hydroperoxide.

^{13}C and ^{1}H spectra of model compounds are compared with their corresponding degradation products in Figures 3.6 and 3.7. An extended series of ^{1}H spectra of degraded model polyacetal is presented in Figure 3.8. These spectra reflect the progress of the degradation past the point when polymer is no longer present. The signals in the upper spectra are due only to degradation products.

3-1d Discussion

On first observation of the ^{13}C and ^{1}H spectra of the degrading polyacetal, the sequence MMMEM in ^{13}C spectra (Figures 3.1 and 3.2) and the sequence MMM in ^{1}H spectra (Figures 3.3 and 3.4) appear to be the most stable microstructures. These observations are not internally consistent, i.e the oxymethylene carbon in the ^{1}H triad (A) cannot be the same oxymethylene carbon in the ^{13}C pentad (B).

(A) $\sim\sim\sim CH_2O\underline{-CH_2O}-CH_2O\sim\sim\sim$

M M M

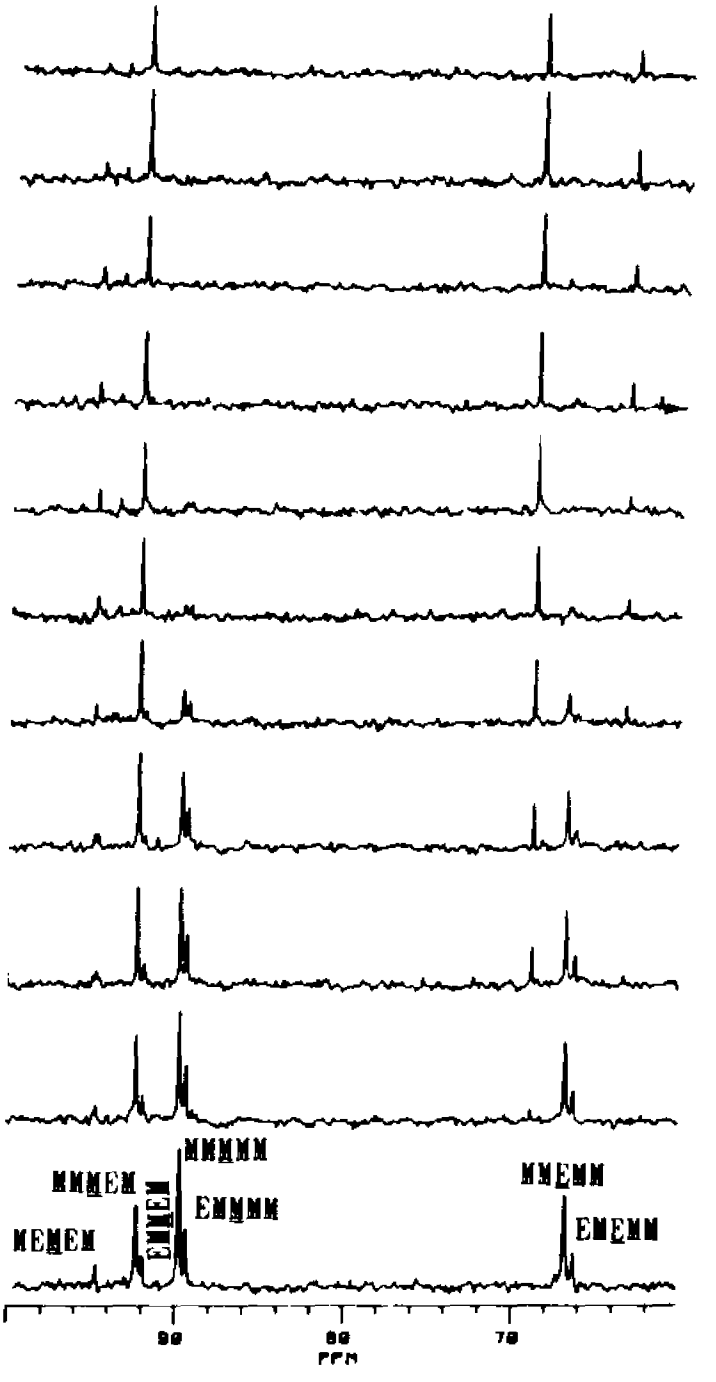

Figure 3.1

^{13}C NMR spectra of degrading model polyacetal, spectra of sample with increasing degree of degradation appear in ascending order (DMSO-d_6, heated at 126°C with trifluoroacetic acid) (200 scans, 15 minute waiting time between spectra)

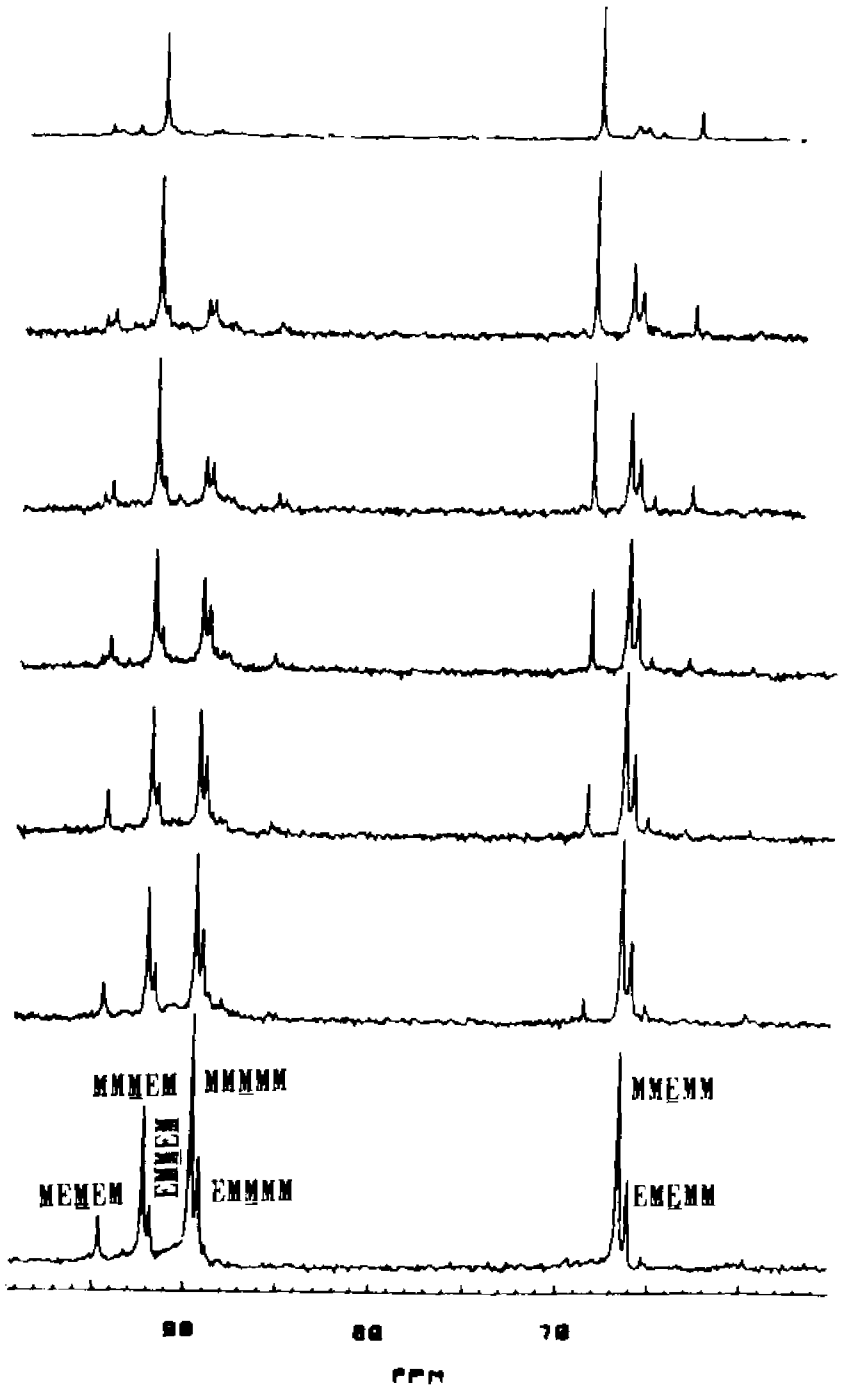

Figure 3.2

^{13}C NMR spectra of degrading model polyacetal, spectra of sample with increasing degree of degradation appear in ascending order (DMSO-d_6, heated at 126°C with hydroperoxide) (200 scans, 15 minute waiting time between spectra, 45 minutes between 2 upper-most spectra)

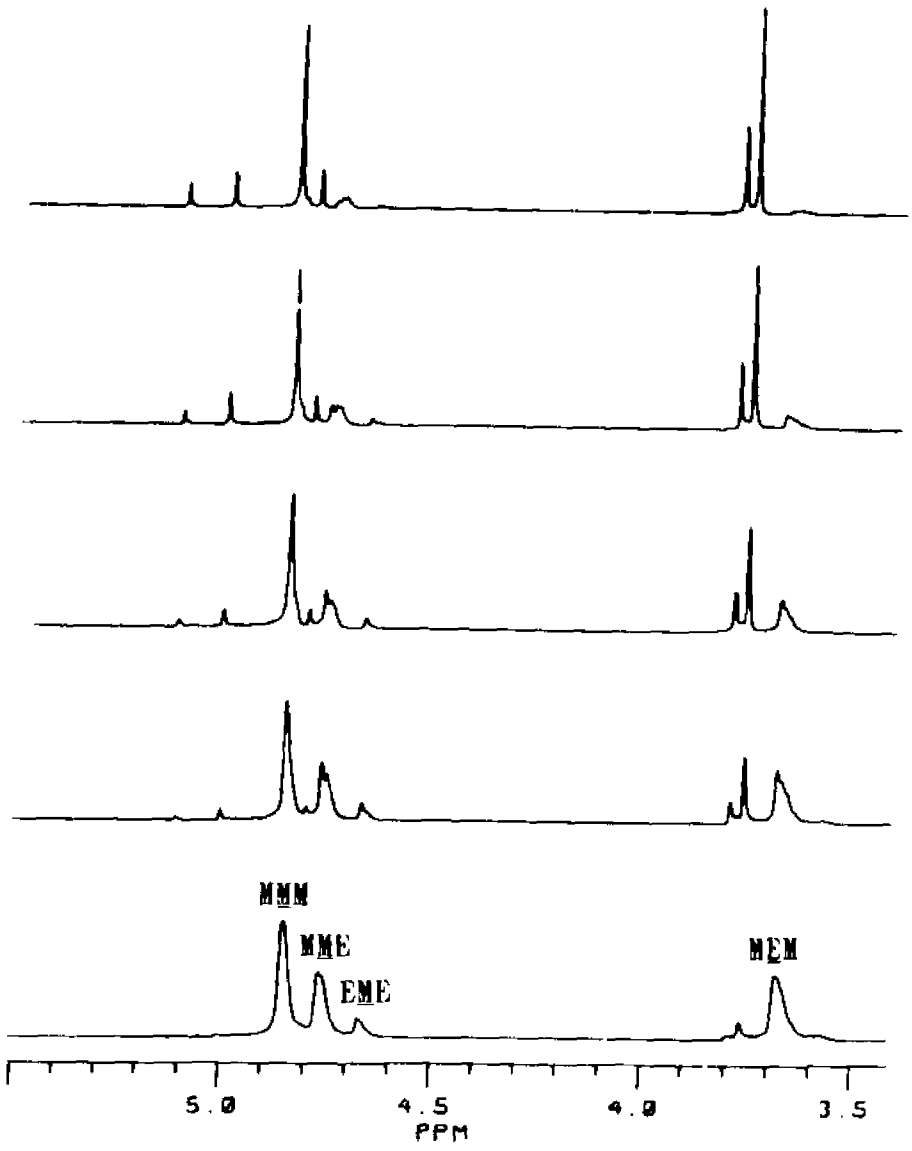

Figure 3.3

^{1}H NMR spectra of degrading model polyacetal, spectra of sample with increasing degree of degradation appear in ascending order (DMSO-d_6, heated at 126°C with trifluoroacetic acid) (64 scans, 30 minute waiting time between spectra)

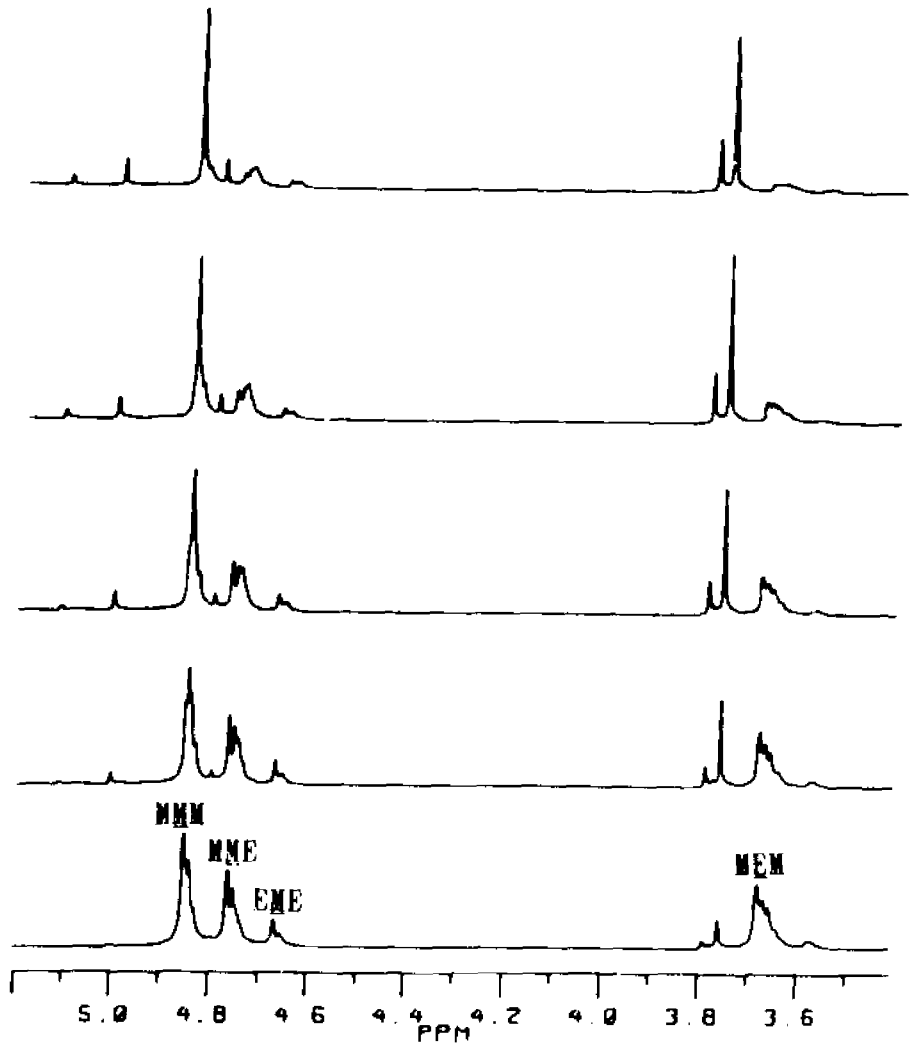

Figure 3.4

^{1}H NMR spectra of degrading model polyacetal, spectra of sample with increasing degree of degradation appear in ascending order (DMSO-d_6, heated at 126^{0}C with hydroperoxide) (64 scans, 30 minute waiting time between spectra)

(B) $\sim\sim\sim CH_2O\text{-}CH_2O\text{-}CH_2O\text{-}CH_2CH_2O\text{-}CH_2O\sim\sim\sim$

M M M E M

where M = $-CH_2O-$
E = $-CH_2CH_2O-$

This suggests the possibility of species fortuitously having the same chemical shift.

In the degradation spectra the appearance of several new signals in the oxymethylene and oxyethylene regions of both the ^{13}C and ^{1}H spectra are observed. Based on the previous discussion of polyacetal degradation, it is expected that hydroxy endgroups, and especially hydroxyethyl endgroups, should grow in concentration as degradation proceeds. However, the chemical shift of the observed signals do not match those of such groups.

The COSY 2D spectrum in Figure 3.5 establishes that the observed signals are not due to hydroxyethyl endgroups. The information given therein was important for detailed spectral assignment. The 2D spectrum, devoid of off-diagonal signals, indicates that there is no coupling between any of the four proton signals in that spectrum. These four signals correspond to protons 3,4,5 and 6 in Figures 3.3, 3.4 and 3.6. The absence of coupled signals eliminates any non-symmetrical oxyethylene units such as $\sim\sim CH_2CH_2OH$. Oxymethylene units have oxygen on both sides and are not expected to show coupling. This information gives significant hints as to the origins of the observed signals. A further restriction is that the assignments for the

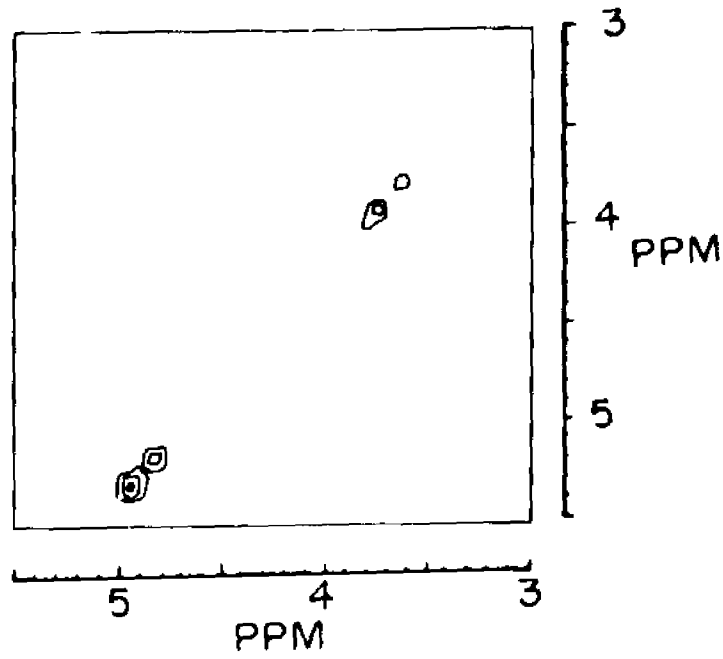

Figure 3.5

COSY-2D NMR spectrum of degraded model polyacetal, (DMSO-d_6, 25°C)

^{13}C and ^{1}H spectra must, of course, be consistent within the system.

Evaluating all of the known information and considering that the degradation is taking place in solution, we propose a reasonable explanation for the observations. Compounds corresponding to known information are cyclic acetals such as 1,3-dioxolane and 1,3,5-trioxepane.

1,3-dioxolane (DOL)

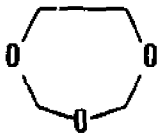

1,3,5-trioxepane (TOP)

The assignments were confirmed by the ^{13}C and ^{1}H spectra of both compounds. Chemical shifts and signal intensities were in complete agreement with the observed signals in both the ^{13}C and ^{1}H spectra, as demonstrated in Figures 3.6 and 3.7.

Two additional signals observed in Figures 3.3, 3.4 and 3.8 but not in the 2D spectra are likewise assigned to cyclic compounds. These are 1,3,5-trioxane and 1,3,5,7-tetraoxane.

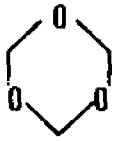

1,3,5-trioxane (TOX)

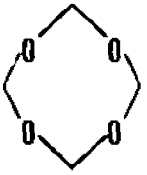

1,3,5,7-tetraoxane (TEX)

Again there was complete agreement of chemical shifts and signal intensities in both the ^{13}C and ^{1}H spectra (see Figures 3.6 and 3.7).

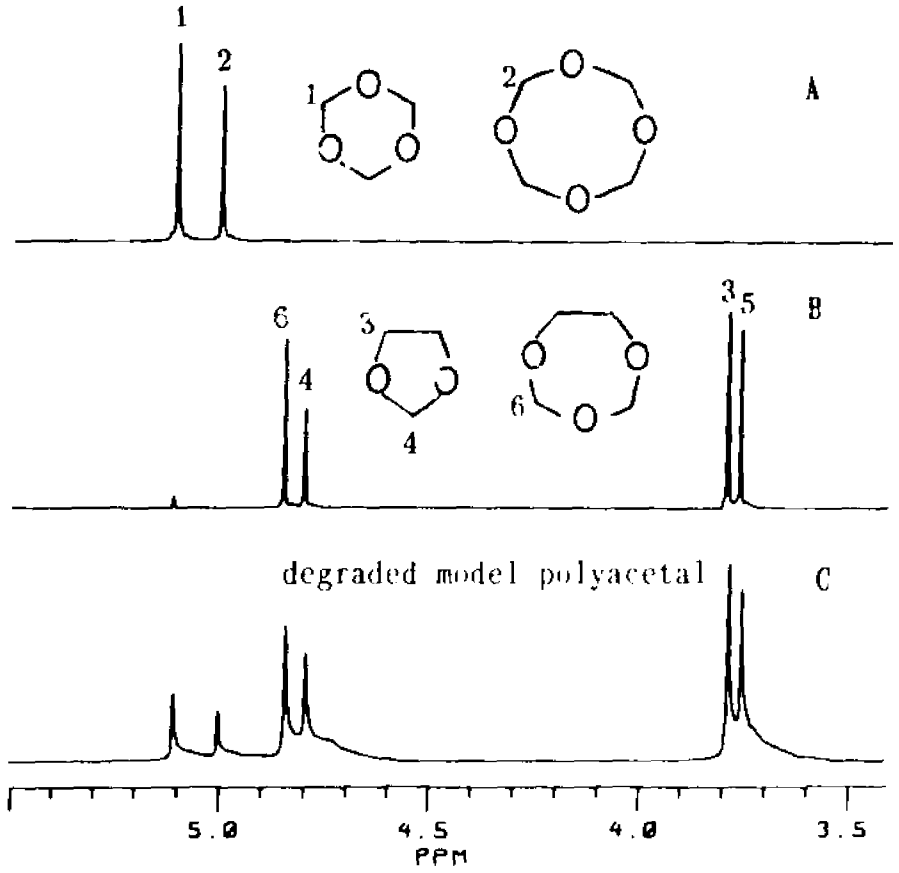

Figure 3.6

^{1}H NMR spectra, comparing known compounds with degraded model copolymer (DMSO-d_6, 126°C)

A : trioxane and tetraoxane
B : dioxolane and trioxepane
C : degraded model polyacetal

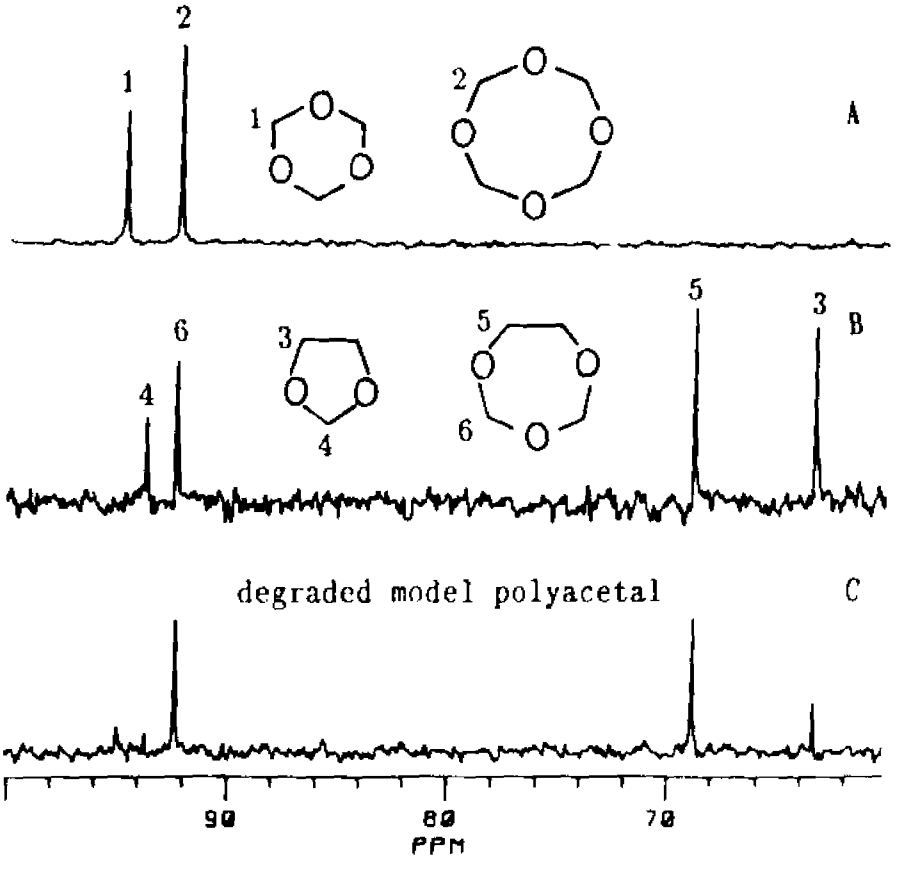

Figure 3.7

^{13}C NMR spectra, comparing known compounds with degraded model copolymer (DMSO-d_6, 126°C)

A : trioxane and tetraoxane
B : dioxolane and trioxepane
C : degraded model polyacetal

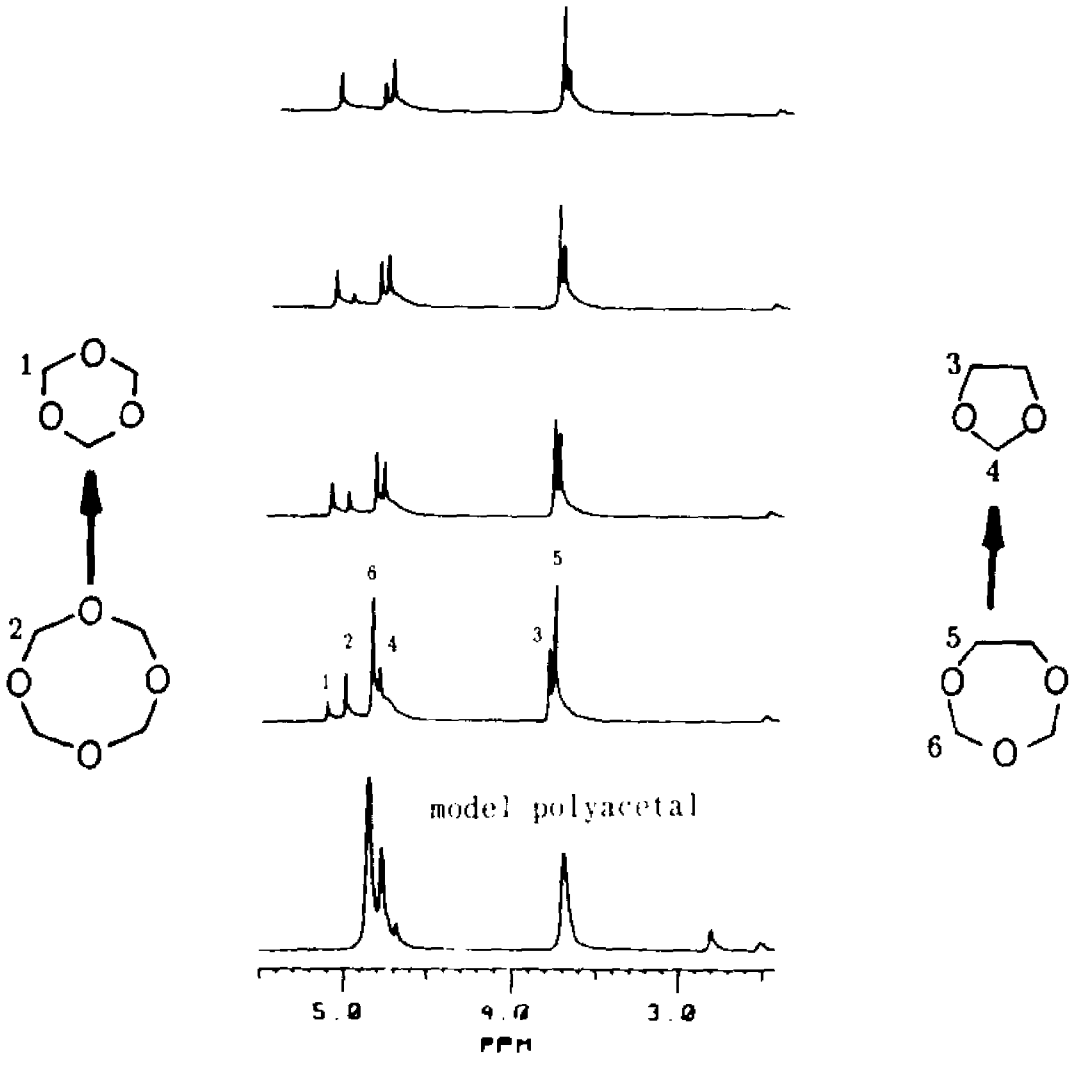

Figure 3.8

^{1}H spectra of degrading model polyacetal illustrating the degradation of cyclic acetal degradation products, spectra of sample with increasing degree of degradation appear in ascending order (DMSO-d_6, heated at 126^{0}C with trifluoroacetic acid)

During the later stages of degradation there is a decrease in the intensity of signals 5 and 6 relative to 3 and 4. Likewise, signal 1 appears to grow with respect to signal 2. These observations may be explained by considering the equilibrium

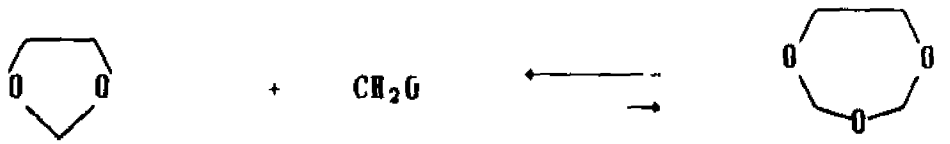

It was exactly this reaction that was used to synthesize the TOP used as a model compound for identification of degradation products. It appears that under the experimental conditions, the equilibrium shifts to the left. A similar argument can be made to explain the decrease in TEX signals, i.e. the equilibrium also shifts in favor of the smaller ring.

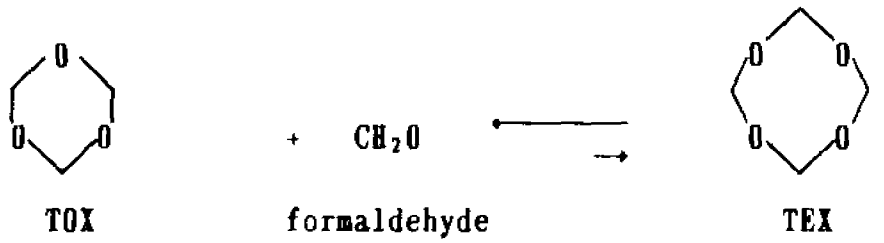

The process involved in the degradation can now be suggested based on the established identity of the degradation products and the observed changes in signal intensity. The first degradation products to be observed are the larger rings, i.e. TEX and TOP. TOP emerges very quickly and remains the dominant product until it is later converted to DOL. TEX also emerges quickly but its concentration grows at a much slower rate. These observations may be explained by the

process known as backbiting. The formation of TOP by backbiting is illustrated as follows:

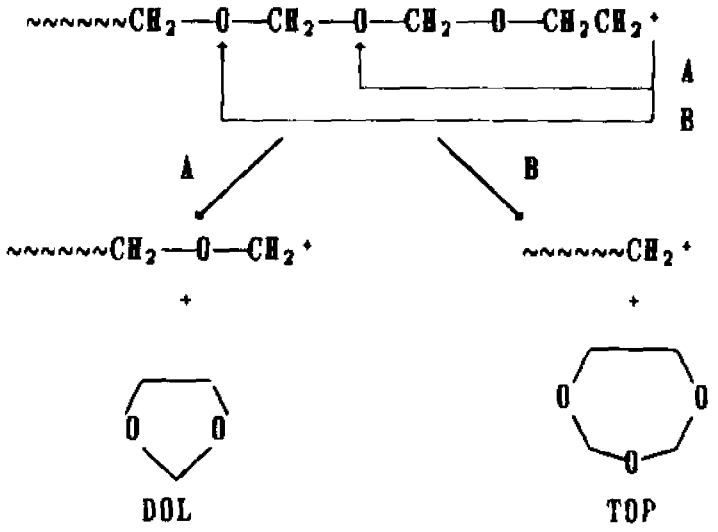

The process requires sufficient segmental motion of the degrading chain end so that it can attack an oxygen of its own chain. The result is a TOP molecule and a chain end that continues to degrade. TEX can be generated in a similar fashion.

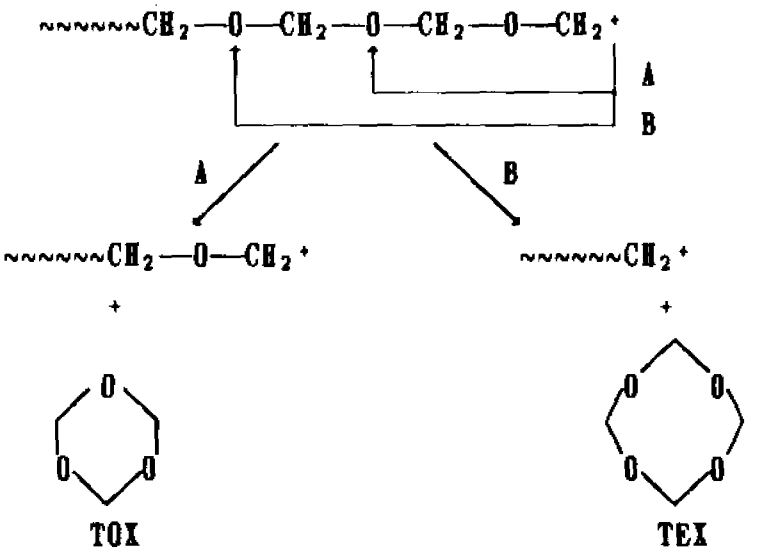

The observation that there is so much less TEX and TOX than DOL and TOP clearly indicates that unzipping of POM blocks is faster than backbiting. If unzipping ceases at an oxyethylene unit, and the chain end can backbite, then either DOP or TOP will be formed.

The kinetic behavior of degradation observed by NMR clearly establishes the relative stabilities of different sequences in the copolymer. Units surrounded by stopper units are the most stable, and units with four or more consecutive oxymethylene units are the least stable. The degradation experiments followed the same route regardless of whether they were initiated by acid or hydroperoxide. Again this is not unexpected since it has been shown that formaldehyde is oxidized to formic acid in these systems (9).

In both acid and hydroperoxide catalyzed polyacetal degradation the autoacceleratory nature of the process is clearly illustrated. That is, the rate of disappearance of oxymethylene units increases with time. This is, of course, a consequence of the degradation products formaldehyde and formic acid.

3-2 Formaldehyde Acceptors

3-2a Summary

The goal of this investigation was to develop a method for evaluating formaldehyde-accepting stabilizers that may be incorporated into the polyacetal system. Formaldehyde can react with amines and amides to form methylolamines according to the following reactions:

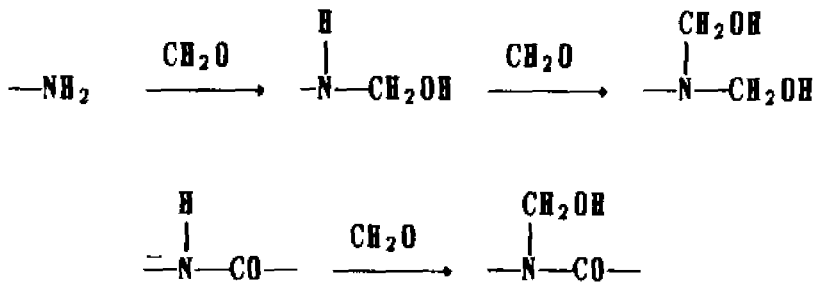

Based on acceptor-adduct equilibrium studies, efficiency of the family of acceptors presented in Figure 3.9 rank in the following order: CNG > melamine > CTU guanamine > benzoguanamine > caprinoguanamine $\cong$ butyroguanamine $\cong$ propioguanamine $\cong$ acetoguanamine $\cong$ diacetyl melamine > triacetyl melamine. The alkyl substituted guanamines did not perform well and are considered unsuitable for reaction with formaldehyde at the processing temperature of acetal copolymers. Under reaction conditions, the amide groups of tri- and diacetyl melamine did not react with formaldehyde. The four other acceptors were effective to varying degrees. Judgement of acceptor efficiency is based on the ratio of weight loss to percent weight of bound formaldehyde. Weight loss was determined by thermogravimetric analysis. Bound formaldehyde was determined via titration of an aqueous formaldehyde solution before

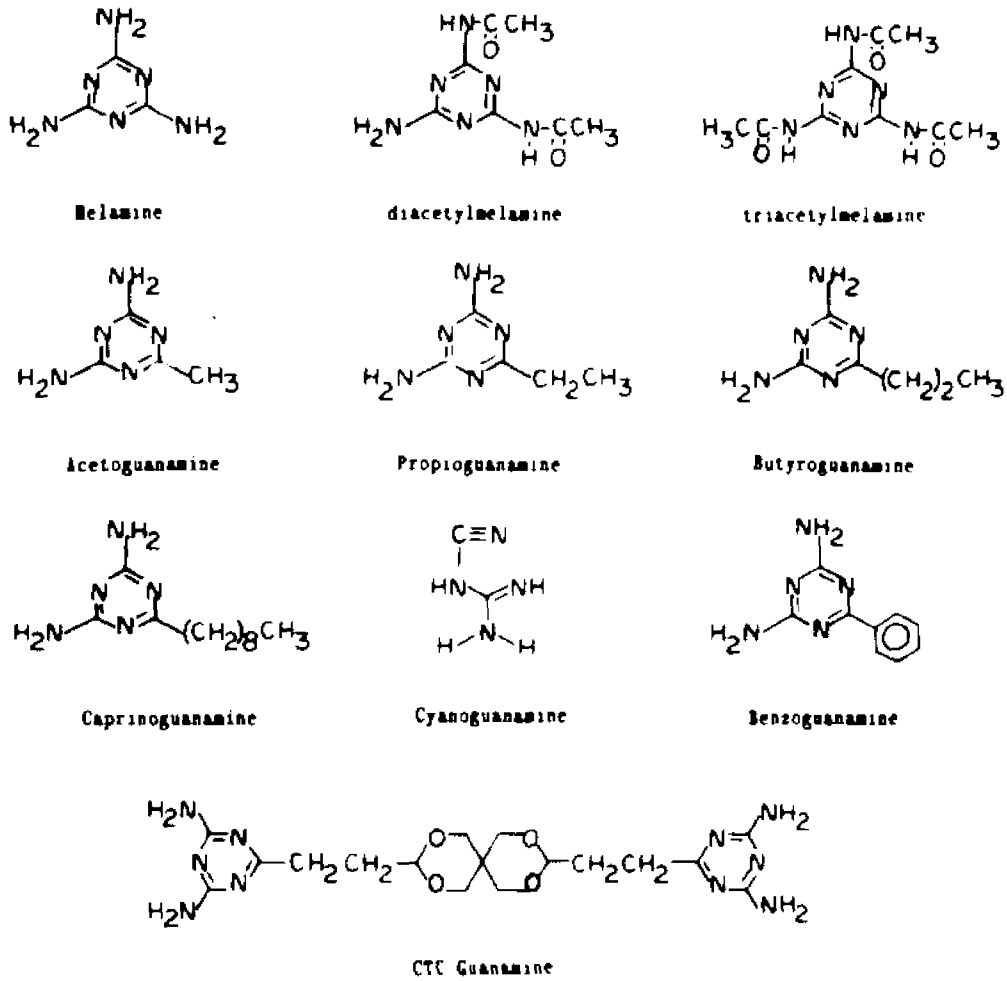

Figure 3.9

Compounds evaluated for use as polyacetal stabilizers

and after reaction with water soluble acceptors or by comparison of ^1H NMR spectra before and after exposure to formaldehyde in the form of a solution of paraform in hexafluoroisopropanol at room temperature.

3-2b Experimental

3-2b-1 Solid phase reactions

The general strategy was first to examine reagents at 220°C and to observe any changes in physical or chemical properties in the absence of formaldehyde. After the effect of heat on the reagents alone was observed, formaldehyde gas was generated in the presence of the potential stabilizer and changes in the system were observed. Reactions were carried out in a modified Parr bomb. (Figure 3.10)

A 13 X 100 mm test tube was suspended from the lid of the reactor with a steel wire. In this test tube were placed trioxane and nitric acid. This modification was made because it was necessary to use an acid to catalyze the generation of formaldehyde and at the same time keep the acid away from the rest of the system. In order to facilitate the cleaning of the reactor, a glass beaker was used to contain the potential stabilizer. An additional modification of the system was made by placing an 18 X 150 mm test tube around the shaft of the stirrer. This was done to provide a surface for the deposition of vaporized components. Since the material was not deposited on the reactor itself, it was much easier to recover. Unreacted formaldehyde was scrubbed by bubbling through a solution of sodium sulfite.

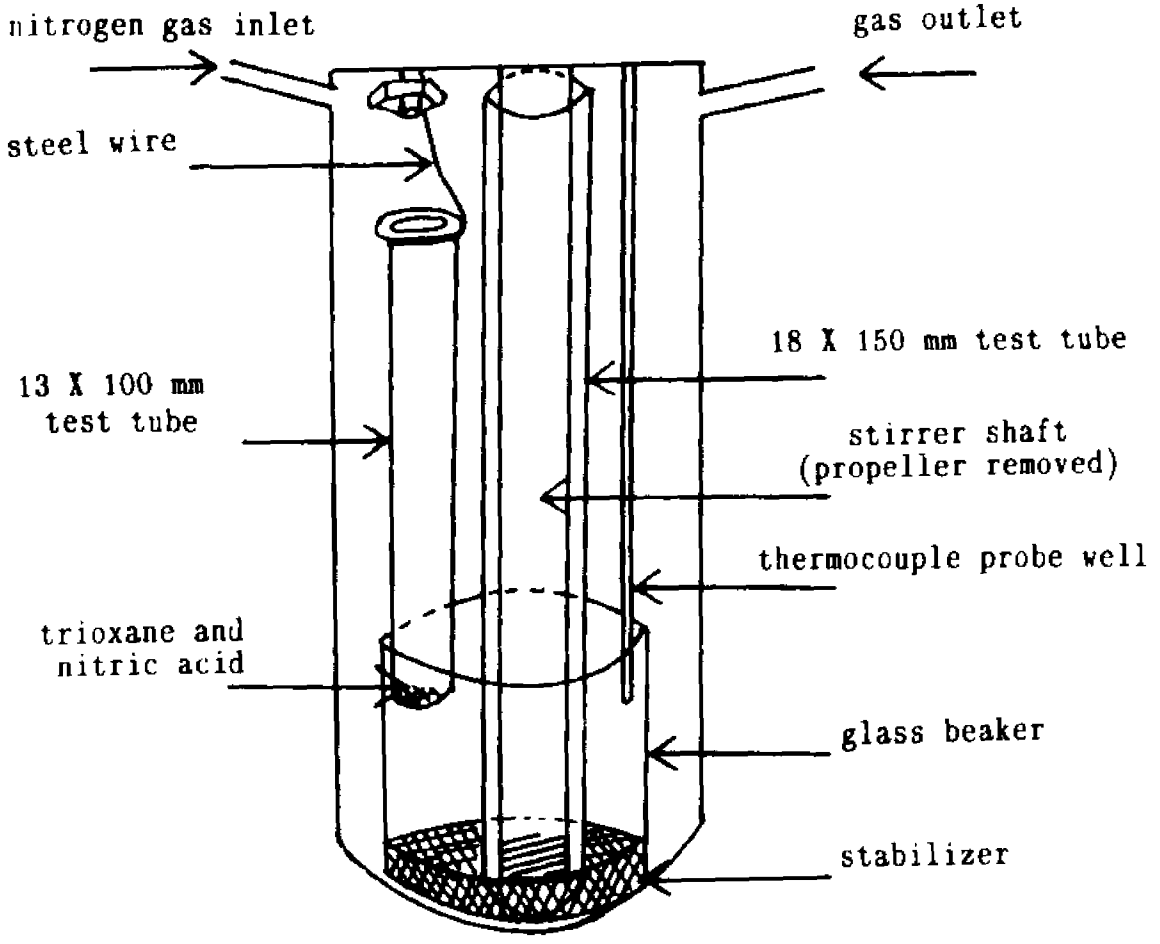

Figure 3.10

Modified Parr bomb reactor

3-2b-2 Solution phase reactions

3-2b-2a Aqueous reaction system

The material recovered at the end of the reactions in the Parr bomb was a mixture of adduct, unreacted stabilizer, and possibly polyoxymethlyene. In order to simplify the isolation of the adducts, the reactions were done in solution. These were accomplished by dissolving approximately 0.01 mole of stabilizer in an aqueous formaldehyde solution (pH adjusted to 8.5 to prevent polymerization).

The formaldehyde solution was prepared by dissolving paraform in distilled water (26). The mixture was refluxed in a round bottom flask fitted with a condenser, and then allowed to cool. The cooled solution was then filtered to remove any undissolved paraform. The formaldehyde content of the solution was determined by reacting an aliquot with sodium sulfite and titrating with standard acid to a thymolphthalein end point (27):

$$CH_2O(aq) + Na_2SO_3 + H_2O \rightarrow NaOH + CH_2(NaSO_3)OH$$

The reactions of formaldehyde with acceptors were carried out in a 50 mL round bottom flask fitted with a condenser. The mixtures were heated to a temperature of 65°C in an oil bath until clear solutions were obtained. The resulting solutions were then transferred to 50 mL Erlenmeyer flasks for further observation.

The choice of reaction conditions was based on the knowledge that melamine can react with almost neutral or mildly alkaline formaldehyde solutions to produce methylolmelamines. From one to six moles of formaldehyde can react with one mole of melamine, apparently yielding all of the methylol derivatives theoretically possible. According to

the literature, hexamethylolmelamine can be obtained by dissolving 0.1 mole of melamine in 0.8 mole of neutral formaldehyde while heating in a boiling water bath for 10 minutes. The crystalline product should gradually crystallize over the course of two days and then be filtered from solution,washed with alcohol, and dried at 60°C for five hours (27). Another procedure calls for the dissolution of the melamine in slightly alkaline (pH=8.0 to 8.5) formaldehyde solution and heating to a temperature of 50 to 85°C (28). The latter procedure was used in this investigation. The precipitates from each solution were filtered and dried under vacuum at 50°C for five hours.

In order to determine the approximate number of moles of formaldehyde consumed by each acceptor, the solutions were titrated in the same manner as the original formaldehyde solution (i.e. by addition of sulfite and titration with standard acid to a thymolphthalein endpoint). The amount of formaldehyde was determined by calculating the difference between the nitial and final concentration of formaldehyde in the reaction solution.

3-2b-2b Nonaqueous reaction system

3-2b-2b-1 Sample Preparation

Sample preparation for formaldehyde uptake experiments was carried out as follows. Paraform and stabilizers were dissolved in a minimum volume of hexafluoroisopropanol, HFIP. Table 3.1 gives the quantities used for each solution. The values chosen for paraform are such that a sufficient amount of formaldehyde was provided for reaction with amine and/or amide without excess. Samples were stirred in a stoppered 12 X

75 mm test tube at 25°C for 20 hours. Solvent evaporation was achieved by slowly dropping the reaction mixture onto a watch glass. Care was taken to keep the area of the residue to a minimum to facilitate collection when dry. Remaining solvent was removed by heating the sample at 60°C under vacuum for 4 hours.

Table 3.1: Composition of stabilizer/paraform solutions for non-aqueous method of stabilizer evaluation

Stabilizer	Stabilizer (g)	Paraform (g)	HFIP (mL)
Diacetyl Melamine	0.1	0.06	1.0
Triacetyl Melamine	0.1	0.04	1.5
Propioguanamine	0.1	0.06	1.0
Benzoguanamine	0.1	0.08	1.0

3-2b-2b-2 NMR samples

DMSO-d_6 solutions of each stabilizer/CH_2O adduct were prepared in 5 mm tubes. ^1H NMR spectra of stabilizers before and after exposure to formaldehyde were obtained on an IBM 200 SY NMR spectrometer. Integration was performed using Bruker software. Proper parameters e.g. pulse angles and relaxation delay, were selected to permit semi-quantitative comparison among absorption peaks.

3-2b-3 Thermogravimetric analysis

Thermogravimetric analysis was carried out on samples obtained by the aqueous and non-aqueous methods. The conditions for the analysis

are given as follows:

Time constant:	1	Range:	2 mV/min
Program rate:	10°C/min	X-axis:	10°C/cm
N_2 Flow Rate:	50 mL/min	Temperature Range:	40-280°C

3-2c Results

3-2c-1 Solid phase studies

The two samples chosen for initial analysis were the parent compound, melamine, and one of the alkyl derivatives, caprinoguanamine. The analysis of melamine was complicated by the fact that it sublimes at elevated temperatures. The time required for the removal of condensed melamine from the bomb interior and more importantly from the gas inlet and outlet, led to very low sample throughput. Samples heated to higher temperatures, i.e. 270°C, became slightly caked, possibly caused by self-condensation (29). Melamine/CH_2O adducts were found to be insoluble in water and in HFIP, indicating that crosslinking had occurred.

For caprinoguanamine, it was observed that on heating to 220°C (in the absence of formaldehyde) the sample had blackened and become viscous. Material deposited on the upper portion of the reactor walls was off-white in color and had a waxy texture. The decomposition of the stabilizer in the bomb is consistent with the results of the TGA thermogram of caprinoguanamine (Figure 3.12) which clearly shows the inherent instability of the compound.

3-2c-2 Solution phase products

3-2c-2a Aqueous reaction system

In this method, water soluble samples were reacted with aqueous formaldehyde. Melamine/CH_2O adducts were expected to precipitate within two days based on literature reports (27). The product was observed to precipitate in less than one day. Other adducts also precipitated relatively rapidly, while still others required nearly a week (see Table 3.2).

All adducts were soluble in water and DMSO; most were soluble in DMF. All were insoluble in chloroform, and except for the caprinoguanamine adduct, were also insoluble in THF (see Table 3.3).

Formaldehyde uptake by each stabilizer was calculated from the difference in formaldehyde concentration of the standardized solution before and after reaction with each stabilizer. Results are presented in Table 3.4.

The results of thermogravimetric analysis of adducts are given in Table 3.5. Mass losses are given for two temperatures,i.e. 210°C and 270°C. TGA thermograms obtained before and after exposure to formaldehyde are presented in Figures 3.11 and 3.12.

3-2c-2b Nonaqueous reaction system

Semiquantification of formaldehyde uptake was accomplished by integration of ^1H NMR spectra of stabilizer/CH_2O adducts. Spectra of stabilizers before and after exposure to formaldehyde are presented in Figures 3.13, 3.14, 3.17, and 3.18. TGA thermograms for amide stabilizers before and after exposure to formaldehyde are given in Figures 3.16 and 3.17. Thermograms comparing the results of adducts

Table 3.2 : Solubility of adducts formed by aqueous method of stabilizer evaluation

Adduct	DMF	THF	Chloroform	DMSO	Hot water
Melamine/CH_2O	i	i	i	s	s
Benzoguanamine/CH_2O	vs	i	i	vs	s
Acetoguanamine/CH_2O	ss	i	i	s	s
Propioguanamine/CH_2O	ss	i	i	s	s
Butyroguanamine/CH_2O	ss	i	i	s	s
Caprinoguanamine/CH_2O	s	s	i	s	s
CTU Guanamine/CH_2O	vs	i	i	vs	s
CNG/CH_2O	ss	i	i	s	vs

i = insoluble s = soluble
ss = slightly soluble vs = very soluble

Table 3.3 : Time required for precipitation of adducts formed by aqueous method of stabilizer evaluation

Adduct	Days necessary for pptn. to occur
Melamine/CH_2O	< 1 day
Benzoguanamine/CH_2O	< 1 day
Acetoguanamine/CH_2O	4 days
Propioguanamine/CH_2O	6 days
Butyroguanamine/CH_2O	3 days
Caprinoguanamine/CH_2O	< 1 day
CTU guanamine/CH_2O	< 1 day
CNG/CH_2O	6 days

Table 3.4 : Formaldehyde uptake by stabilizers in aqueous method of formaldehyde evaluation

Stabilizer	moles CH_2O/moles stabilizer	grams CH_2O/gram adduct
Melamine	5.04 ± 0.03	0.569 ± 0.002
Benzoguanamine	3.37 ± 0.03	0.373 ± 0.002
Acetoguanamine	1.68 ± 0.46	0.303 ± 0.058
Propioguanamine	1.96 ± 0.01	0.317 ± 0.001
Butyroguanamine	2.23 ± 0.19	0.334 ± 0.009
Caprinoguanamine	2.56 ± 0.35	0.264 ± 0.026
CTU guanamine	4.66 ± 0.35	0.261 ± 0.014
CNG	1.24 ± 0.12	0.328 ± 0.020

Table 3.5 : TGA weight losses for adducts obtained by aqueous method of stabilizer evaluation

Adduct	% mass lost at 210°C	% mass lost at 270°C
Melamine/CH_2O	20	32
Benzoguanamine/CH_2O	31	32
Acetoguanamine/CH_2O	44	47
Propioguanamine/CH_2O	42	45
Butyroguanamine/CH_2O	47	51
Caprinoguanamine/CH_2O	20	35
CTU guanamine/CH_2O	15	26
CNG/CH_2O	7	17

obtained by the aqueous and nonaqueous reaction systems are presented in Figures 3.20 and 3.21.

3-2d Discussion and conclusions

Solution phase investigations mainly reflect the inherent ability of the acceptors to react with formaldehyde. The acceptors studied by the aqueous method include CNG and six compounds structurally related to melamine. On a molar basis, the number of formaldehyde molecules reacted per acceptor molecule should be related to the number of amine groups available. Thus, melamine and CTU guanamine react with more formaldehyde molecules than butyroguanamine, for example. Based on this approach we would expect that benzoguanamine and butyroguanamine, having equal number of amine groups available, should react with equal amounts of formaldehyde. Experimentally, it is learned that benzoguanamine is more reactive towards formaldehyde than butyroguanamine, as well as aceto-, propio-, and caprinoguanamine. These observations may be related to electron density of the amino groups and the solubility of the acceptors and adducts, among other factors.

It was observed that each stabilizer gave a clear solution when reacted with aqueous formaldehyde at 60°C. This indicates that water soluble-adducts were formed. Adducts precipitated over various periods of time depending on the acceptor, when allowed to stand at room temperature. All of the isolated products can be redissolved in hot water. Two of the factors influencing the time necessary for precipitation are the symmetry of the adduct's molecular structure and

the adduct's hydrophobicity.

In the case of melamine, the adducts should be relatively symmetrical and should fit well into the crystal lattice. The caprinoguanamine adduct, though less symmetric, did not remain in solution when cooled because of its large aliphatic substituent. Other adducts are effected by these factors to different degrees. For instance, acetoguanamine is more symmetrical than butyroguanamine, yet its adduct takes longer to precipitate. Here, perhaps, the hydrophobicity acted as a more important factor.

When an amine group in melamine is replaced by an alkyl substituent, the number of formaldehyde molecules lowered from five for the parent molecule to ca. two (see Table 3.5). However, when the substituent group is a benzene ring, the number of formaldehyde units reacted is three. The higher efficiency for benzoguanamine may be caused by its electronic structure, which is markedly different from the alkyl groups. Resonance from the benzene ring may serve to be electron donating than the alkyl groups, and may activate the amines toward reaction with formaldehyde.

The series of TGA experiments reflects the stability of the adducts once formed. There exists an equilibrium for each acceptor-adduct system :

$$\text{Acceptor} + CH_2O \rightleftharpoons \text{Adduct}$$

It is desirable to find a system whose equilibrium favors the formation of the adduct at high temperatures (i.e. 210°C). The TGA thermogram indicates that acetoguanamine, propioguanamine and butyroguanamine (see

Figure 3.11) each lose all of their formaldehyde between the temperatures of 150-180°C and are not suitable for stabilizing acetal copolymers. Caprinoguanamine also seems to be unsuitable because it not only gives up its formaldehyde before 210°C, but also appears to decompose further. The yellowish color of the acceptor and the adduct also make it an unlikely candidate for stabilization. The adduct of CTU guanamine begins to show weight loss at 150°C. At 210 C it releases one-half of its bound formaldehyde. Its performance is at the same level as melamine. The weight loss between 60 and 90°C for the CTU guanamine adduct is, perhaps, caused by degradation of the acceptor itself (see Figure 3.12). Based on thermal analysis, the most efficient acceptors in the melamine series rank as follows: melamine > CTU guanamine > benzoguanamine. The acceptor CNG, not directly related to the melamine series, shows the best performance. When evaluating thermograms, consideration must be given to the amount of bound formaldehyde as well as the the amount lost on heating.

The ^1H NMR spectra presented in Figures 3.13 and 3.14 indicate that only one of the two amide containing stabilizers reacted with formaldehyde. It can be seen in Figure 3.13A that there is neither a decrease in the ratio of the areas of the H_{amide} to H_{methyl} signals (as compared to Figure 3.13B) nor is any new signal observed. These observations suggest that the amide groups of triacetyl melamine were not reactive towards CH_2O under experimental conditions.

TGA thermograms similarly indicate that there is no difference between triacetyl melamine before and after exposure to formaldehyde

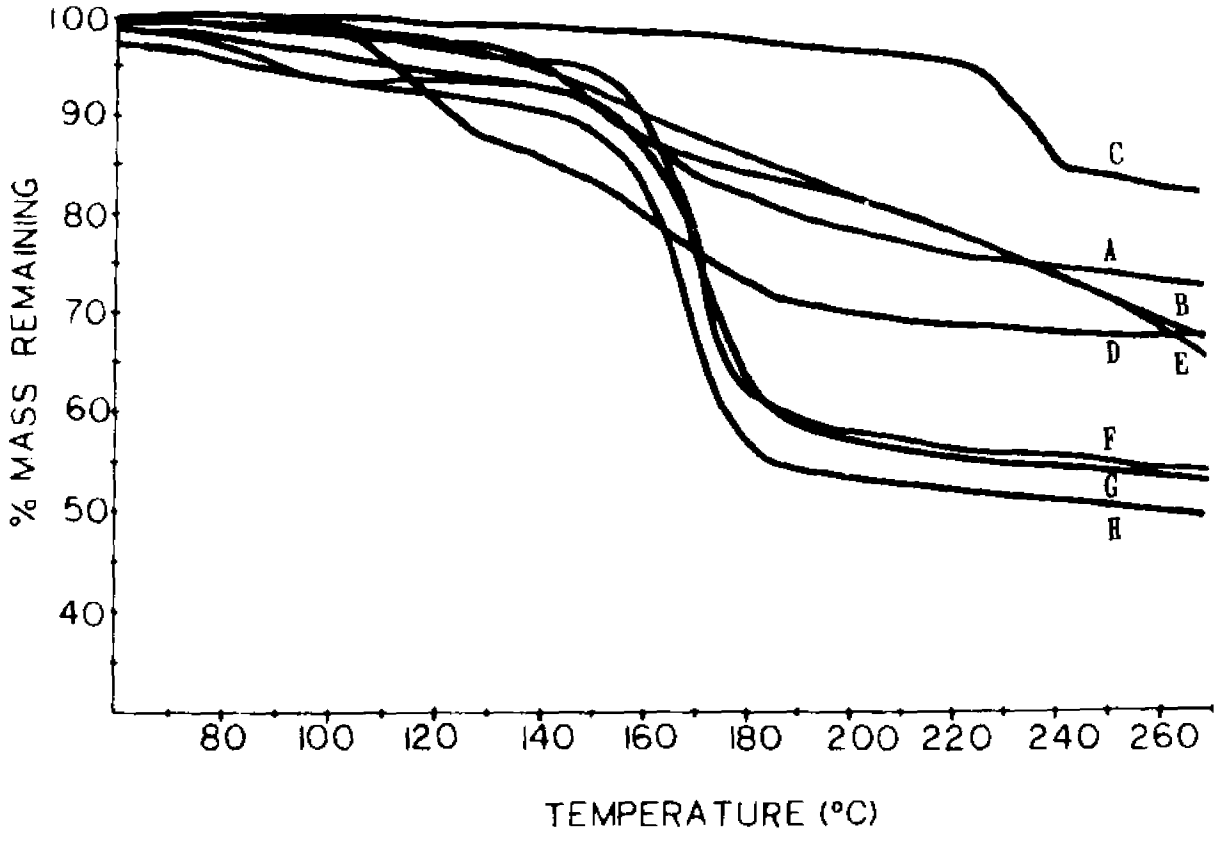

Figure 3.11

TGA thermograms of water soluble stabilizers after exposure to formaldehyde. (heating rate = 10°C/min)

A : CTU guanamine
B : melamine
C : cyanoguanamine
D : benzoguanamine
E : caprinoguanamine
F : propioguanamine
G : acetoguanamine
H : butyroguanamine

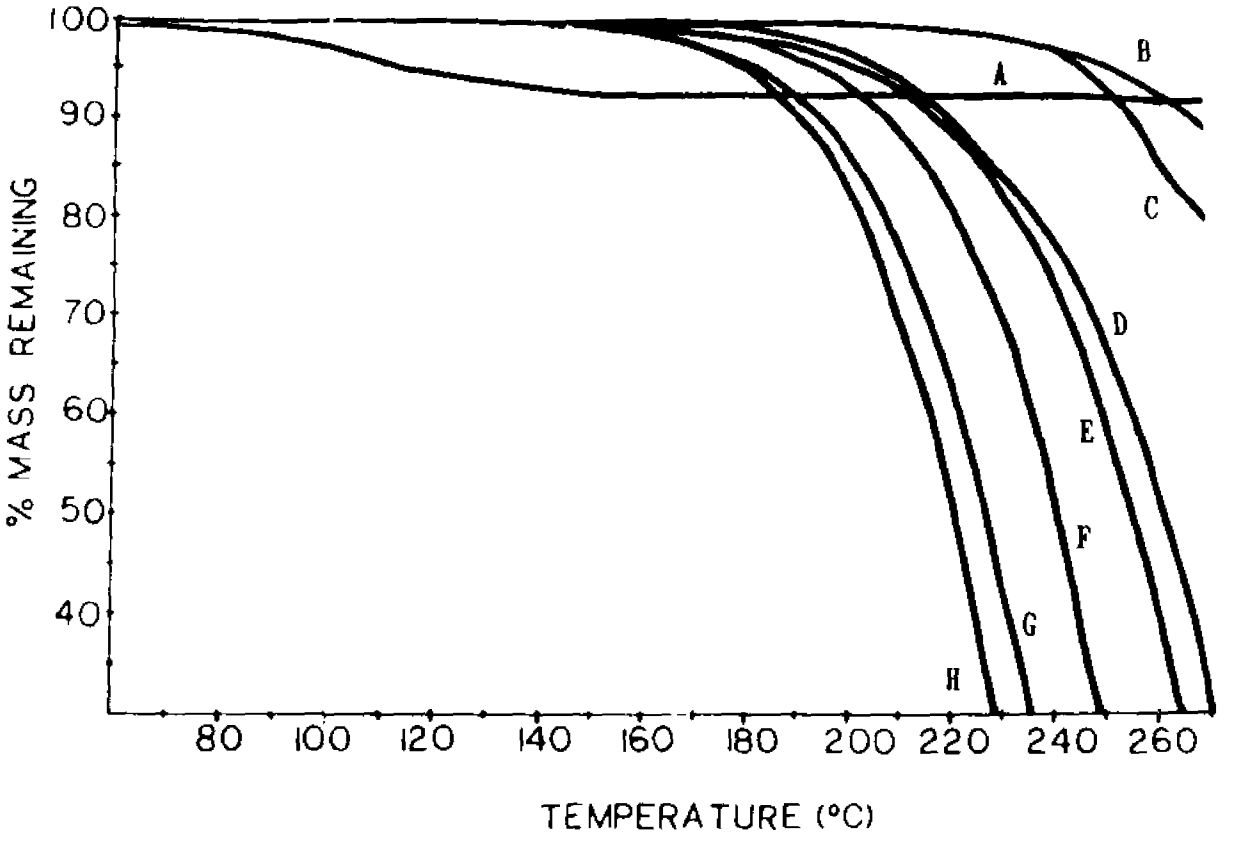

Figure 3.12

TGA thermograms of water soluble stabilizers before exposure to formaldehyde. (heating rate = 10°C/min)

A : CTU guanamine
B : melamine
C : cyanoguanamine
D : benzoguanamine
E : caprinoguanamine
F : propioguanamine
G : acetoguanamine
H : butyroguanamine

(see Figure 3.15). The weight loss that occurs at approximately 100°C is attributed to loss of water not removed on vacuum drying.

In sharp contrast to triacetyl melamine, diacetyl melamine shows a marked change in its ^1H NMR spectrum after exposure to formaldehyde Figure 3.14). First, one observes a significant decrease in the ratio of the H_{amine} to H_{methyl} peak areas. Second, new signals appear in the region of 4.5-5.5 ppm. These signals are assigned to aminomethylol groups ($-NH-CH_2OH$) generated by reaction of formaldehyde with the amine group. As was observed for diacetyl melamine, the amide groups does not appear to be reactive towards formaldehyde. Comparison of the area of the methylol $C\underline{H}_2$ signal (3 units) to the acetyl $C\underline{H}_3$ signal (6 units), reveals that approximately 1.5 moles of formaldehyde reacted with each mole of diacetyl melamine. This corresponds to 0.18 g CH_2O per gram of stabilizer.

The TGA thermograms of diacetyl melamine and its formaldehyde adduct also show a striking difference. The unreacted stabilizer begins to lose mass at 240°C, whereas the dried adduct shows two regions of mass loss (see Figure 3.16). A mass loss of approximately 4% was caused by water loss between 100 and 110°C. A mass loss of approximately 20% due to another species, presumably formaldehyde, occurs between 130 and 170°C. This 20% mass loss is consistent with the loss of 1.5 methylol units per molecule of diacetyl melamine and supports the value obtained by NMR analysis.

Based on NMR and thermal analysis it is concluded that each mole of diacetyl melamine reacts with 1.5 mole of formaldehyde and loses all bound formaldehyde at temperatures lower than 170°C.

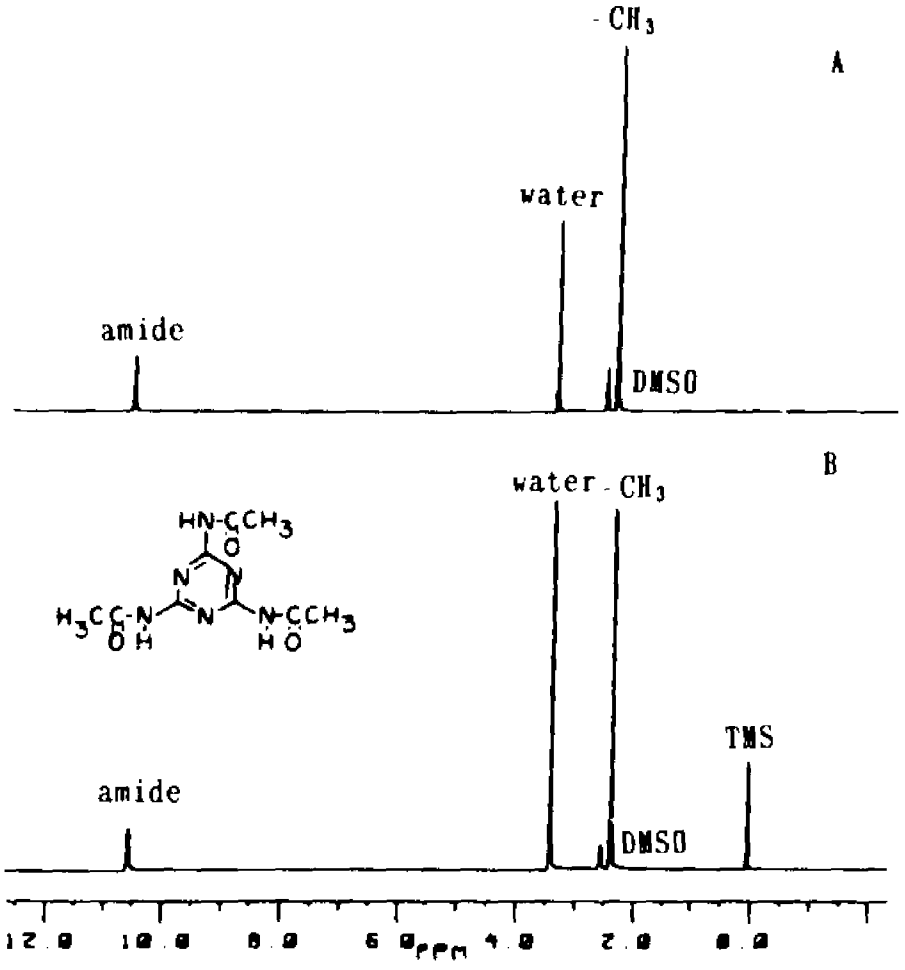

Figure 3.13

^{1}H NMR spectra of triacetylmelamine (DMSO-d_6, 25°C)

A : after exposure to formaldehyde
B : before exposure to formaldehyde

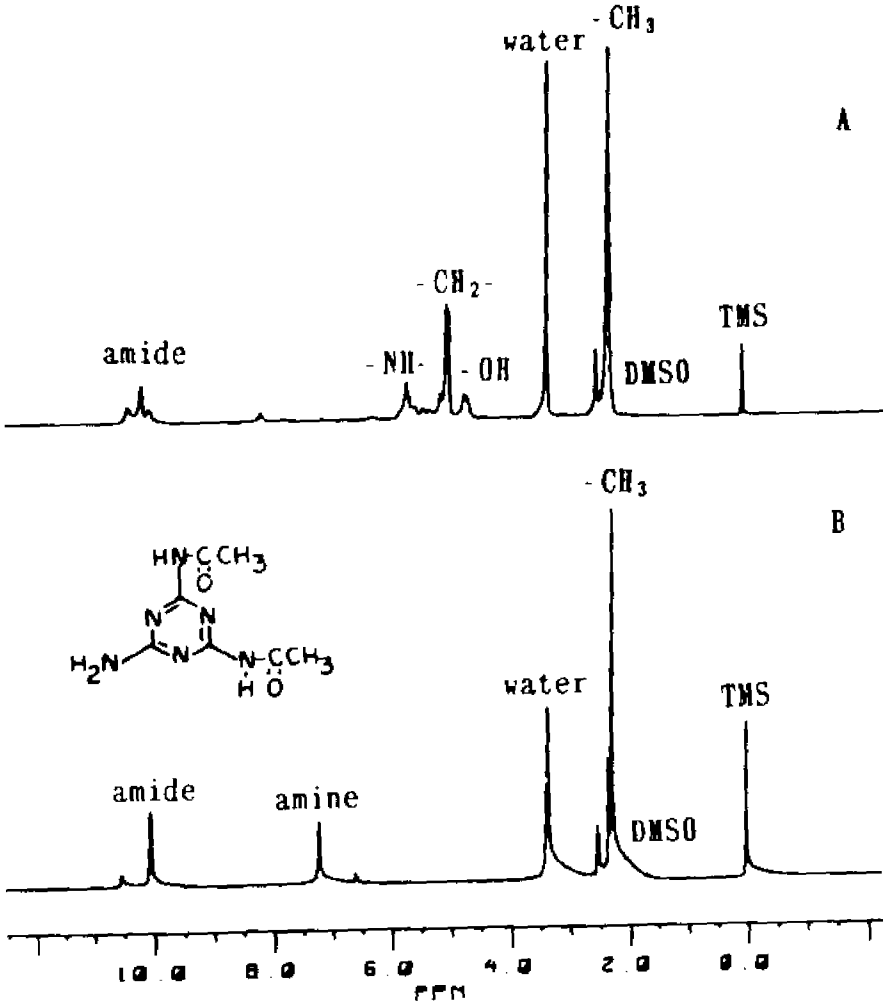

Figure 3.14

^{1}H NMR spectra of diacetylmelamine (DMSO-d_6, 25°C)

A : after exposure to formaldehyde
B : before exposure to formaldehyde

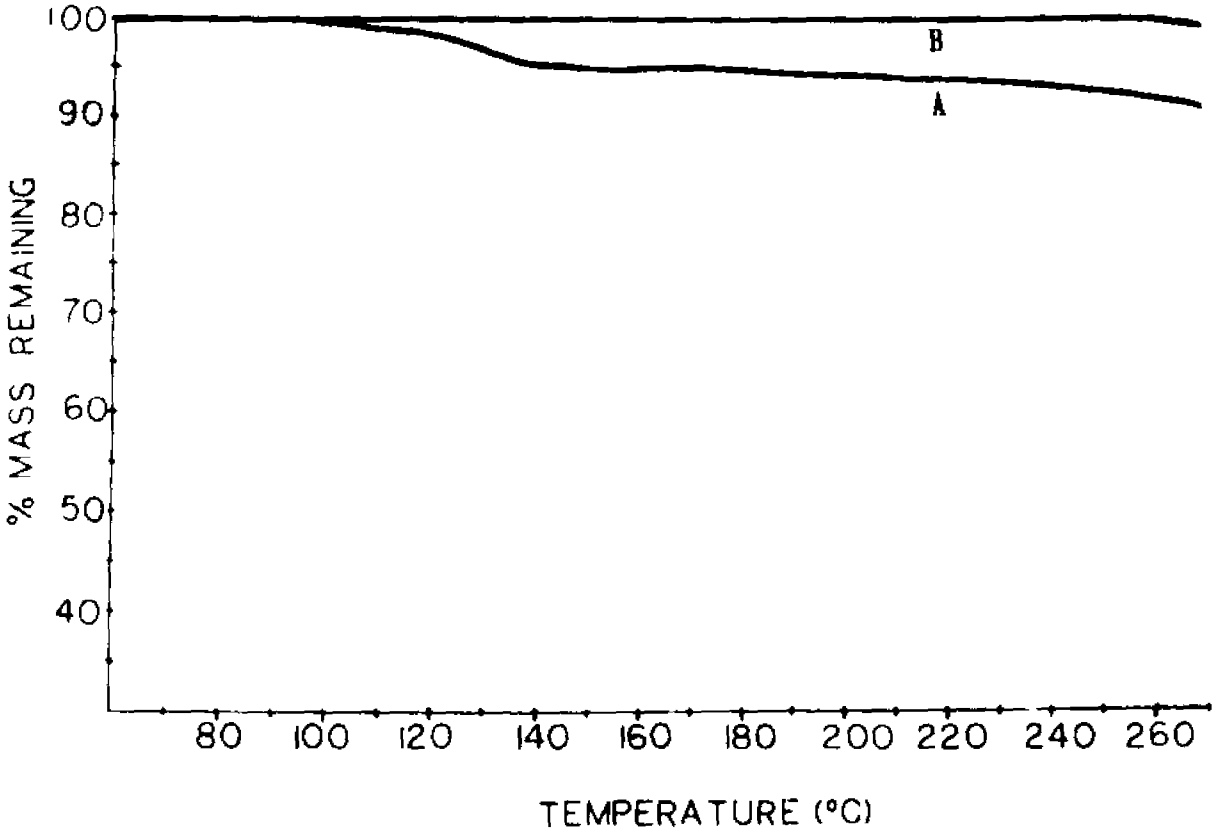

Figure 3.15

TGA thermogram of triacetyl melamine (heating rate = 10°C/min)

A : after exposure to formaldehyde
B : before exposure to formaldehyde

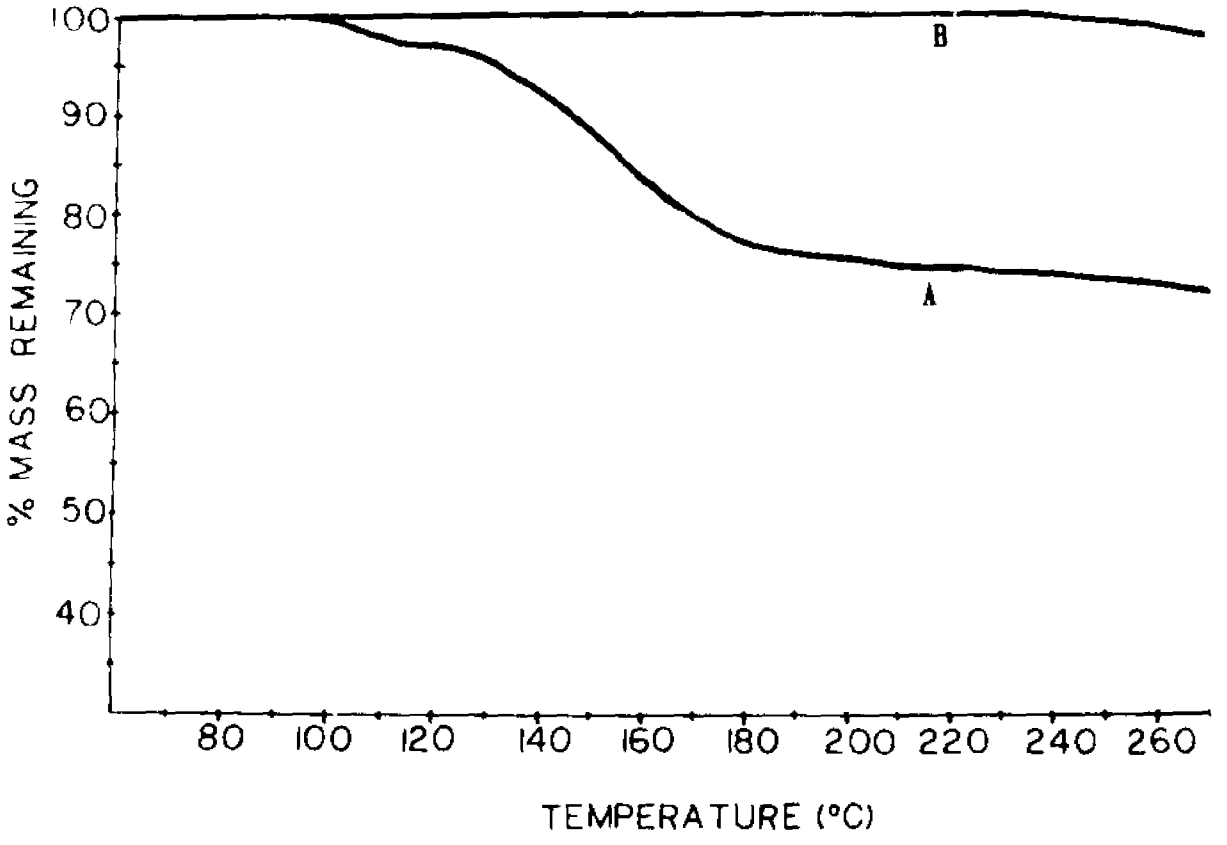

Figure 3.16

TGA thermogram of diacetyl melamine (heating rate = 10°C/min)

A : after exposure to formaldehyde
B : before exposure to formaldehyde

The ^{1}H NMR spectra for propioguanamine and benzoguanamine before and after exposure to formaldehyde via the nonaqueous method, are given in Figures 3.17 and 3.18. These spectra indicate that the experimental conditions are conducive to reaction with formaldehyde. This is evidenced by the absence of the primary amine signal and the presence of aminomethylol signals in both "after exposure" spectra. Semiquantitative determination of the amount of formaldehyde reacted with each stabilizer was accomplished by comparison of the area of the aminomethylol $C\underline{H}_2$ proton signal with those of the alkyl or aromatic proton signals for propioguanamine and benzoguanamine respectively. The ^{1}H NMR spectra obtained after exposure to formaldehyde indicates that approximately 2 moles of CH_2O react with each mole of propioguanamine, and that approximate 3 mole react with each mole of benzoguanamine.

The splittings in Figure 3.18A are attributable to various hydrogen bondings e.g. aminomethylol $-O\underline{H}$ with ring nitrogen:

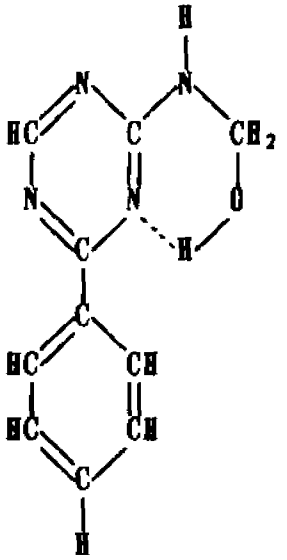

At higher temperatures, molecular motion increases and these interactions decrease. The absence of splittings is clearly demonstrated in Figure 3.19 which gives the ^1H NMR spectra of the benzoguanamine/CH_2O adduct at room temperature and at 60°C.

TGA thermograms support the NMR results and confirm that the above described method is comparable to the previous method. Figures 3.20 and 3.21 show comparisons of thermograms for propioguanamine and benzoguanamine adducts obtained by both methods. Within experimental error, the results are equivalent.

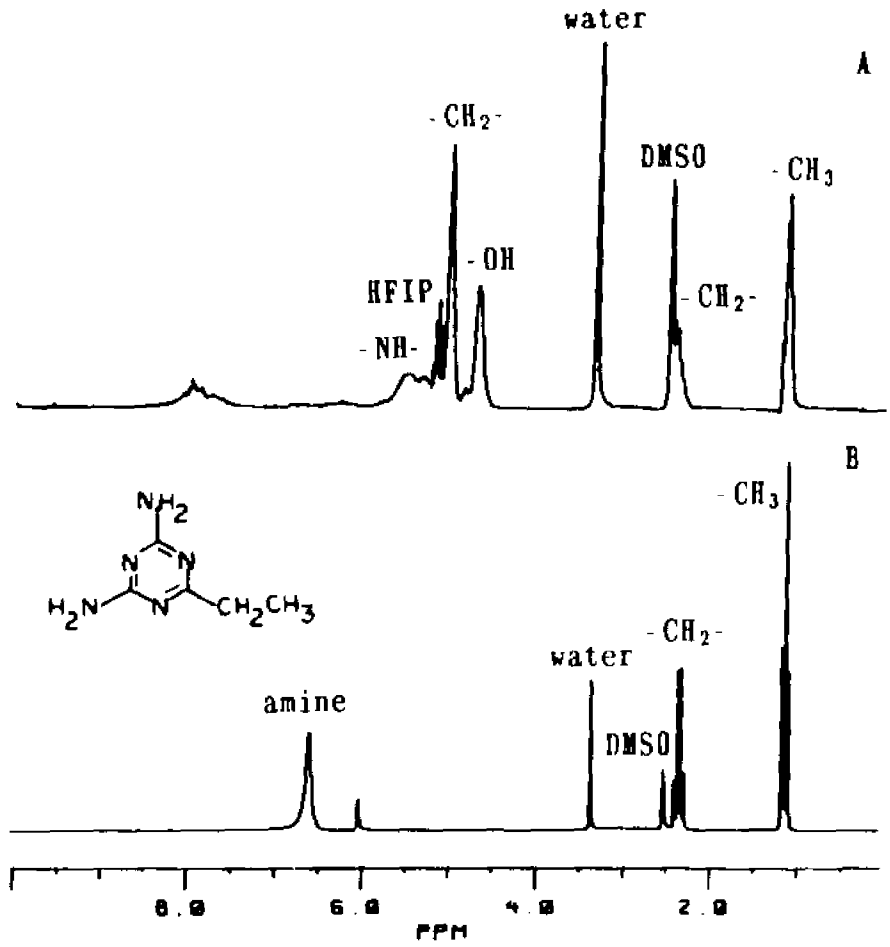

Figure 3.17

^{1}H NMR spectra of propioguanamine (DMSO-d_6, 25°C)

A : after exposure to formaldehyde
B : before exposure to formaldehyde

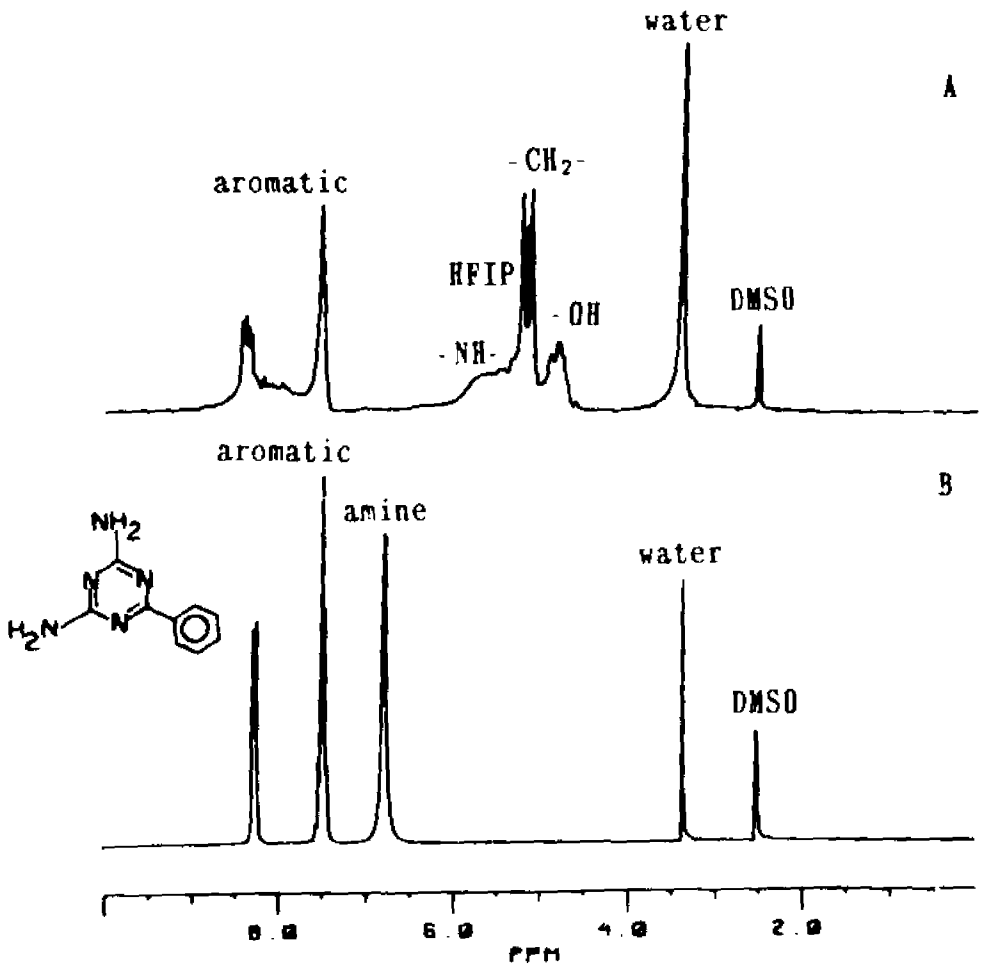

Figure 3.18

^{1}H NMR spectra of benzoguanamine (DMSO-d_6, 25°C)

A : after exposure to formaldehyde
B : before exposure to formaldehyde

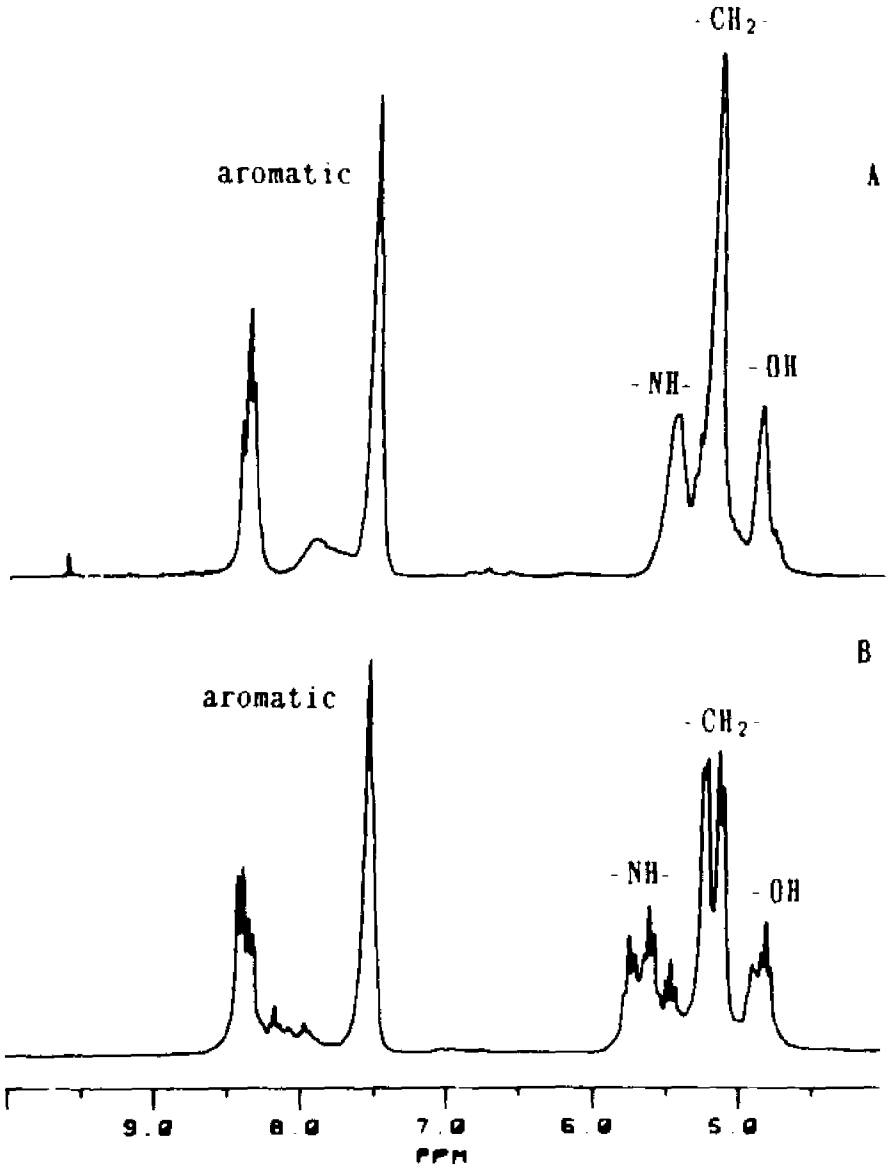

Figure 3.19

^{1}H NMR spectra of benzoguanamine after exposure to formaldehyde (DMSO-d_6, 126°C)

A : spectrum obtained at 60°C
B : spectrum obtained at 25°C

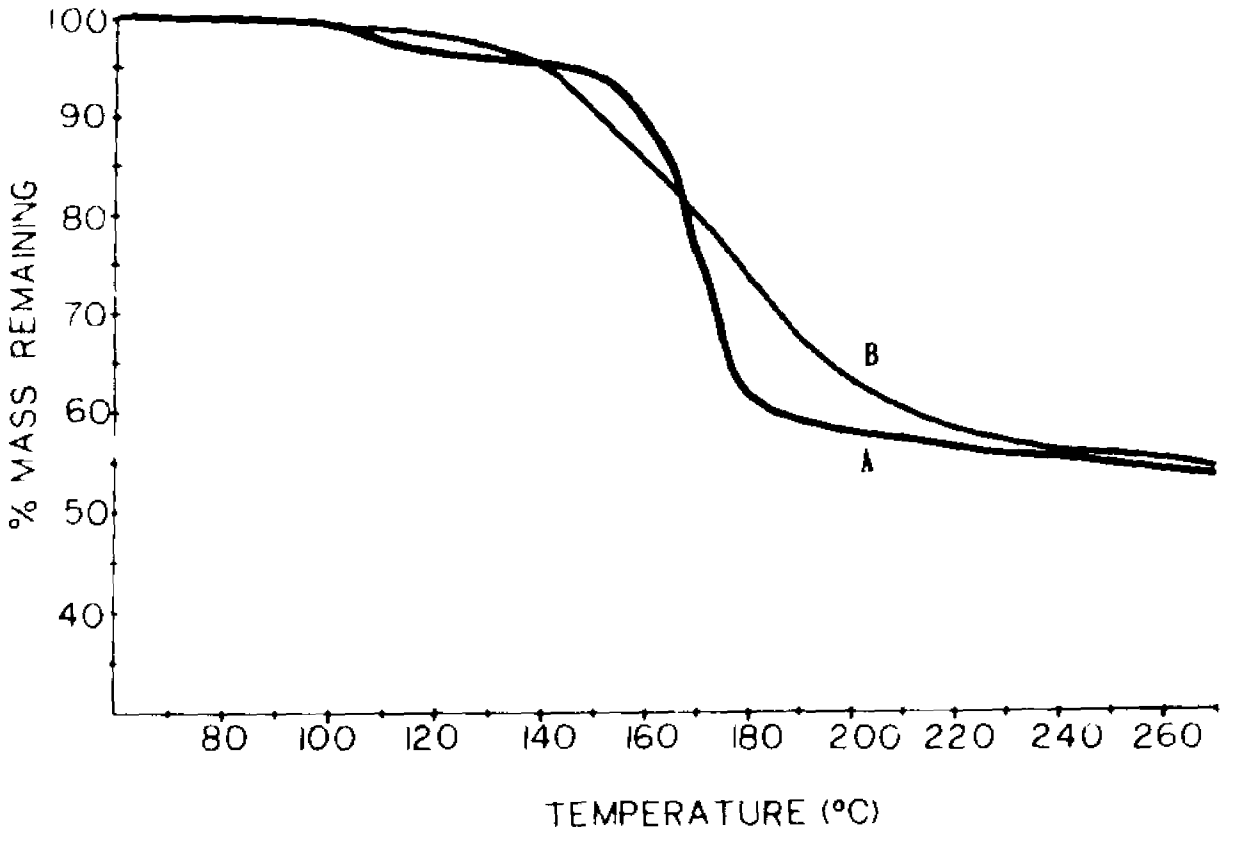

Figure 3.20

TGA thermogram of propioguanamine (heating rate = 10°C/min)

A : adduct obtained from aqueous evaluation method
B : adduct obtained from non-aqueous evaluation method

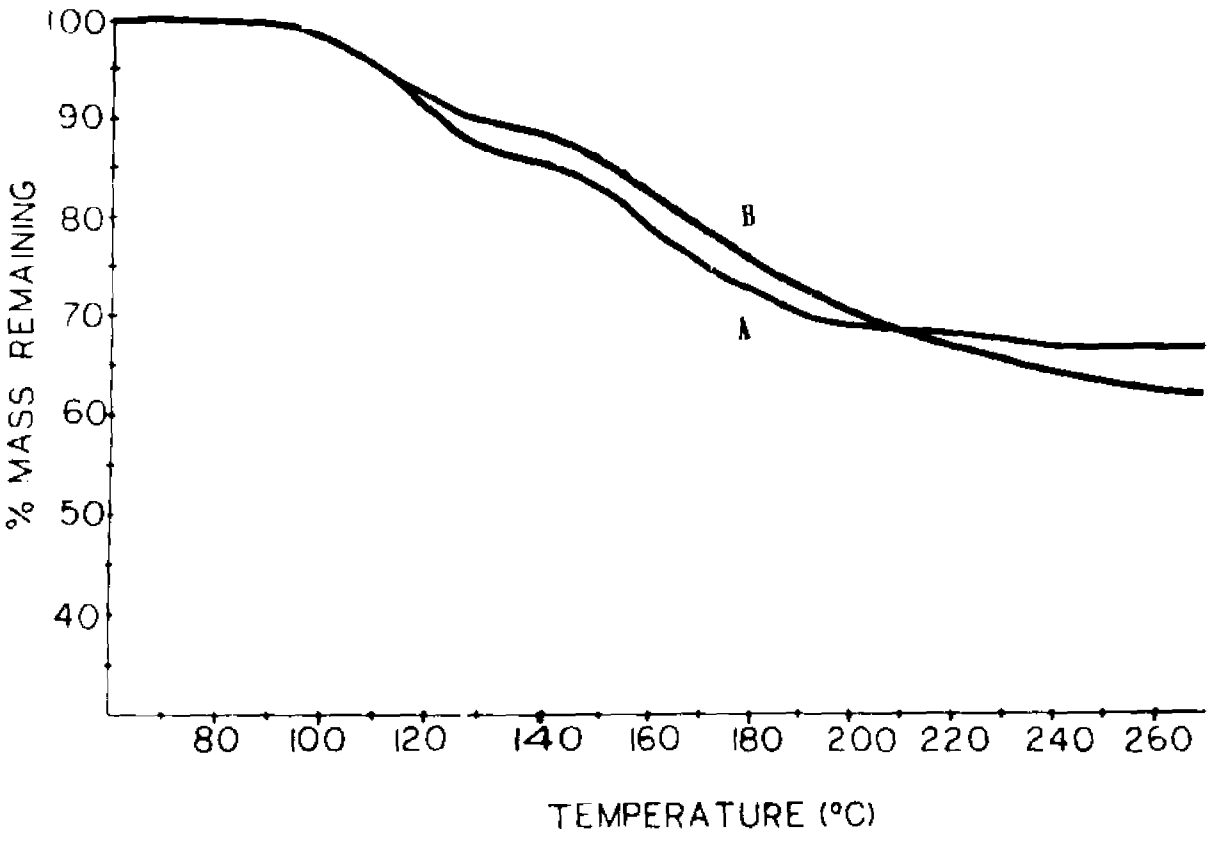

Figure 3.21

TGA thermogram of benzoguanamine (heating rate = 10°C/min)

A : adduct obtained from aqueous evaluation method
B : adduct obtained from non-aqueous evaluation method

4 POLYACETAL STABILIZATION BY COPOLYMERIZATION

4-1 Trioxane - (1,3-dioxep-5-ene) Copolymers

4-1a Summary

The preparation of polyacetal copolymers with backbone double bonds through the cationic copolymerization of trioxane, TX, with 1,3-dioxep-5-ene, DIPE, has been demonstrated recently (20,21,22).

1,3-dioxep-5-ene (DIPE)

We report here the first systematic detailed investigation of the copolymerization system, including studies of copolymer structure and properties. The resulting polymer can be considered as an acetal copolymer with methylene oxide, $-CH_2O-$, and 1-oxy-2-butene, $-O-CH_2CH=CHCH_2-$, comonomer units. The relationship between feed ratio and copolymer composition, end groups, thermal stability and crystallinity of the final product, obtained through base catalyzed hydrolysis of the nascent copolymer, have been established in the present work. The copolymer, compared to the trioxane-ethylene oxide copolymer, was demonstrated to show far better stability against degradation by bromine. Modifications of the copolymer backbone double bond, including grafting, epoxidation and incorporation of a urea group, are also reported.

4-1b Experimental

4-1b-1 Synthesis

The comonomer, 1,3-dioxep-5-ene, was synthesized through an acid catalyzed reaction of *cis*-2-butene-1,4-diol with paraformaldehyde based on a reported procedure (30,31). Trioxane was purified by distillation from sodium metal before use.

Copolymerization of trioxane with 1,3-dioxep-5-ene, DIPE, was carried out as follows: A dry test tube (25 X 150 mm) was charged with 18 grams of trioxane and the desired amount of DIPE. The tube was then capped with a serum stopper, purged with nitrogen and evacuated. The contents of the tube were brought to a temperature of 65°C. Then, the required amount of boron trifluoride etherate was injected through the serum stopper into the completely melted mixture. A typical amount of initiator was 2 μL for a total comonomer charge of 20 grams. After addition of the initiator, the colorless mixture became yellow, then green and finally brown. The polymerization was allowed to proceed at 60°C for 20 hours. At the conclusion of the polymerization, the polymer was removed and pulverized in a Waring blendor. The crude polymer was then stirred in 60 mL of methanol containing 1% triethanolamine, TEA, for one hour and then collected by filtration. The typical product yield was about 80%. Unstable end groups were removed by base hydrolysis through the procedure described below.

The crude polymer (16 g), dimethylformamide (120 mL), benzyl alcohol (120 mL) and TEA (1% of total volume) were placed in a 500 mL, two-necked round bottom flask fitted with a thermometer and an

air-cooled, straight-through condenser. The mixture was heated and stirred at 160-170°C to dissolve the solid. The contents were maintained at refluxing conditions until evolution of formaldehyde was no longer visible. The polymer solution was cooled to room temperature and the solid polymer was removed and washed with acetone three times. The polymer was then filtered and dried under vacuum at 40°C. The yield was about 60%.

4-1b-2 Copolymer modifications

4-1b-2a Copolymer grafting

A demonstration of the modification of the trioxane-DXPE copolymer through grafting with sodium acrylate, was performed as follows. A 12 X 75 mm test tube was charged with 10 mg copolymer sample (finely powdered), 5 mg sodium acrylate (Polyscience) and 0.5 mg Luperox (2,5-dihydroperoxy- 2,5-dimethylhexane) (Penwalt Corp.). One mL of a deaerated HFIP solution containing 0.03 mL TEPA (tetraethylenepentamine) per mL was then added to the test tube. The contents of the tubes were stirred with small magnetic stirrers and heated in a 55°C water bath. After one hour the samples were removed from the water bath. At that time, 4 mL of distilled water were added to each tube to precipitate the copolymers and to remove any unbound acrylate. The contents of each tube were then centrifuged and washed repeatedly with water and acetone.

Dye treatment was achieved by adding several drops of concentrated aqueous methylene blue to samples test tubes which contained the washed grafted copolymer and 4 mL of distilled water (pH adjusted to 9.5 with

NaOH). The samples were then stirred magnetically for several hours. Treated samples were then repeatedly washed with acetone and water. The relative color intensities of the samples were then observed.

4-1b-2b Epoxidized copolymers (30,31,32)

Epoxidized copolymer was obtained as follows. A dry 100 mL round bottom flask was charged with 0.6 g of copolymer (4 mole percent comonomer incorporation) and 40 mL of dimethylformamide (DMF). The contents were stirred magnetically and heated to 130°C in order to dissolve the solid. The polymer solution gelled after cooling in an ice bath. 3-Chloroperoxybenzoic acid (0.1g) dissolved in 20 mL of DMF was then added to the gelled mixture. The stirred mixture was allowed to reacted for six hours at 0-5°C under an inert atmosphere. A white precipitate (m-chlorobenzoic acid) began to separate from the reaction mixture after about thirty minutes. The reaction continued to proceed overnight at room temperature. The cooled mixture was poured into 100 mL of water. The polymer was then collected by filtration and washed once with 5% aqueous sodium bicarbonate and three times with hot water. The polymer was dried at 40°C under vacuum for 4 hours. The yield was approximately 0.5 grams.

3-1b-2c Incorporation of urea functional group (30,33,34,35)

Surface modification of the copolymer was achieved by reaction of 0.5 g copolymer (4 mole percent comonomer incorporation) with 50 mL of a preformed iodine isocyanate solution. A preformed solution of iodine isocyanate, rather than a mixture of iodine and silver cyanate, was

used to facilitate purification of the product. Since the copolymer does not dissolve in acetonitrile, it remains a solid throughout the reaction and is difficult to separate from the nonreactive inorganic salts. The copolymer/isocyananate mixture was allowed to react overnight at room temperature, under an inert atmosphere. Upon termination of the reaction, the copolymer was collected by filtration and washed with acetonitrile to remove unreacted iodine isocyanate. The product was then dried under vacuum to remove remaining solvent.

Further modification of the isocyanate group was achieved by passing excess anhydrous ammonia through 50 mL of acetonitrile containing the modified copolymer. The product was again filtered and washed with acetonitrile.

A modified DXPE ring monomer was also prepared as a suitable model compound for NMR analysis. This was done by reacting 0.02 moles of 1,3-dioxepene, dissolved in 50 mL of acetonitrile, with 5 g (0.02 mole) of iodine and excess silver cyanate (6 g, 0.04 mole). The solution was allowed to react for one hour under an inert atmosphere. After one hour, the reaction mixture was filtered to remove inorganic salts The remaining solution was then reacted with anhydrous ammonia. The brown color of the mixture was observed to dissappear after several minutes. The solid product obtained was then washed with acetonitrile to remove unreacted iodine isocyanate. Solvent was evaporated by means of a rotary evaporater.

4-1b-3 NMR analysis

Proton and carbon-13 NMR spectra were obtained on an IBM WP-200 SY

FT NMR spectrometer. For unmodified copolymer samples, the solvent used was perdeuterated dimethylsulfoxide, DMSO-d_6. The temperature of measurement was 126°C. For quantitative NMR measurement, sufficient relaxation times were used to insure that all protons were completely relaxed. Pulse angle of 26° and relaxation time of 20 seconds were typical for quantitative determinations. Further increase in relaxation time did not lead to change in quantitative results. Integration of area of absorption peaks was carried out using Bruker software provided. Solid state spectra were obtained using magic angle spinning and cross polarization. Signals labelled "SSB" are spinning side bands.

4-1b-4 Thermal analysis

4-1b-4a DSC determination of heat of fusion, ΔH_f, and percent crystallinity

Samples of copolymers, ranging in mass from 2 mg to 4 mg, were analyzed using a DuPont 990 thermal analyzer with a DSC cell. The samples were heated rapidly to a temperature of 120°C and then further heated at a rate of 10°C/minute. The time base setting was 0.25 min/cm. Samples were heated until they melted. Immediately after melting, the heater was turned off and the samples were allowed to slowly cool. No cooling accessory was used. The melt crystallized samples were again quickly reheated to 120°C and then further heated at 10°C/min until they melted for a second time.

Samples were reweighed after analysis to determine whether any of

the sample had volatilized and escaped from the DSC pan during the analysis.

Heat of fusion, ΔH_f, was calculated by the time base method, using a weighed indium sample as standard. Percent crystallinity was based on a ΔH_f equal to 58.7 cal/g for 100% crystallinity (19). The effect of comonomer units on ΔH_f was assumed to be negligible.

ΔH_f was calculated according to the following formula:

$$\Delta H_f = (A/m)\ 60\ B\ E\ qs$$

where A = peak area in cm^2

m = sample mass in mg

B = time base setting in min/cm (0.25 min/cm)

E = calibration coefficient in mV/mV
(0.20529 mV/mV based on indium standard)

ΔH_f = heat of fusion in mcal/mg

qs = Y-axis sensitivity setting (5 mV/cm)

giving:

$$\Delta H_f = \frac{\text{area } cm^2}{\text{mass mg}} \times \frac{60 \text{ sec}}{\text{min}} \times \frac{0.25 \text{ min}}{\text{cm}} \times \frac{0.20529 \text{ mV}}{\text{mV}} \times \frac{5 \text{ mV}}{\text{cm}} \times \frac{1 \text{ mcal}}{4.18 \text{ mJ}}$$

Percent crystallinity was calculated by the following formula:

$$\% \text{ crystallinity} = \frac{\Delta H_f}{\Delta H_f^*} \times 100\%$$

where ΔH_f^* is the ΔH_f of a hypothetical 100% crystalline sample (58.7 mcal/mg)

4-1b-4b Thermogravimetric analysis

TGA thermograms were obtained under a nitrogen atmosphere with a heating rate of 10°C/min. See Section 3-2b-2 for additional conditions.

4-1b-4b Bromine resistance test

Copolymer samples at a concentration of 0.2 % (wt/wt) were prepared by dissolving 31.9 mg of polymer (TX-EO or TX-DXPE with 2 mole % comonomer incorporation) in 10.00 mL of hexafluoroisopropanol (HFIP, ρ=1.506 g/mL) obtained from Aldrich Chemical Company and distilled before use. Using a 10 μL syringe, 10.00 μL of a 3 X 10^{-2} M bromine solution were added to these copolymer solutions. The bromine solution was prepared by dissolving 1.5 μL of bromine (dispensed from a 2 μL syringe) in 1.00 mL HFIP. The samples were quickly mixed and then introduced directly into a Ubbelohde viscometer. The temperature of measurement was 25°C. Reduced viscosities were calculated using a predetermined solvent flow time of 128.0 seconds according to the formula:

$$\eta_{red} = \frac{\eta_{sp}}{c} = \frac{(t/t_o) - 1}{c} = \frac{(t/128) - 1}{0.319\ g/dL}$$

4-1c Results and conclusions

4-1c-1 Copolymer structure

Figure 4.1 illustrates details of copolymer stucture revealed by proton NMR spectra. The singlet, S, represents the methylene oxide units from TX; the doublet, D, proton next to the double bond in the DXPE unit; and the triplet, T, protons on the carbon atoms of the

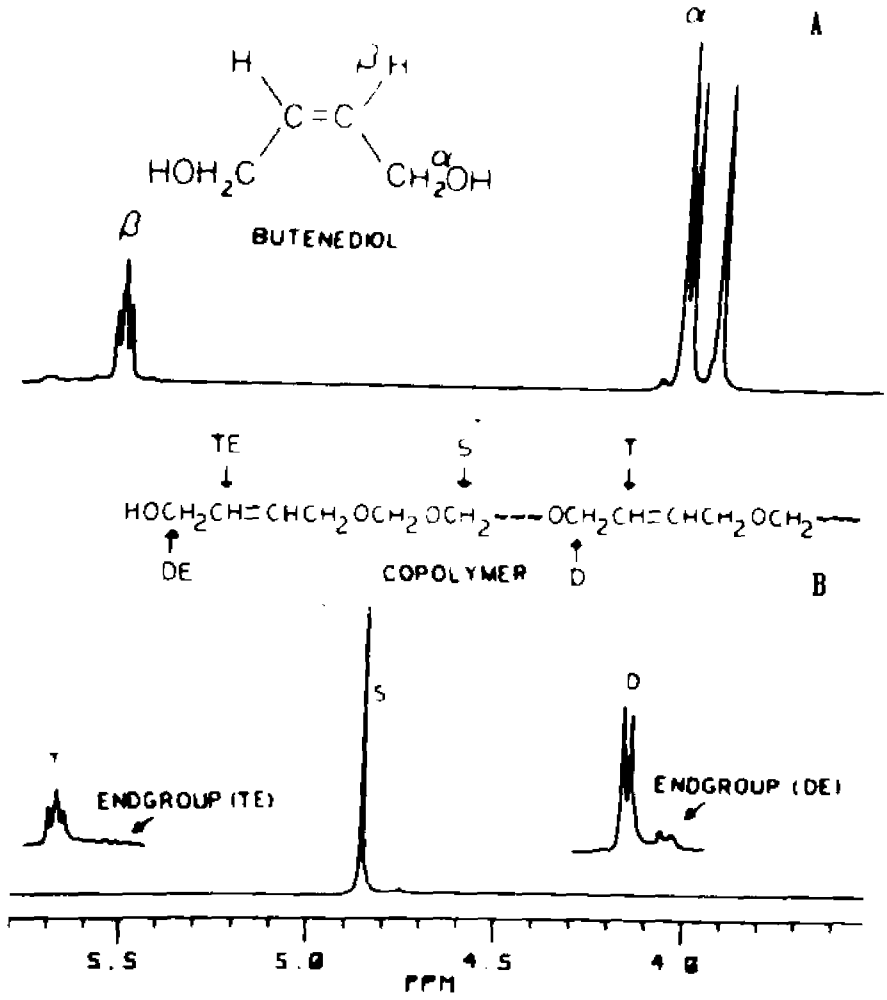

Figure 4.1

^{1}H NMR spectra (DMSO-d_6, 126°C)

A : *cis*-2-butene-1,4-diol
B : trioxane-1,3-dioxep-5-ene copolymer

double bond. Comparing the copolymer spectrum with that of the *cis*-1,4-butenediol, one can clearly identify the end group signals, DE and TE. The absorption peaks, TE, cannot be due to *trans*-double bonds, since a *trans* configuration would lead to a downfield shift from T (37). The integral of copolymer absorption peaks can be used to calculate the number average degree of polymerization, $\overline{DP}_n$, and mole percent incorporation:

$$\overline{DP}_n = \frac{S + (D/2) + (DE/2)}{(DE/2)} \quad \text{(Assuming 2 end groups per chain)}$$

$$\text{Mole \% DIPE incorporated in the copolymer} = \frac{(D/2) + (DE/2)}{S + (D/2) + (DE/2)} \times 100\%$$

All expressions of mole percent are based on formaldehyde, CH_2O, as a comonomer unit although trioxane was used in the feed. The relationship, D = 2T, serves as verification for internal consistency. There are a number of small absorption peaks around the main peak for CH_2O, S. These are due to methylene oxide units next to comonomer units and reflect comonomer sequence distribution.

Table 4.1 summarizes the values calculated for the DIPE incorporation in mole percent.

The comonomer DIPE is much less reactive than trioxane. For feeds above 6.8% DIPE, copolymerization was not observed. The comonomer forms a complex with BF_3 as evidenced by the appearance of a brownish color.

As expected, the number average degree of polymerization, $\overline{DP}_n$ is dependent on the initiator to comonomer concentration ratio. A $\overline{DP}_n$ of 2×10^3, i.e. $\overline{M}_n = 6 \times 10^4$, was obtained for copolymerization of 19

Table 4.1 : Mole percent feed and incorporation for copolymers of trioxane and 1,3-dioxep-5-ene

Sample #	% DXPE in Feed	% DXPE Incorporated
17,18,21	1.5	1.8 ± 0.2
19,20	3.2	2.4 ± 0.1
11,13	6.8	3.9 ± 0.5

Table 4.2 : Heat of fusion and percent crystallinity for acetal copolymers

Sample number	% DXPE (by NMR)	First Heating ΔH_f (mcal/mg)	% Cryst.	Second Heating ΔH_f (mcal/mg)	% Cryst.
17	1.8 ± 0.2	41 ± 4	70 ± 6	31 ± 2	53 ± 3
20	2.4 ± 0.1	38 ± 6	64 ± 10	30 ± 1	52 ± 1
11	3.9 ± 0.5	34 ± 2	57 ± 4	27 ± 1	47 ± 1
TX-EO copolymer	1.4	35 ± 3	60 ± 5	29 ± 3	50 ± 5

grams of TX with 1 gram of DIPE initiated by 2 μL of BF_3 etherate. A viscosity average molecular weight, M_v, of 8 X 10^4 was obtained based on a GPC calibration curve determined through differential viscosity data. This result further buttresses our ^1H NMR assignments for end groups.

4-1c-2 Properties

The TX-DIPE copolymer with a 1.8% by mole incorporation of double bond shows thermal stability comparable to that of polyacetal copolymer with the same level of ethylene oxide incorporation (Figure 4.2). Thus the comonomer unit functions efficiently as a stopper against unzipping.

Comparison of sample mass before and after DSC determination indicates no mass lost during the analysis. It was also observed that the calculated percent crystallinity was higher for the samples' first heating (solution crystallization) than for their second heating (melt crystallization). Apparently, a greater degree of crystallinity was achieved from solution than from the melt.

The calculated percent crystallinity and heats of fusion, ΔH_f, are presented in Table 4.2.

The results presented in the table above indicates that all of the copolymer samples analyzed show crystallinity within a narrow range of values and have crystallinity comparable to that of corresponding trioxane-ethylene oxide copolymers.

Although exact melting points of the TX-DIPE copolymers have not been determined, it has been observed that the onset of melting, as well as the temperature of the melting endotherm minimum, decrease as

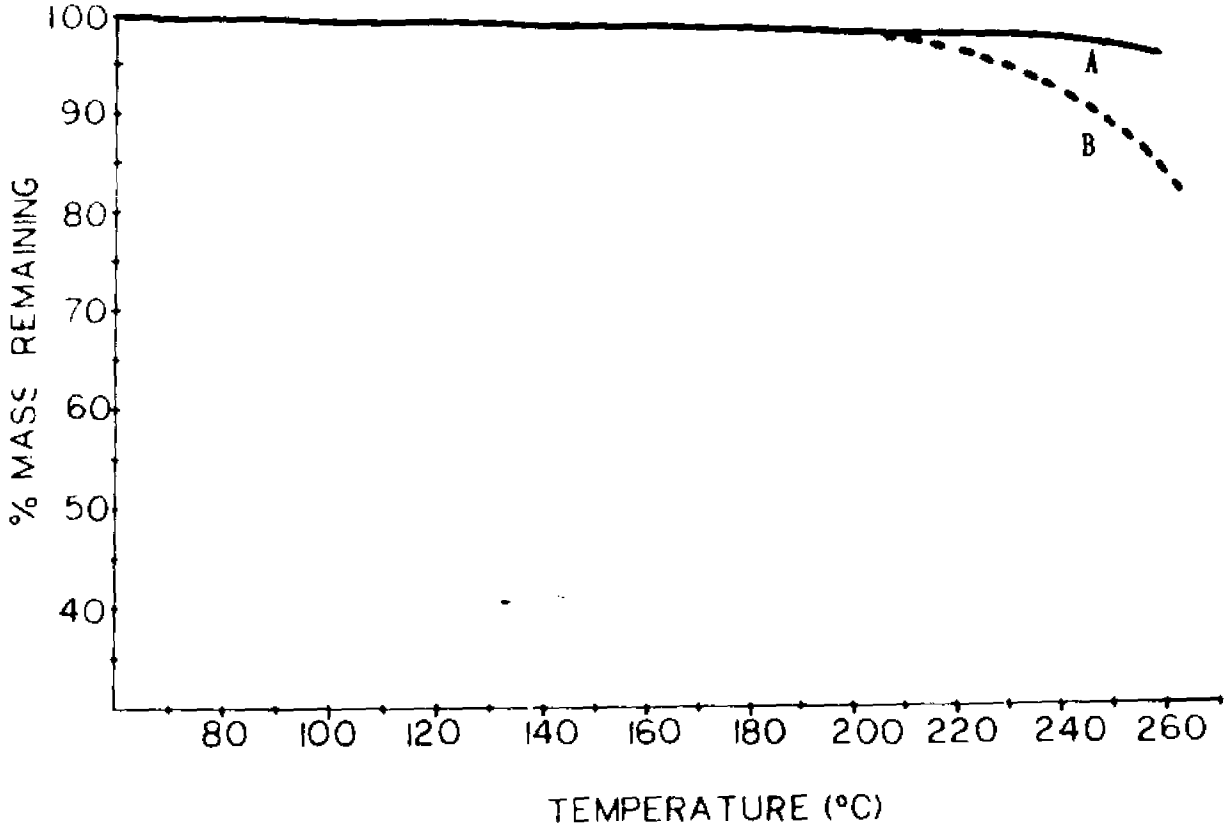

Figure 4.2

TGA thermogram of acetal copolymers (heating rate = 10^0C/min)

A : trioxane- 1,3-dioxep-5-ene copolymer (1.8 mol% incorporation)
B : trioxane-ethylene oxide copolymer (1.4 mol% incorporation)

the percent comonomer incorporation increases. This is consistent with Inoue's study (38) of trioxane copolymers, where he reports that copolymers with ethylene oxide, dioxolane and dioxepane have melting temperatures which follow Flory's equation:

$$(1/T_m) - (1/T_m^o) = -(R/\Delta H_u) \ln X_a$$

where T_m^o is the melting temperature of the trioxane homopolymer, ΔH_u is the heat of fusion per crystallizing unit, R is the gas constant and X_a is the mole fraction of the crystallizing unit. (47,48) The derivation of this empirical equation requires several assumptions, including that the polymer has a very small fraction of comonomer, a random comonomer distribution, a large molecular weight and that $(\Delta H/\Delta S)$ is constant for polymer units from T_m^o to T.

Compared to a TX-EO copolymer of comparable incorporation, the TX-DXPE copolymer was found to be much less susceptable to degradation by bromine (Figure 4.3). In the presence of bromine at a concentration as low as 3×10^{-5} M, the reduced viscosity of the TX-EO copolymer was found to decrease from 1.7 dL/g to 0.2 dL/g in less than 20 minutes at 25°C. Under the same conditions, the reduced viscosity of a TX-DXPE copolymer sample was found to decrease only from 1.1 dL/g to 1.0 dL/g. However, when the bromine concentration is increased by a factor of 10^2, both copolymers experienced considerable degradation (see Figure 4.4).

The double bond units of the TX-DXPE copolymer may remove

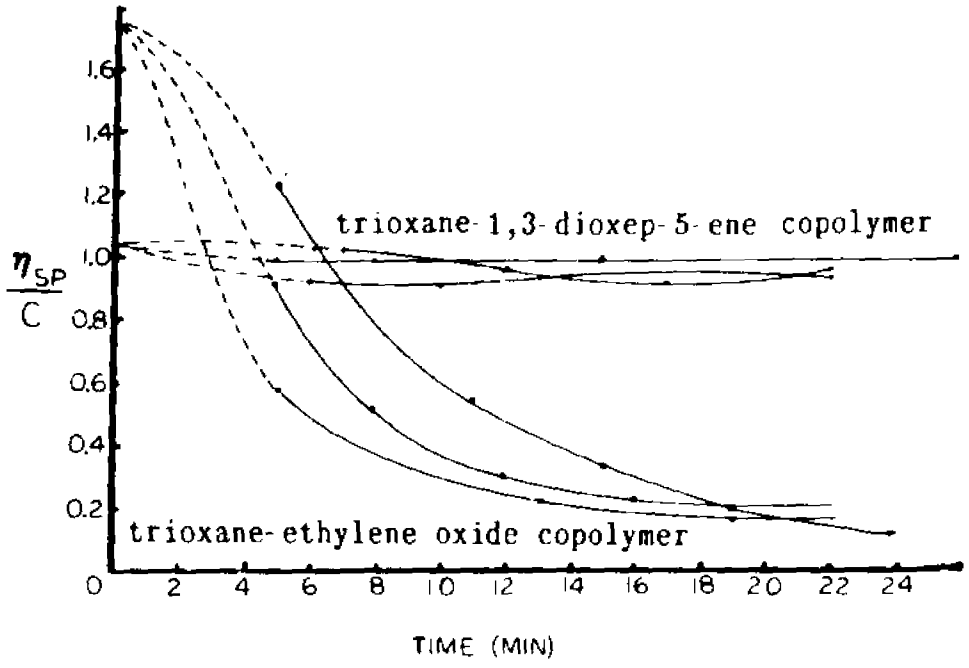

Figure 4.3

Copolymer stability against Bromine degradation
as determined by monitoring η_{sp}/c as a function of time
[polymer] = 0.310 g/dL. $[Br_2]$ = 3 X 10^{-5} M,
25°C in hexafluoroisopropanol

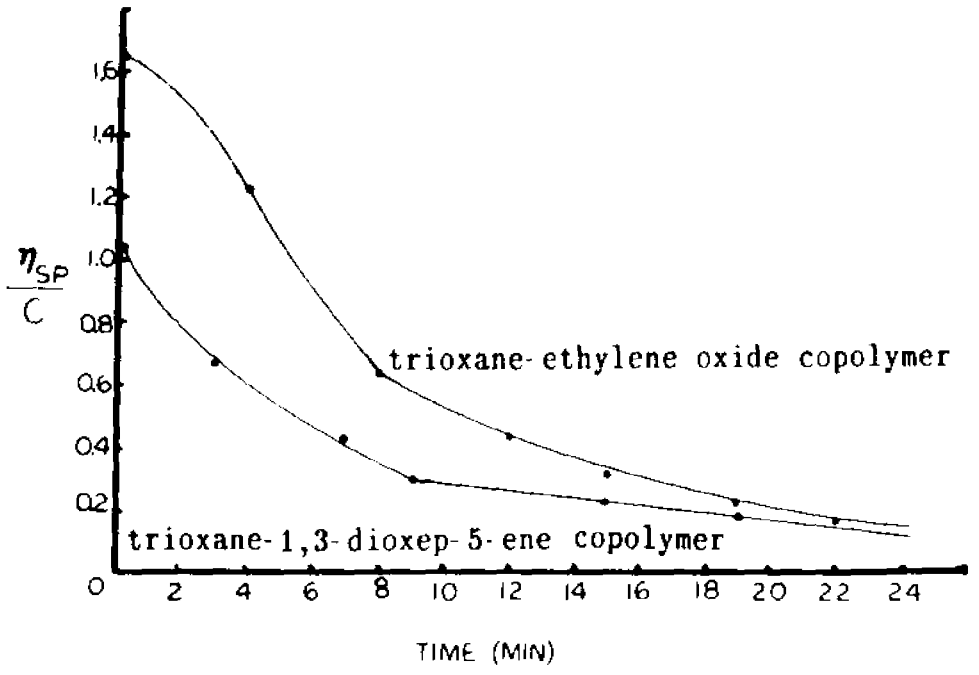

Figure 4.4

Copolymer stability against Bromine degradation as determined by monitoring η_{sp}/c as a function of time [polymer] = 0.310 g/dL. $[Br_2] = 3 \times 10^{-3}$ M, 25°C in hexafluoroisopropanol

potentially harmful species such as bromine through the formation of stable products:

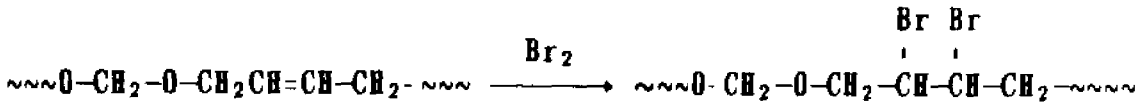

Degradation of polyacetals by bromine may occur by either a radical or an acidolytic mechanism:

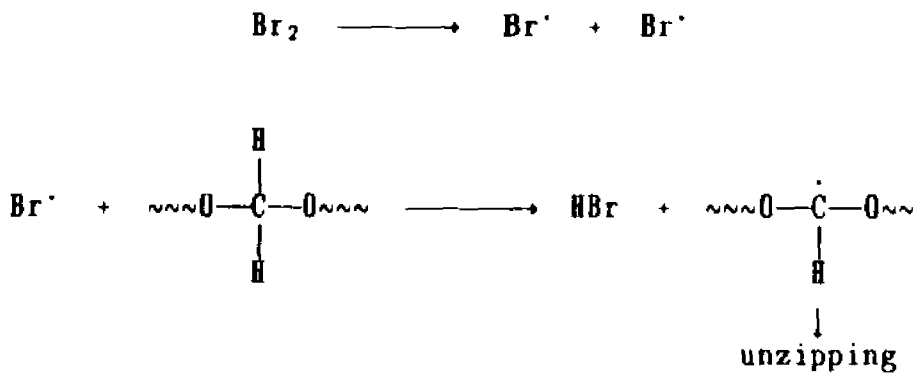

H^+ resulting from the ionization of HBr generated by hydrogen abstraction can also attack the polymer:

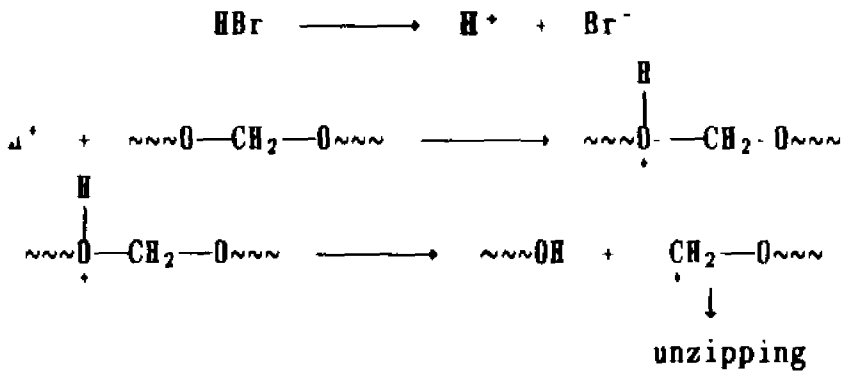

4-1c-3 Copolymer modifications

4-1c-3a Graft copolymers

Copolymer samples haveing been modified by grafting with sodium acrylate were observed to become colored after staining with methylene blue, a cationic dye. Table 4.3 presents the results for the modified copolymer as well as for a control copolymer (trioxane- ethylene oxide copolymers) referred to as copolymer "C". The TI-DIPE copolymer samples refers to as "A" and "B" have 2 and 4 mole percent incorporation of DIPE respectively.

It was observed that sodium acrylate does not demonstrate significant solubility in HFIP. After stirring and heating the system for one hour, however, it was found to form very finely dispersed particles. It was also observed that tubes containing hydroperoxide appeared to be clearer and more yellow that those without.

Table 4.3 Results of dye treatment on grafted copolymer

Sample	Luperox	Color
Copolymer A	none	pale blue
Copolymer A	0.5 mg	dark blue
Copolymer B	none	pale blue
Copolymer B	0.5 mg	dark blue
Copolymer C	none	pale blue
Copolymer C	0.5 mg	pale blue

The results in the column labelled "Color" are reproducible, but vary if the quantities of amine and peroxide are not carefully controlled. The relative intensity of the blue color of each dye treated sample is believed to reflect the extent of grafting with sodium acrylate. In a basic environment, the polyacrylate chains will be negatively charged. Methylene blue, a cationic dye, is positively charged and is expected to be attracted to acrylate branches. In a few isolated instances where the peroxide concentration was not carefully controlled, it was observed that even the control copolymer, which contains no unsaturated units and therefore should not react with sodium acrylate, had a dark blue color after dye treatment. The explanation for this can be found in the discussion of polyacetal degradation and susceptibility to radical degradation. If a polymer chain is attacked by a peroxide radical an initiation point for grafting is established. Just as in the case of TX-DXPE stabilization against low levels of bromine, an increase in the "stress" (such as higher bromine or peroxide levels) on the system results in an overload on the system that cannot be tolerated. The chain must respond by degrading in the case of bromine radicals and by grafting for hydroperoxide radicals in the presence of a vinyl monomer. These observations are consistent with a reported grafting procedure (39) that claims to graft methyl methacrylate onto TX-EO copolymer fibers by means of ionizing radiation.

4-1c-3b Epoxidized copolymers

Trioxane copolymers with epoxy functional groups can be obtained through epoxidation of the *cis*-2-butene stopper unit.

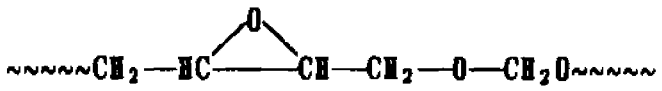

Figure 4.5 shows a solid state ^{13}C (CP/MAS) spectrum of the epoxidized copolymer. There is only a faint hint of absorption at 56 ppm where the epoxide carbon should occur. The substantial chemical shift anisotropy of epoxide carbons may lead to broad absorption peaks. It is very likely that the apparently low epoxide content arises from epoxidation only at the copolymer surface. As described in Section 4-1b-2b, the copolymer was not completely dissolved during the modification reaction. Complete epoxidation is not expected under such conditions.

TGA thermograms given in Figure 4.6 demonstrate that epoxidation, however minimal, improves the thermal stability of the copolymer.

4-1c-3c Incorporation of urea functional group

Due to difficulties with respect to copolymer solubility, copolymer modification by incorporation of the urea moiety also appears to have had limited success. Figure 4.7 gives the IR spectra of urea and modified DIPE for use as model compounds for spectral identification. The IR spectra of modified and unmodified copolymers

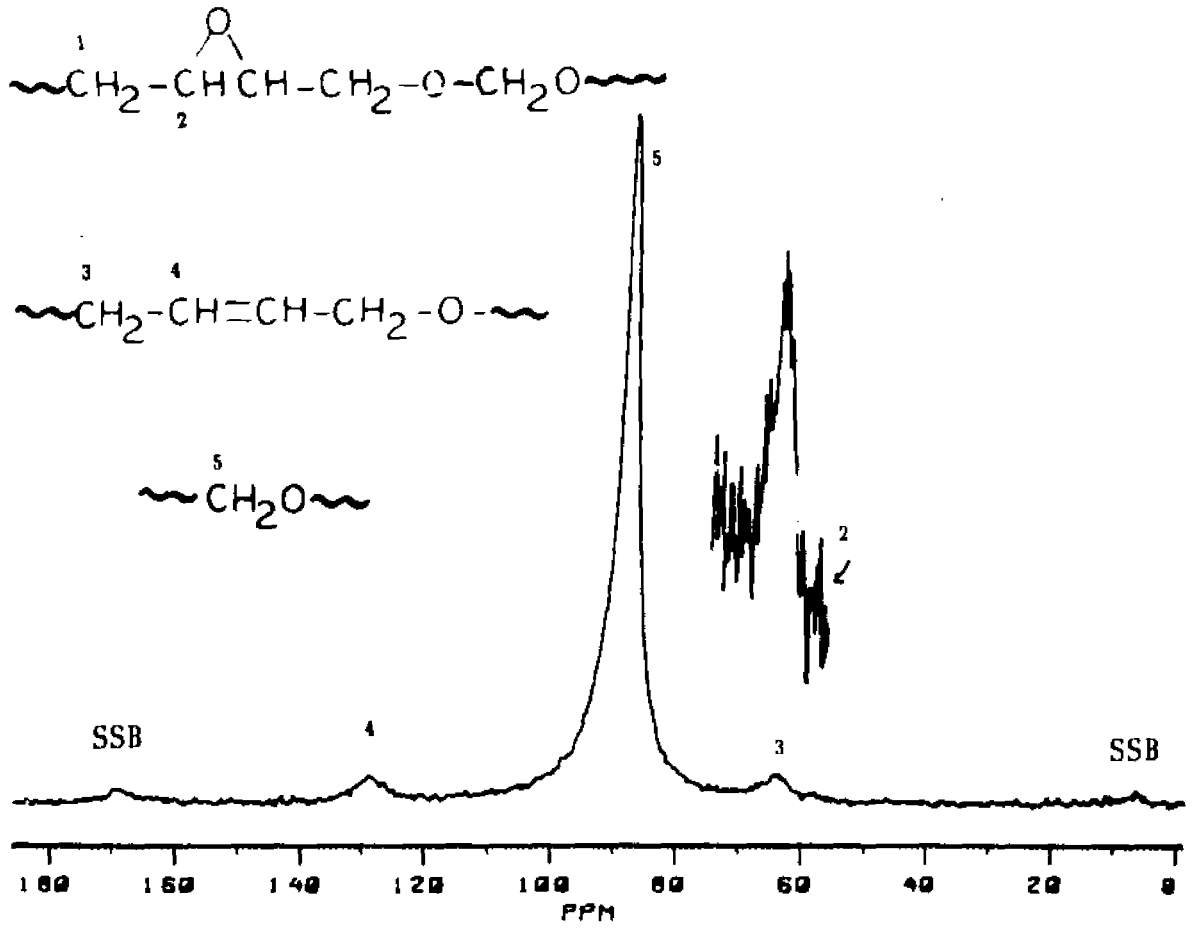

Figure 4.5

Solid state ^{13}C NMR spectrum of an epoxidized trioxane-1,3-dioxep-5-ene copolymer, obtained using cross polarization and magic angle spinning.

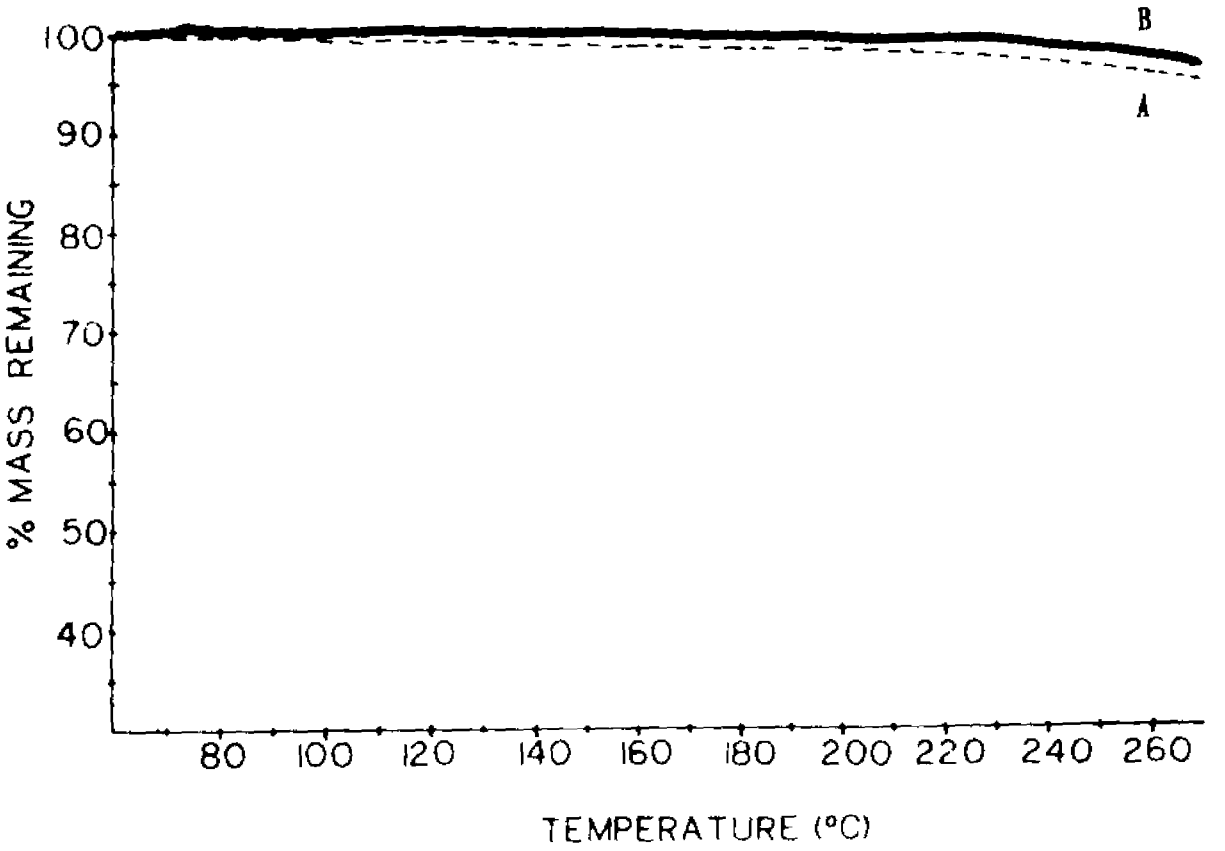

Figure 4.6

TGA thermograms of trioxane-1,3-dioxep-5-ene copolymers before and after expoxidation.

A : before epoxidation
B : after epoxidation

are given in Figure 4.8.

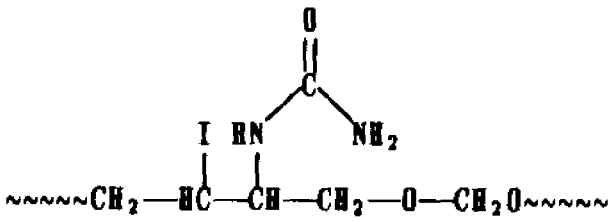

The copolymer spectra show characteristic acetal peaks (2900, 1460, 1360, 1240, 1100 and 900 cm^{-1}) as well as weak signals at 1740 (C=O stretching), 1700 (-NH bending) and a broad signal at 3400 (-NH stretching) indicating that the desired modification had been at least partially achieved.

The intended modification would have the advantage of providing an excellent site for stabilizer binding. The unit's urea moiety can act as a polymer-bound stabilizer even without further modification. (see section 3-2 for discussion of formaldehyde acceptors).

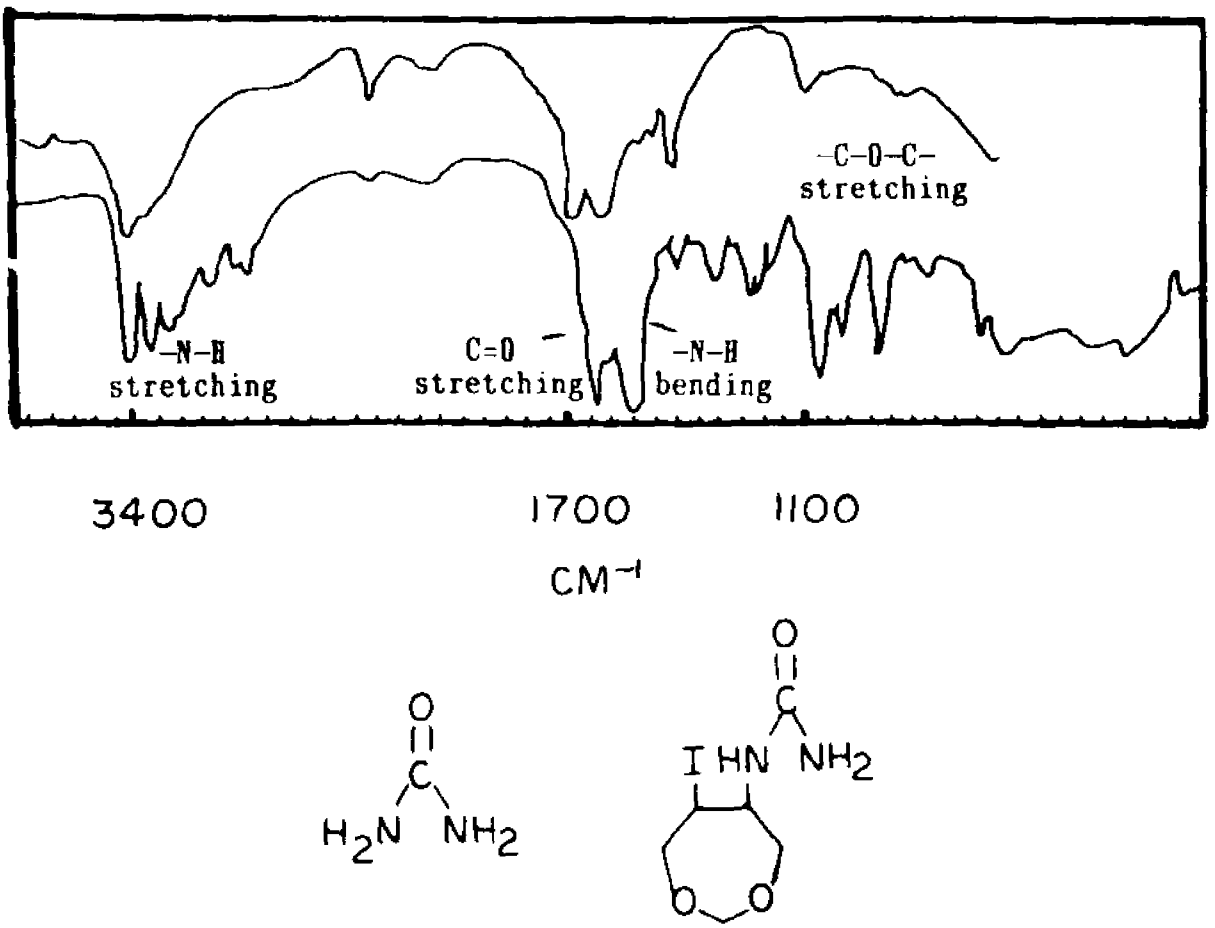

Figure 4.7

IR spectra of urea and epoxidized 1,3-dioxep-5-ene comonomer

A : urea
B : modified 1,3-dioxep-5-ene comonomer

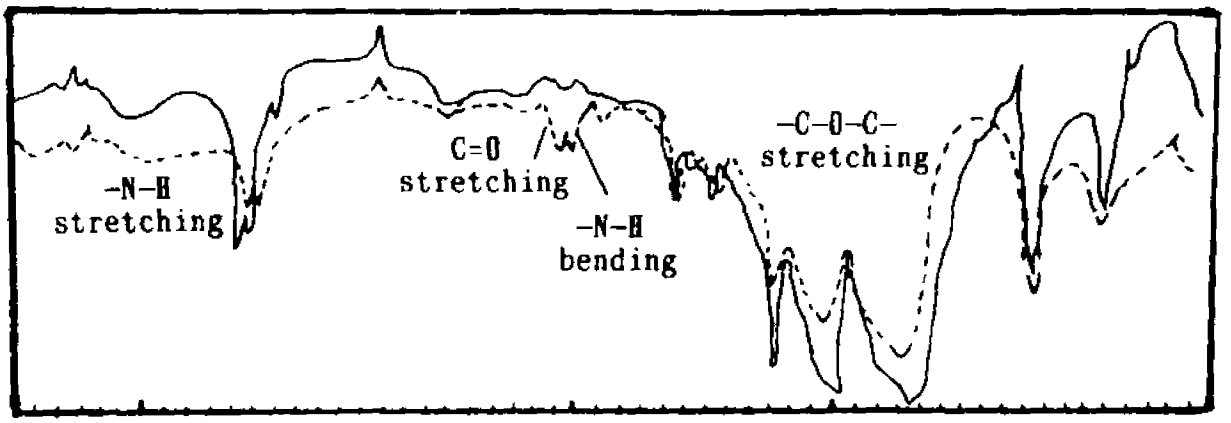

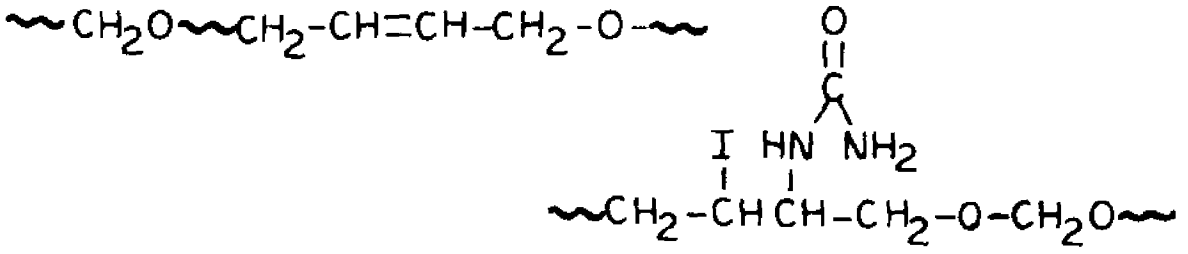

Figure 4.8

IR spectra of epoxidized and unmodified trioxane-1,3-dioxep-5-ene copolymer

A : unmodified trioxane-1,3-dioxep-5-ene copolymer
B : epoxidized trioxane-1,3-dioxep-5-ene copolymer

4-2 Trioxane-Glycerol Formal Copolymers

4-2a Summary

Functionalized copolymers of trioxane have been synthesized by cationic ring opening copolymerization with glycerol formal. Base hydrolyzed copolymers with 3 mole % comonomer incorporation have been found to show thermal stability comparable to that of trioxane-ethylene oxide copolymers with 1.4 mole % comonomer incorporation. Characterization by ^{13}C NMR spectroscopy revealed that the hydrolyzed copolymers are composed of the following structural units:

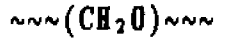

1

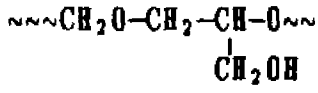

2

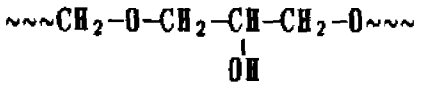

3

The ratio of unit 2 to unit 3 appears to be approximately 1:1, but is difficult to determine because of overlapping signals in the ^{13}C NMR spectrum. Possible endgroups include:

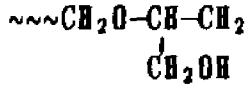

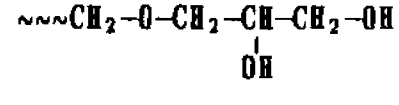

Viscosity molecular weight for these copolymers was determined to be less than 5×10^3. All copolymers were observed to be soluble in hexafluoroisopropanol, HFIP, as well as hot dimethylsulfoxide, DMSO, and dimethylformamide, DMF. The resulting functionalized polyacetals

have the potential for further modification.

4-2b Experimental

4-2b-1 Synthesis

Copolymerization of trioxane, TX, with glycerol formal, GF, (obtained from Aldrich Chemical Co.) was carried out as described in Section 4-1b-1 Typically, 10 μL of initiator was used for a total comonomer charge of 15 grams. The base hydrolysis process used to remove unstable end groups from trioxane-glycerol formal copolymers is also described in Section 4-1b-1. Homopolymerization of the glycerol formal monomer was attempted by adding 10 μL of BF_3OEt_2 to a 15 g charge. The reaction was carried out as described for the copolymerization above.

4-2b-2 NMR analysis

Carbon-13 NMR spectra were obtained on an IBM WP-200 SY FT NMR spectrometer using Bruker software. The solvent used was perdeuterated dimethlysulfoxide, DMSO-d_6. The temperature of measurement is indicated in the caption for each spectrum. Pulse angles and relaxation delays were selected to permit semiquantitative comparison among absorption peaks.

4-2b-3 Thermal analysis

TGA thermograms were obtained on a DuPont 990 Thermogravimetric Analyzer under a nitrogen atmosphere with a heating rate of 10°C/min. Sample masses were typically 3-5 mg. See Section 3-2b-3 for further

details.

Differential scanning calorimetry, DSC, was used to determine copolymer heat of fusion and percent crystallinity. (Sect. 4-1b-4a)

4-2c Results

4-2c-1 Product yields

Table 4.4 summarizes the yields after methanol/TEA washing (crude product) and after hydrolysis (final product). Since unreacted trioxane is removed by washing with methanol, these results serve as an approximate measure of percent conversion. Also presented are the values of yields after base hydrolysis. Since copolymer is expected to be thermally stable, and polyoxymethylene homopolymer to be unstable, these values reflect the extent of comonomer incorporation and loss due to homopolymerization of trioxane.

4-2c-2 NMR analysis

Table 4.5 presents calculated and observed chemical shift values for signals in spectra of glycerol formal and trioxane-glycerol formal copolymers. Calculations are based on correlation tables compiled by Brown (40). Numbering assignments are given in Figure 4.10.

4-2c-3 Thermal analysis

In Figure 4.16 the thermograms resulting from the thermogravimetric analysis of a trioxane-glycerol formal copolymer is compared with that of a trioxane-ethylene oxide copolymer with 1.4 mole percent ethylene oxide incorporation.

Table 4.4 : Product yields for copolymerization of trioxane and glycerol formal

wt.% GF in Feed	Crude Product Yield	Final Product Yield
4.8	63	18
7.2	98	45
7.5	84	37
14.4	--	32
14.7	71	30
15.8	68	26
17.7	--	13

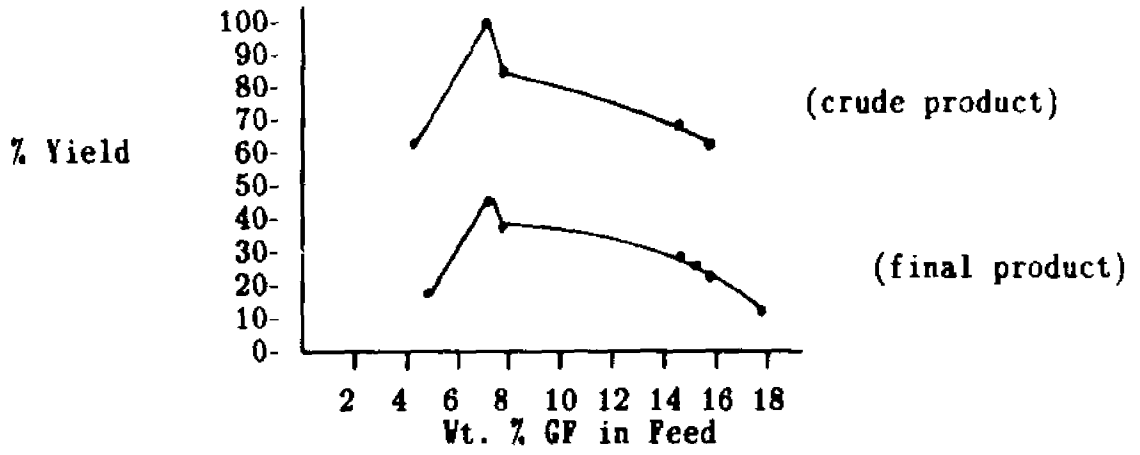

Figure 4.9

Percent yield vs. wt. % GF in feed for CH_3OH/TEA wash (crude product) and base hydrolysis (final product)

Table 4.5 Calculated vs. observed ^{13}C chemical shift values for trioxane-glycerol formal copolymers

Carbon #	Calculated Chemical Shift (ppm)	Observed Chemical Shift (ppm)
9	67.3	67.8
10	74.7	74.3
11	65.5	65.7
12	72.7	73.4
13	69.4	68.3
14	75.5	75.0
15	64.0	64.1
16	69.0	68.5
17	71.0	71.5
18	67.0	68.0
19	72.2	73.0
20	69.5	69.5

Figure 4.10 Numbering assignments for ^{13}C NMR spectra as given in Figures 4.12, 4.13, and 4.15

1) Glycerol formal monomer (Figures 4.12 and Figure 4.13)

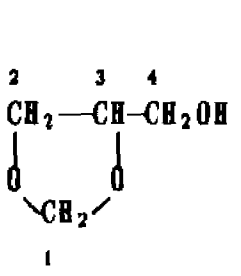

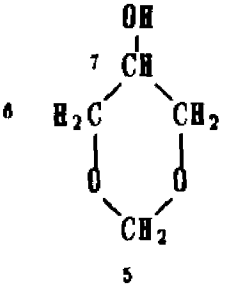

2) Copolymer units (Figure 4.13)

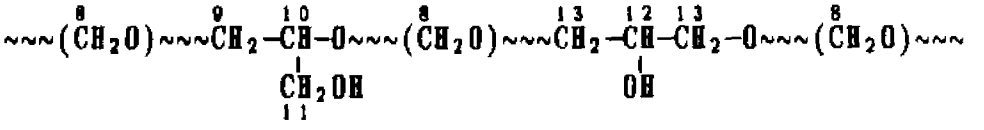

3) Oligomer units (Figure 4.15)

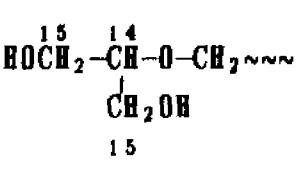

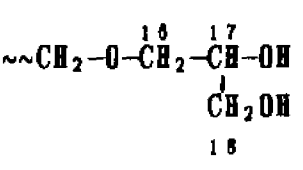

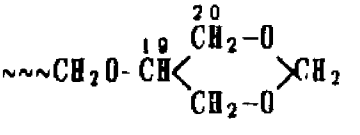

4-2d Discussion

Glycerol formal, GF, is a mixture of isomeric α,α- and α,β-forms prepared from glycerol and formaldehyde (41). In the presence of trioxane and a cationic initiator, such as BF_3OEt_2, there are several possible reaction products. Figure 4.11 outlines these reactions, the symbol "~~~" representing poly(oxymethylene) units.

Based on the scheme in Figure 4.11 there are seven possible structural comonomer units. Comonomer units may be incorporated into the macromolecule through three different paths: chain transfer to monomer, ring-opening chain initiation and ring-opening copolymerization. Base hydrolysis of the nascent product further modifies the initial structure.

End group I and II result from chain transfer to monomer which, in both cases, results in the initiation of a new chain and termination of the growing chain. Ring opening of structures I and II leads to the formation of the branched unit given by structure III. Hydrolysis of this structure may yield structures IV or V. Further hydrolysis of IV or V may yield an endgroup with structure VI or VII. Endgroup structures VI and VII may also result directly from ring-opening chain initiation.

For the purpose of polymer modification, the units IV and V are of interest. The difunctional endgroup units VI and VII may also be useful.

To gain a better understanding of the behavior of the glycerol formal isomers under polymerization conditions, two control experiments were conducted. The first experiment examined the effect of

Figure 4.11 : Glycerol formal reactions in trioxane-glycerol formal copolymerization

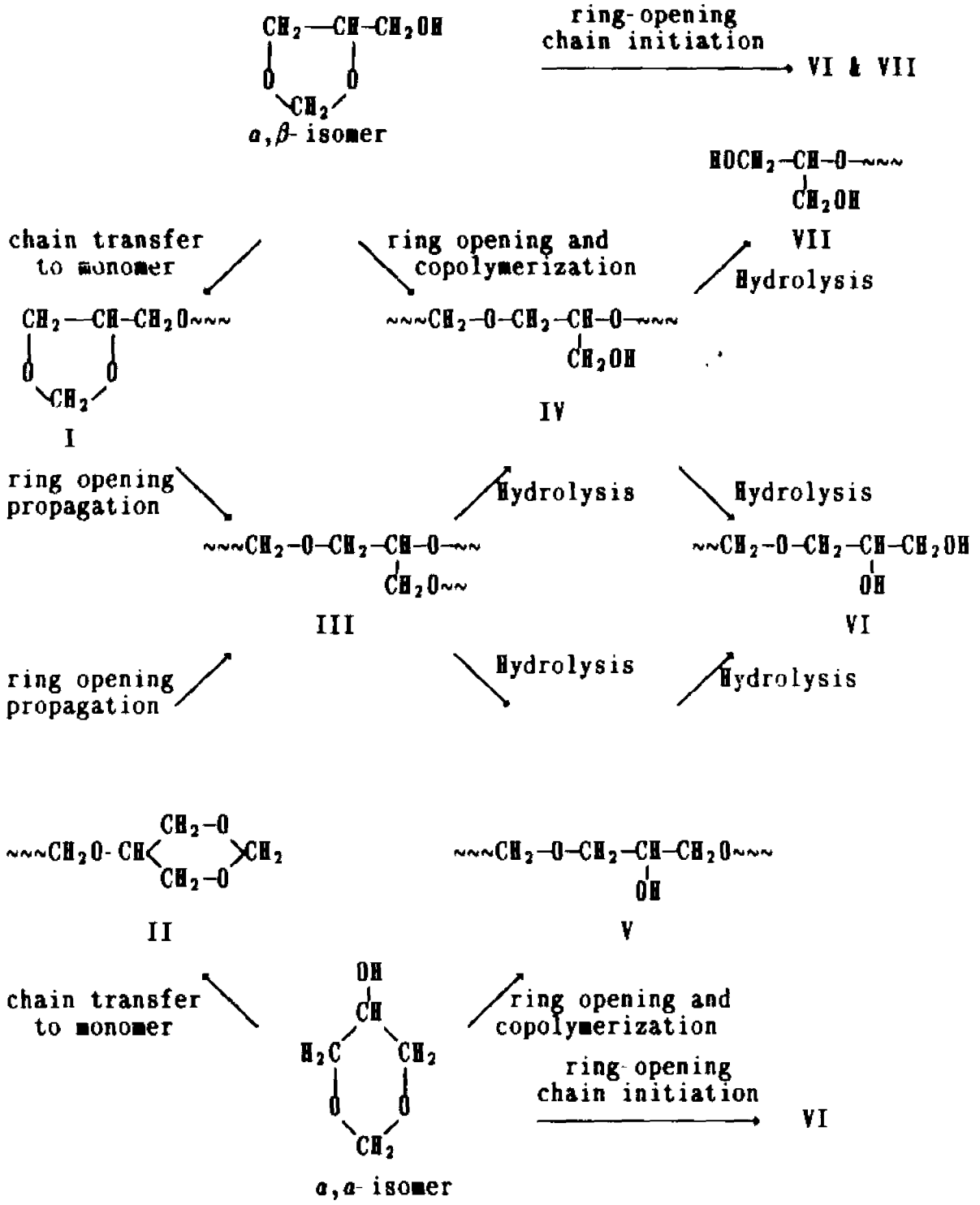

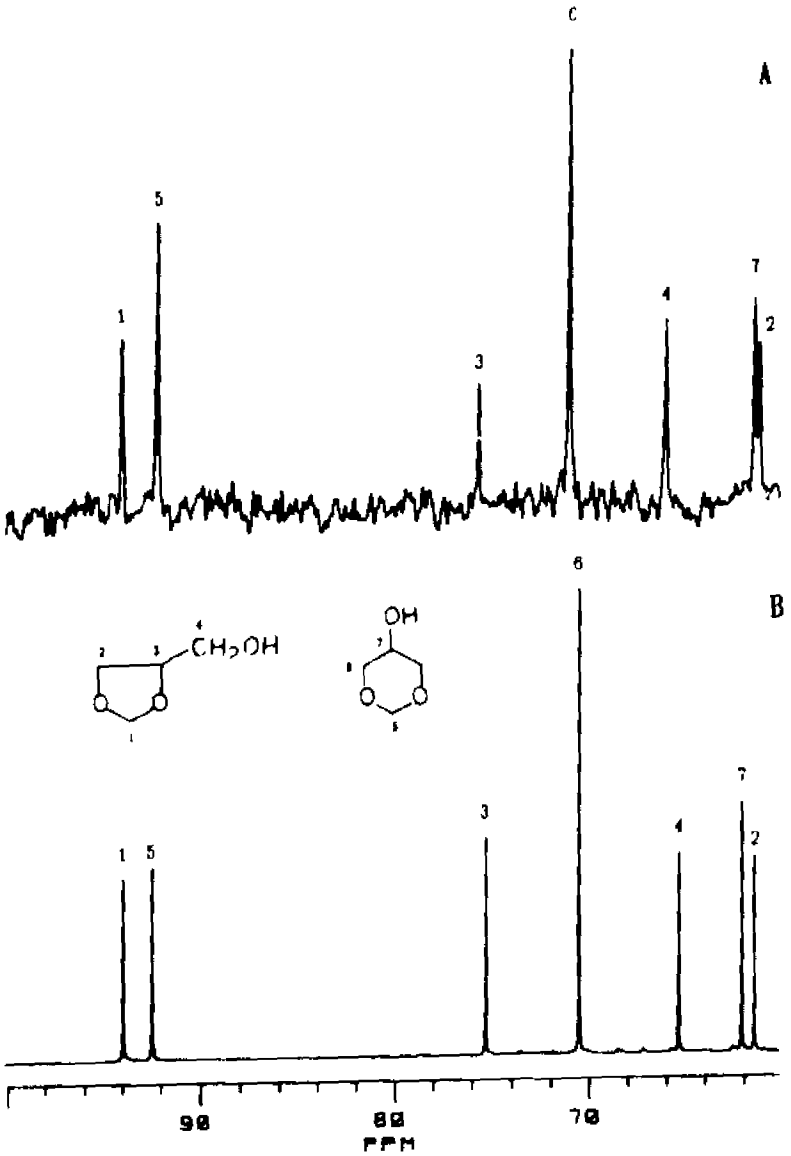

Figure 4.12
^{13}C NMR spectra of glycerol formal comonomer (DMSO-d_6)

A : spectrum obtained at 60°C
B : spectrum obtained at 25°C

temperature on the isomer equilibrium. At room temperature the isomeric ratio is approximately one (42), at higher temperatures the α,α-form is favored. For example at 60°C, the ratio is approximately 3:2 in favor of the α,α-isomer. (See Figure 4.12)

α,β-form α,α-form

The second control experiment involved observation of the behavior of the two isomers in the presence of cationic initiator. Neither form of the comonomer was observed to homopolymerize in the presence of cationic initiator, although there is evidence for dimer formation. "Spectrum B" in Figure 4.13 was obtained on glycerol formal 3 days after the addition of BF_3OEt_2 (10μL to 15g GF). "Spectrum A" corresponds to the initial conditions of approximately equal isomeric concentrations. Comparing "A" with "B", one can clearly observe the preferential depletion of the α,β-isomer. The new NMR absorptions are tentitively assigned to the following structures:

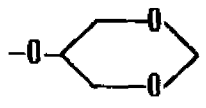

II

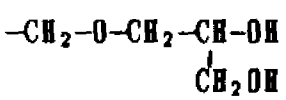

VI

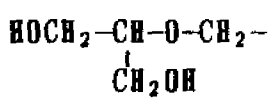

VII

The assignment are based on calculated chemical shifts (40) and internal consistancy of peak intensities of ^{13}C absorptions belonging to the same structural unit.

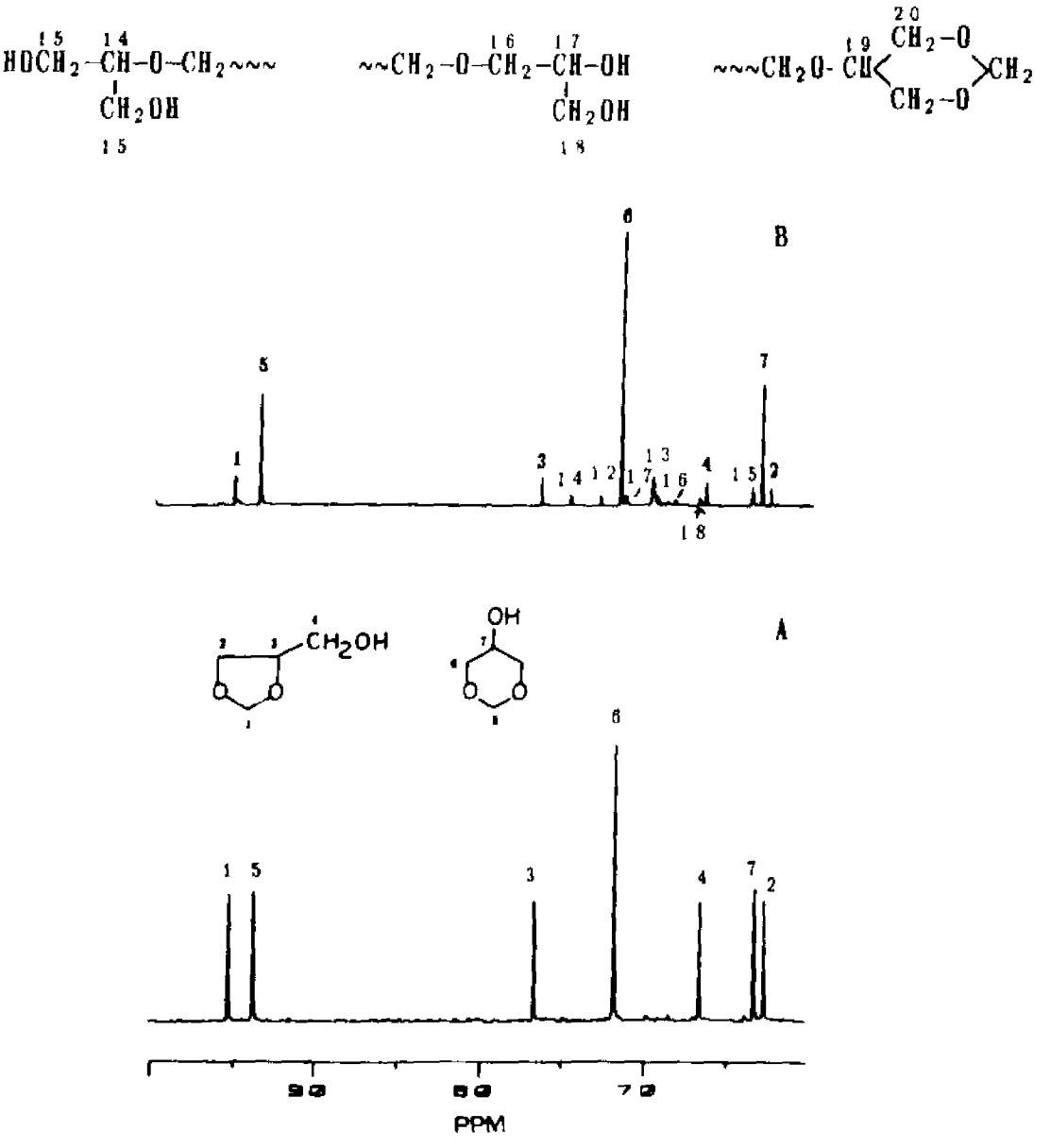

Figure 4.13

^{13}C NMR spectra of glycerol formal comonomer
(DMSO-d_6, 25°C)

A : before addition of BF_3OEt_2
B : several days after the addition of BF_3OEt_2

The formation of dimers consisting of either structures II and VI or II and VII is consistent with the NMR data. The processes involve ring opening of either glycerol formal isomer to form cationic centers which can participate in a number of reactions (see Figure 4.14). The α,β-form gives two different cationic species (VIII and IX). Species VIII is at equilibrium with its original neutral form, and is also capable of chain transfer to monomer to form dimers. Species IX is at equilibrium with both isomers and is likewise capable of forming dimers. For the equilibria of species IX, the thermodynamically more stable α,α-form must be favored. This can contribute to the preferential depletion of the α,β-form as observed by NMR (Figure 4.13). Chain transfer to the α,α-isomer dominates due to its higher prevailing concentration as well as to its stronger basicity at the hydroxy site.

Under conditions of copolymerization, the cationic sites due to the highly reactive trioxane monomer dominates the process. Figure 4.15, a ^{13}C NMR spectrum of a base hydrolyzed copolymer sample, indicates a structure consisting primarily of $-CH_2O-$ units. The relative occurrence of units IV and V appears to be approximately equal based on a comparison of signals 11 and 13. Accurate quantification is difficult due to signal overlapping.

The observed incorporation of these two units may be the result of equal reactivity of both isomers or the reactions of one isomer involving several steps. For example, structural unit IV can originate directly from the α,β-isomer (via ring-opening copolymerization) or from the α,α-isomer through a three step process (i.e. chain transfer

Figure 4.14 : Glycerol formal reactions in the presence of BF_2OEt_2

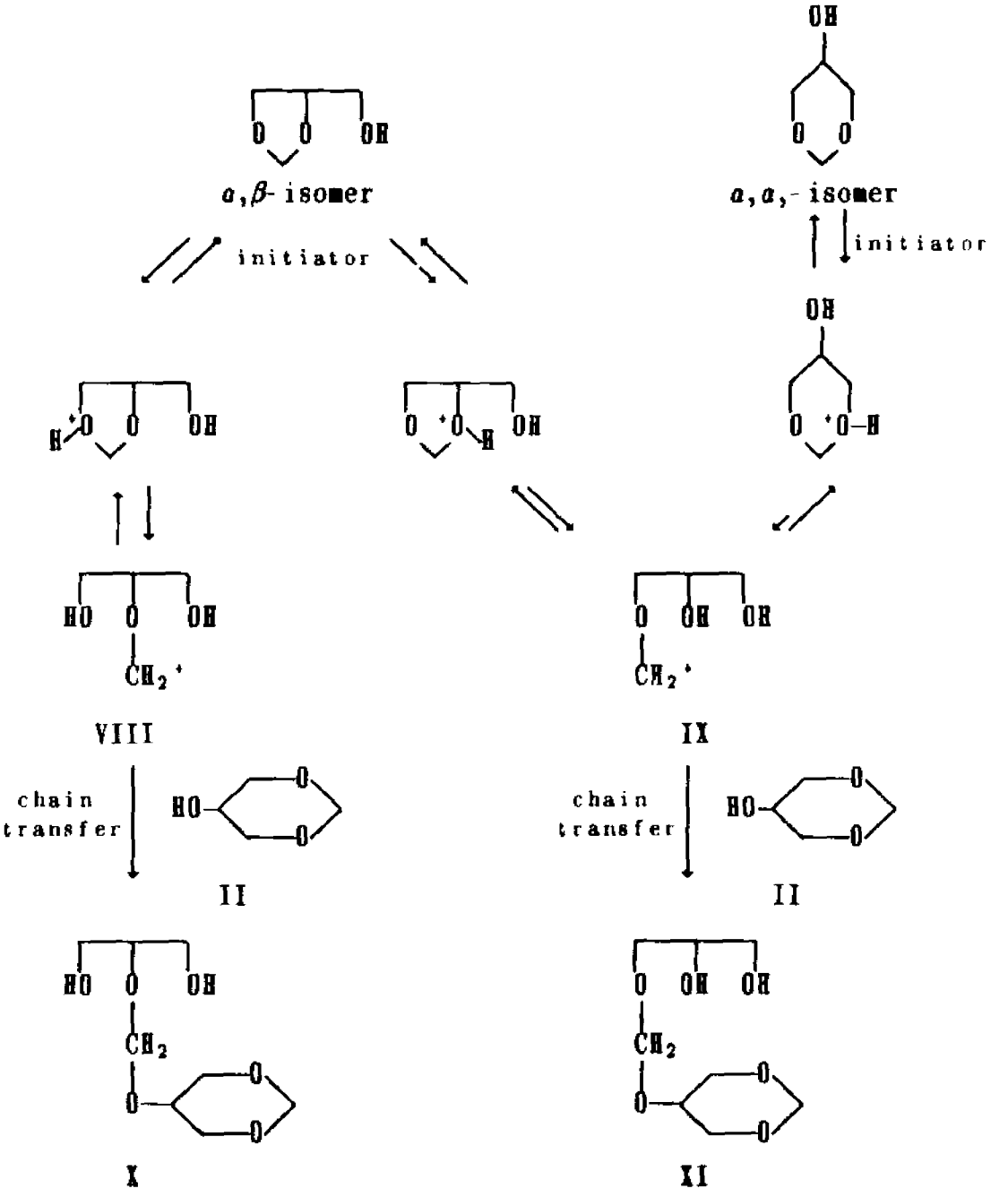

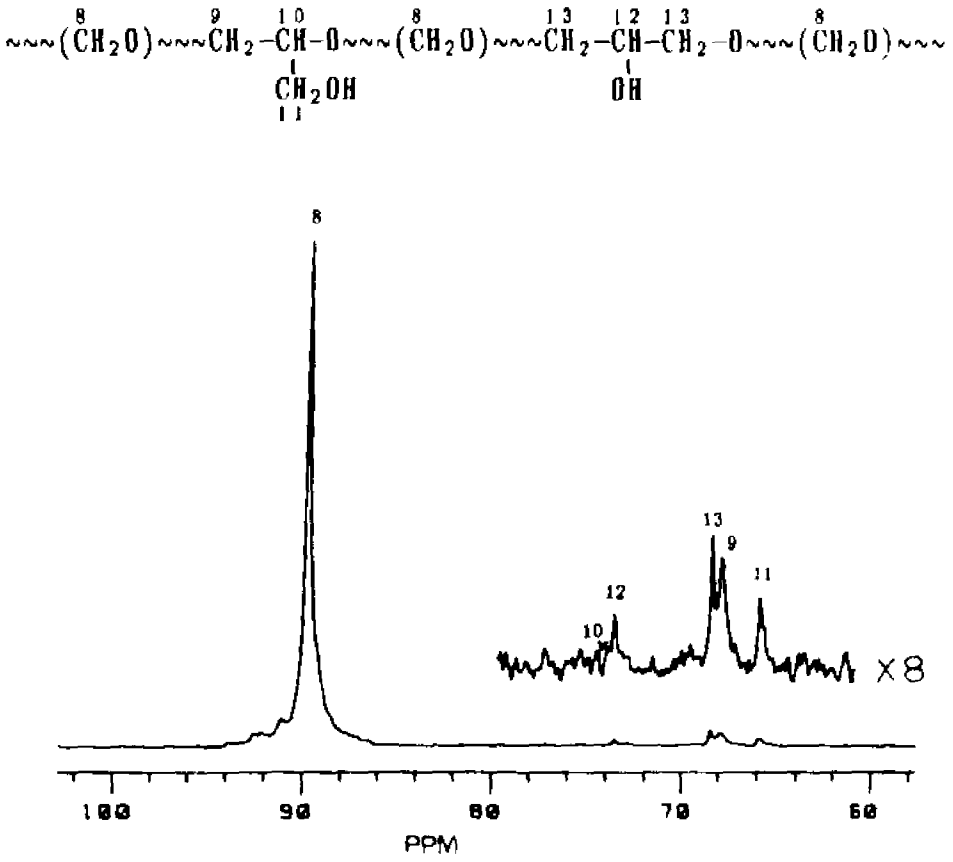

Figure 4.15

Typical ^{13}C NMR spectrum of trioxane-glycerol formal copolymer, DMSO-d_6 126°C.

to monomer, ring opening propagation and then hydrolysis) as depicted in Figure 4.11. However, since end groups resulting from chain transfer to monomer (I and II) and the branched unit (III) are *not* observed in the copolymer spectrum, but may have existed prior to hydrolysis.

The data in Figure 4.9 summarizes the yields after methanol/TEA washing (crude product) and after hydrolysis (final product). The first treatment removes initiator and monomers. This yield includes products due to both homopolymerization and copolymerization. The base hydrolysis step leads to stable end groups. A good final yield is indicative of resonable levels of comonomer incorporation. Product yield data, together with the results of NMR analysis (spectra not shown) indicate that at low feeds (i.e. less than approximately 1.5 mole percent) the product indeed contains little or no comonomer and is nothing more than thermally stable POM. This is not considered to be unusual since hydrolyzed POM homopolymer typically yields a thermally stable fraction of approximately 25% (11). At high feeds (i.e. more than about 2.4 mole percent) chain transfer to monomer or water may be significant, resulting in POM homopolymer and low molecular weight copolymer that is lost on hydrolysis. At feeds of about 2 mole percent, thermally stable copolymers are reproducibly obtained in reasonable yield. NMR spectra indicate an incorporation of ca. 3% by mole (Figure 4.15, comparing peaks #8 with #9 through 13). At a concentration of 2% by weight of copolymer in hexafluoroisopropanol, HFIP, an inherent viscosity of 0.42 dL/g was obtained. The molecular

weights are estimated to be ca. 4 X 10^3 based on comparison with viscosity results from trioxane-ethylene oxide copolymers with molecular weights within this range. The number of comonomer units incorporated per chain is about four. The low molecular weight of trioxane-glycerol formal copolymers is expected because the -OH group of the comonomer readily leads to chain transfer for cationic polymerization.

Figure 4.16 shows a comparison of TGA thermograms obtained from trioxane copolymers with glycerol formal (3 mole % incorporation) and ethylene oxide (1.4 mole % incorporation). Clearly the thermal stability of the copolymer is not adversely affected by incorporation of glycerol formal units.

Differential scanning calorimetry gives a percent crystallinity of 68%, indicating that hydroxyl and methylol pendant groups are being incorporated into the crystal structure with less impediment than $-O-CH_2-CH_2-$ groups on the backbone (36,37).

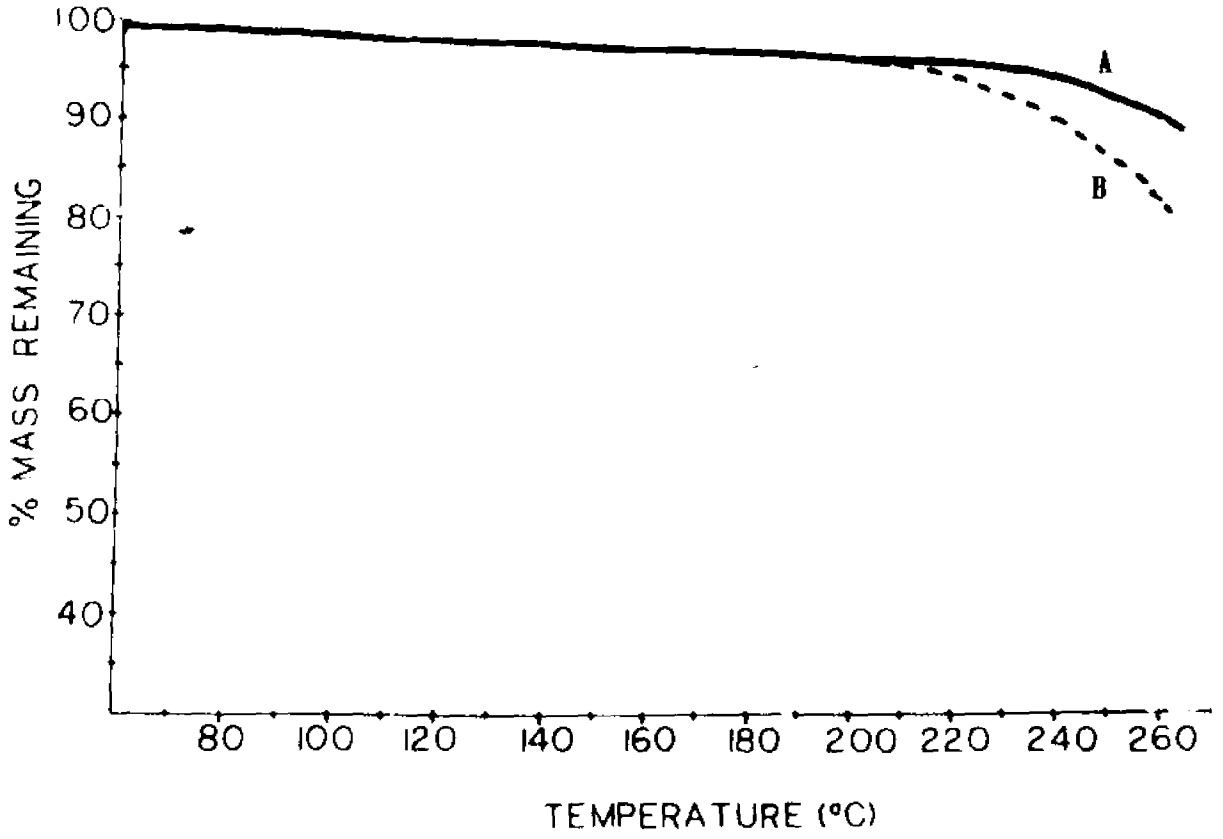

Figure 4.16
TGA thermograms of acetal copolymers (heating rate = 10°C/min)

A : trioxane-glycerol formal copolymer (3.0 mole % incorporation)
B : trioxane- ethylene oxide copolymer (1.4 mole % incorporation)

4-3 Trioxane-Glycidyl Acrylate Copolymers

4-3a Summary

Crosslinked copolymers of trioxane and glycidyl acrylate have been obtained by cationic ring-opening polymerization and subsequent base hydrolysis. The resulting copolymers were found to be thermally stable above 270°C and insoluble in HFIP at room temperature as well as in DMF and DMSO at 170°C. Characterization by solid state ^{13}C NMR spectroscopy (CP/MAS) indicates that the hydrolyzed copolymers consist primarily of structural units I and II:

I II

The following units are believed to be present at a much lower concentration.

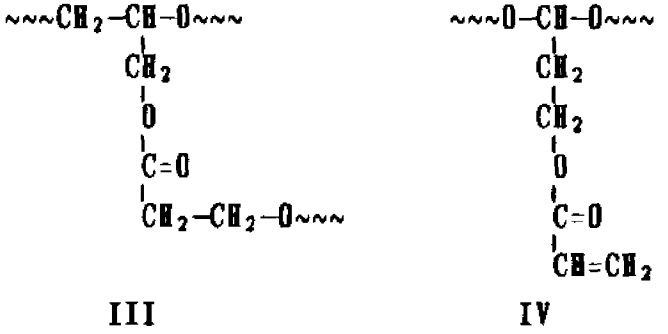

III IV

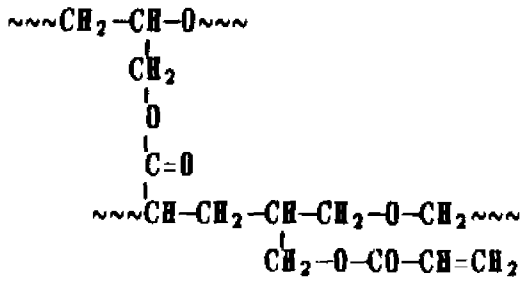

V

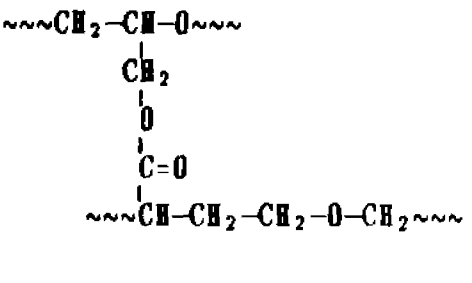

VI

Structures III, V, and VI can lead to crosslinking of the copolymer. The comonomer acrylate group functions as a bound stabilizer in the resulting network, and provides a site for further modification. DSC analysis reveals that copolymer crystallinity is unusually low in comparison with copolymers with comparable levels of other comonomers.

4-3b Experimental

4-3b-1 Synthesis

Copolymerization of trioxane, TX, with glycidyl acrylate, GA, (Aldrich Chemical Co.) was carried out as described in Section 4-1b-1. Typically, 25-50 μL of initiator was used for a total monomer charge of 15-20 grams. Copolymerization tubes were vented by inserting a Pasteur pipet fitted with a drying tube through the serum stopper. This was done to relieve the pressure built up during polymerization. The base hydrolysis procedure used to remove unstable endgroups from trioxane-glycidyl acrylate copolymers is also described in Section 4-1b-1.

Glycidyl acrylate was homopolymerized as follows: A dry test tube (25 X 75) was charged with 5 grams glycidyl acrylate. The tube was

capped with a serum stopper, purged with nitrogen and evacuated. The contents of the tube were brought to a temperature of 65°C in an oil bath and stirred with a magnetic stirrer. Initiator (10 μL, BF_3OEt_2) was then injected through the serum stopper into the comonomer. The polymerization was allowed to proceed at 65°C for 20 hours.

4-3b-2 NMR analysis

Solid state ^{13}C NMR spectra were obtained on an IBM WP-200 SY FT NMR spectrometer equipped with a solid accessory for high power decoupling, cross polarization and magic angle spinning. The cylindrical double air bearing probe was from Doty Scientific (Columbia, SC). Rotors with a sample volume of 0.36 cm^3 made from Al_2O_3 were routinely spun at 4 KHz. For each spectrum, 2 K data points were collected and zero-filled to 4 K. Line broadening was chosen for optimum signal-to-noise ratio without sacrificing resolution. Spinning rates were monitored with a frequency counter and are indicated in the caption for each spectrum. Signals noted "SSB" are due to spinning side bands. Spectra were obtained with a contact time of 2 msec. All reported quantifications are estimated values. Due to differences in NOE effects and efficiency of cross polarization for various carbons, precise quantitative determinations based presented spectra is not possible.

4-3b-3 Thermal analysis

TGA thermograms were obtained on a DuPont 990 Thermogravimetric Analyzer under a nitrogen atmosphere with a heating rate of 10°C/min.

Sample masses were typically 3-5 mg. For further details see section 3-2b-3. For differential scanning calorimetry, DSC, measurements see Section 4-1b-4a.

4-3c Results

4-3c-1 Product yields

The yields for stable copolymer after base hydrolysis increases with increasing comonomer yield (see Figure 4.17). Copolymerization with glycidyl acrylate feeds of greater than 0.7% were observed first to give a translucent gel. After an induction period rapid solidification occured. This induction time decreased with

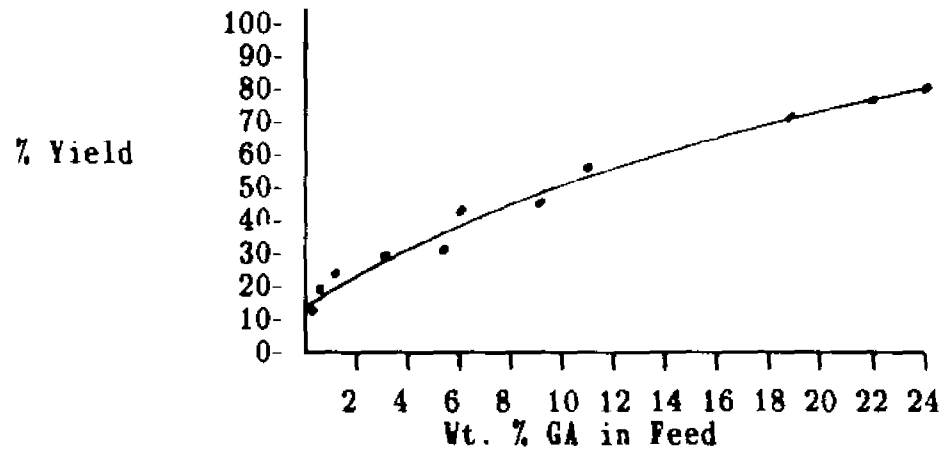

Figure 4.17

Percent yield vs. wt. % GA in feed after base hydrolysis

increasing comonomer feed. The reaction was accompanied by the evolution of a significant quantity of gas. In cases where the

reaction tube was not vented (see Section 4-3b-1), the pressure generated can be significant. The temperature within the reaction tube was observed to rise as high as 90°C during the solidification process.

The gas generated was formaldehyde. Due to the high reactivity of the oxirane ring in the presence of cationic initiator, free formaldehyde rapidly reaches its equilibrium concentration with respect to trioxane as well a to polymer chains. The higher yield for thermally stable copolymer with large GA feeds was due to the incorporation of more GA comonomer units acting as stoppers against unzipping of oxymethylene blocks.

4-3c-2 NMR analysis

A typical solid state CP/MAS ^{13}C NMR spectrum of a TX-GA copolymer is given in Figure 4.19. Absorptions due to both comonomers are identified. Figure 4.20 shows representitive solid state CP/MAS ^{13}C NMR spectra of a trioxane-glycidyl acrylate copolymer at low and high degree of conversion and the glycidyl acrylate homopolymer before and after hydrolysis. Spectrum 4.20A has been enlarged to show detail in the area of the comonomer signals because the comomomer incorporation is low in comparison with methylene oxide. Table 4.6 presents calculated versus observed chemical shift value for the ^{13}C NMR spectra. Calculations are based on correlation tables compiled by Brown (40). Structures noting carbon numbering are given in Figure 4.18. Carbons noted with asterisks are suspected structures. Only carbons 1 through 6 and 21 are confirmed assignments.

Table 4.6 : Calculated vs. observed ^{13}C chemical shift values for trioxane-glycidyl acrylate copolymers

Carbon #	Calculated Chemical Shift (ppm)	Observed Chemical Shift (ppm) spectra a b c	Observed Chemical Shift (ppm) spectrum d
1	63	65	71
2	72	75	78
3	64	65	71
4	166	164	164
5	131	126	134
6	129	122	132
7*	106	109	-
8*	41	41	41
9*	60	-	-
10*	73	-	-
11*	31	32	33
12*	59	-	-
13*	79	-	-
14*	27	26	25
15*	28	29	30
16*	77	-	
17*	44	47	47
18*	59	62	62
19*	175	175	175
20*	65	-	-
21	90	90‡	90

*tentative structures - overlapping signals ‡ spectrum a only

Figure 4.18 : Numbering assignments for spectra in Figures 4.19 and 4.20 A,B,C and D

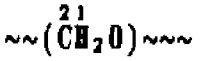

I

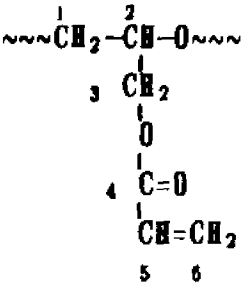

II

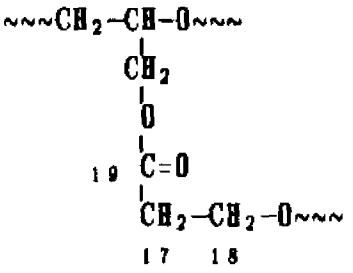

III

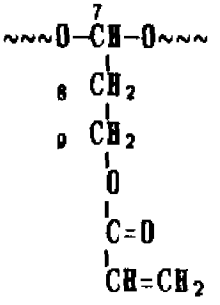

IV

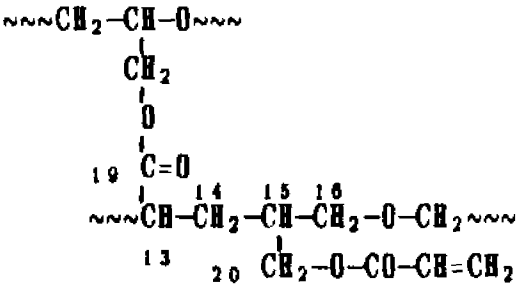

V

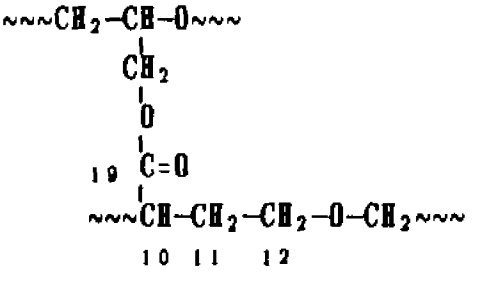

VI

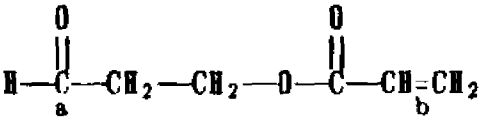

Figure 4.21 gives the high resolution ^{13}C NMR spectrum of the glycidyl acrylate monomer for purposes of comparison. Copolymers with glycidyl acrylate feed of less than 0.7 mole % gave only a methylene oxide signal and were concluded to be polyoxymethylene homopolymer. The incorporation for a copolymer sample with 1.1 mole % comonomer feed was estimated to be ca. 1 mole % based on integration of ^{13}C NMR spectra. (Figure 4.19, peaks 5 and 6 vs. 21).

4-3c-3 Thermal analysis

In Figure 4.22, the thermogram resulting from the thermogravimetric analysis of a trioxane-glycidyl acrylate copolymer (1 mole % incorporation) is compared with that of a trioxane-ethylene oxide copolymer (1.4 mole % incorporation). Figure 4.23 gives TGA thermograms of the glycidyl acrylate homopolymer before and after hydrolysis.

Copolymer samples with a glycidyl acrylate feed of less than 0.7 mole percent melted below 270°C and exhibited thermal behavior similar to thermally stable POM. This suggests that systems with low comonomer feed result not in copolymer but mainly in thermally stable POM (i.e. ~~~O–CH_3 end-capped). The absence of comonomer signals in the NMR spectra of these low feed samples supports this conclusion. This is not considered to be unusual since hydrolyzed POM homopolymer typically yields a thermally stable fraction of approximately 25% (11). Samples with higher GA feeds (i.e. greater than 0.7 mole %) result in products that, unlike the lower feed samples, are insoluble in HFIP and DMSO and DMF at 170°C. All samples with comonomer feeds greater than 0.7 mole

% did not appear to melt when heated to 270°C during thermogravimetric analysis. Decomposition occurs well above 270°C.

Data from DSC (Table 4.7) indicate that the crystallinity of the acetal copolymer is unusually low as compared to linear copolymer with comparable comonomer incorporation. For example, trioxane copolymer with 1.4 mole percent ethylene oxide incorporation shows a percent crystallinity of 60. For the trioxane-glycidyl acrylate copolymer with 1% GA incorporation, only 35% crystallinity was observed. When the incorporation increases to 2.4%, a low 11% crystallinity was obtained.

4-3d Discussion and conclusions

The ^{13}C NMR spectra shown in Figure 4.19 and 4.20 provide some insight to our understanding of the chemistry of the copolymerization of trioxane and glycidyl acrylate. The product obtained in the early stage of copolymerization is found to be only partly soluble on hot DMF and DMSO. The spectrum of this low conversion product (Figure 4.20 D) indicates that the polymer is composed primarily of structure I and II (i.e. POM and the unit resulting from ring-opening polymerization of the oxirane). As expected, the oxirane functionality of the glycidyl acrylate monomer is much more reactive than trioxane, a six-membered ring. The reaction of the acrylate group may result in the formation of the crosslinked structures III,V and VI, leading to the partial insolubility of the products.

The close similarities between the low conversion trioxane-glycidyl acrylate copolymer spectrum (Figure 4.20 D) and that of glycidyl acrylate homopolymer (Figure 4.20 B and C) indicates that the

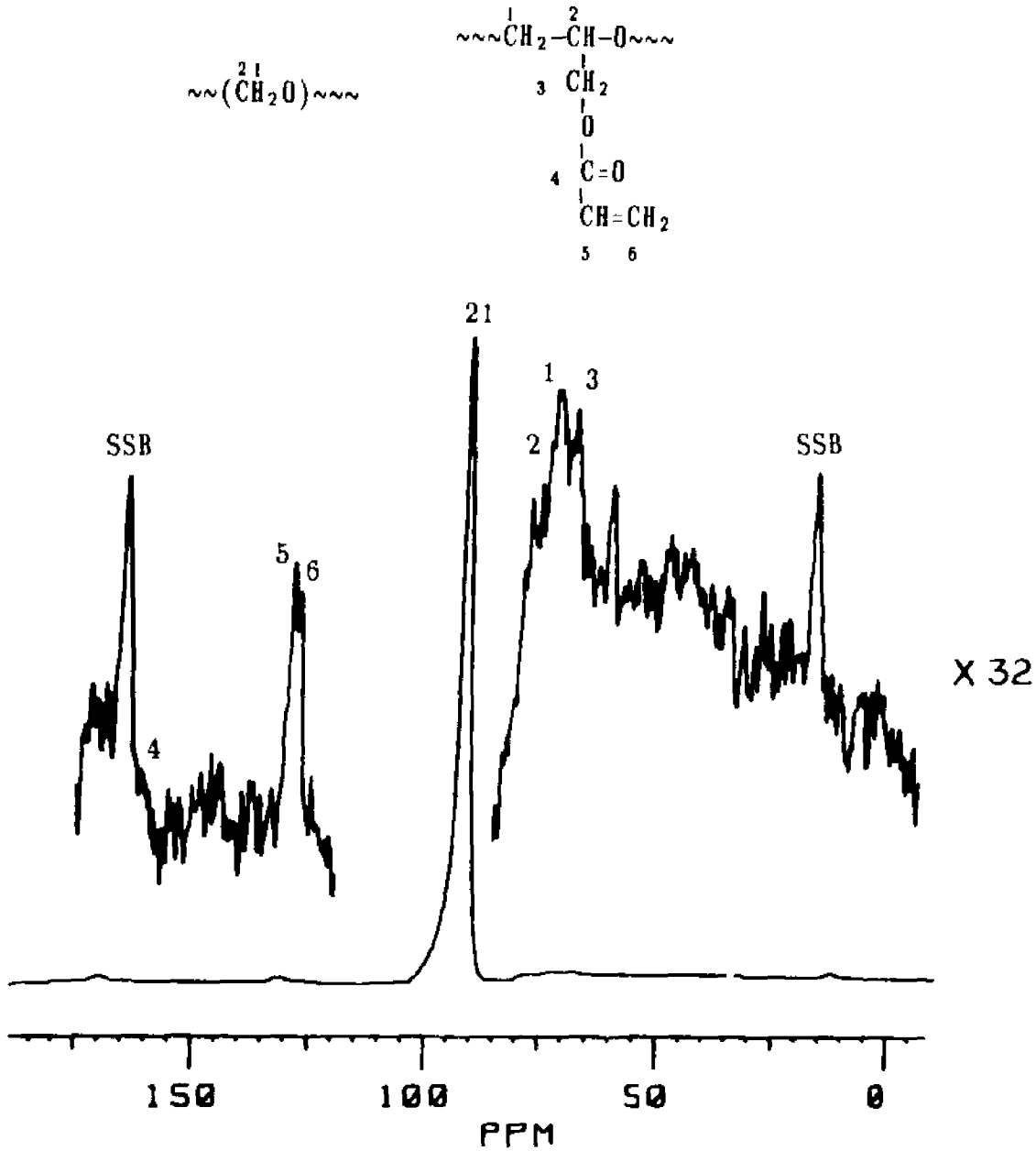

Figure 4.19
Typical solid state ^{13}C NMR spectrum of a trioxane-glycidyl acrylate copolymer, spectrum obtained using cross polarization and magic angle spinning, (25°C,2846 scans, spinning rate = 4.0 KHz)

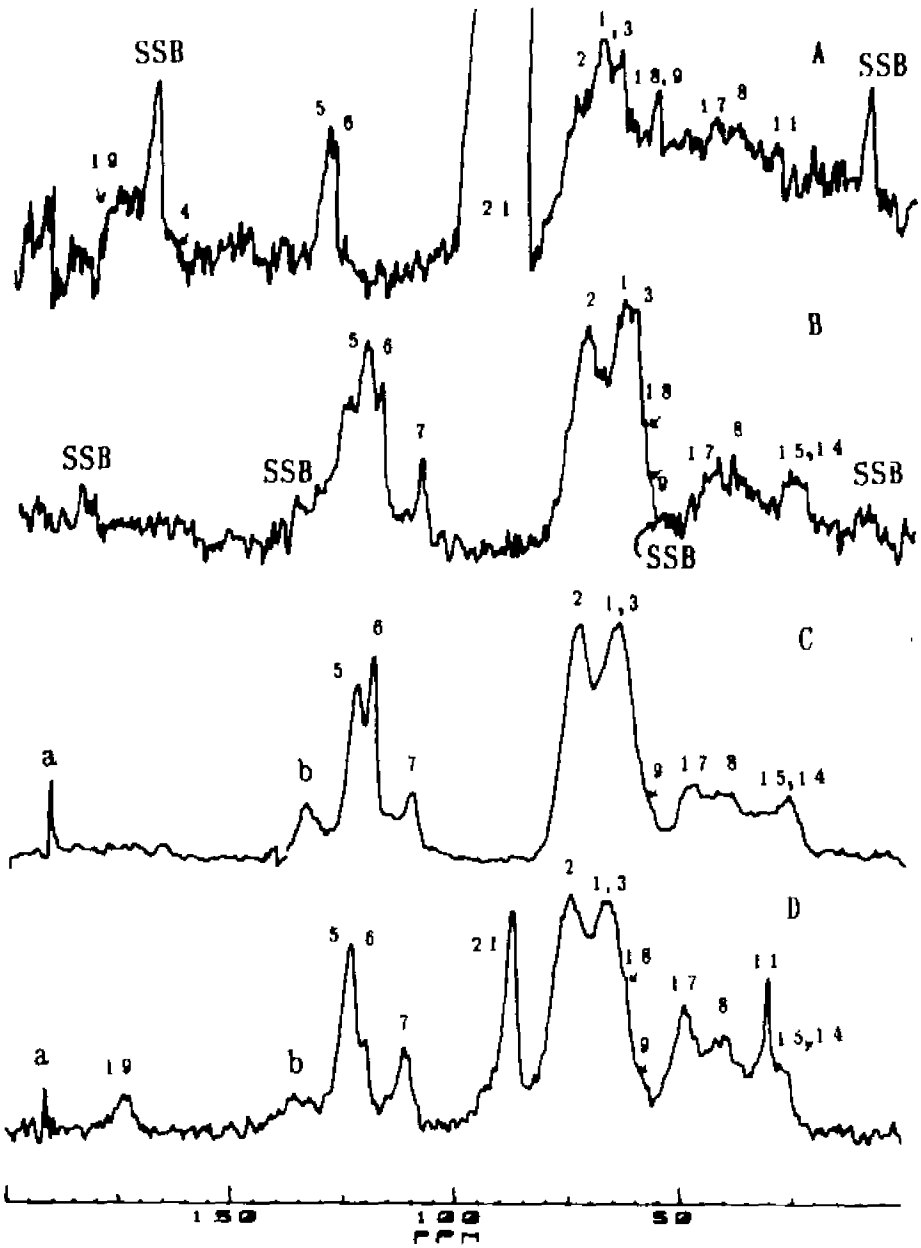

Figure 4.20

Solid state ^{13}C NMR spectra obtained using crosspolarization and magic angle spinning (25°C)

A : trioxane-glycidyl acrylate copolymer, high degree of conversion, after base hydrolysis (spinning rate = 4.0 kHz) 4 wt % feed, 2846 scans

B : glycidyl acrylate homopolymer after base hydrolysis, (548 scans, spinning rate = 3.1 kHz)

C : glycidyl acrylate homopolymer before base hydrolysis,(584 scans, spinning rate = 4.6 kHz)

D : trioxane-glycidyl acrylate copolymer, low degree of conversion, before base hydrolysis (3335 scans, spinning rate = 4.6 kHz)

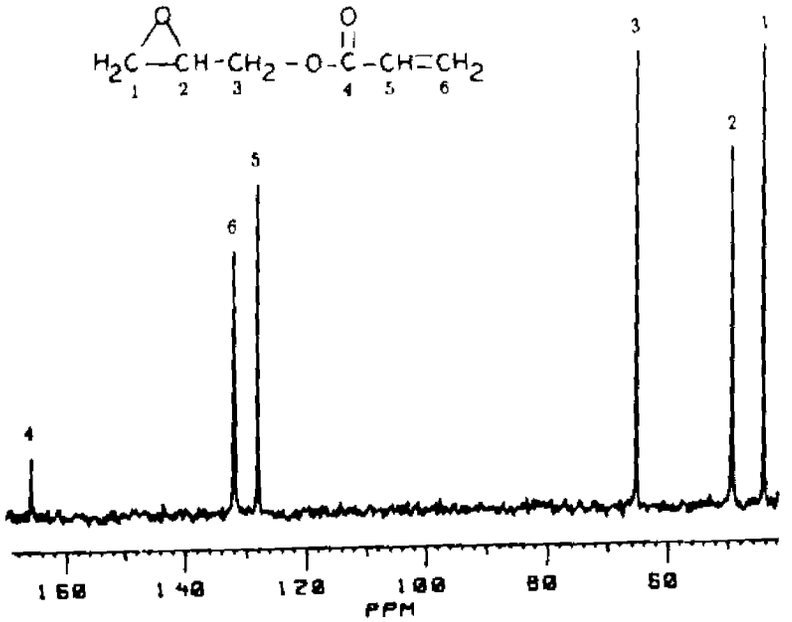

Figure 4.21

^{13}C NMR spectra of glycidyl acrylate comonomer (DMSO-d_6, 25°C)

trioxane-glycidyl acrylate copolymer at low conversion is essentially a glycidyl acrylate homopolymer. The major unit in the homopolymer is, as in the low conversion copolymer, Structure II. Also evident from these spectra is the conspicuous presence of the acrylate group (carbons 5 and 6), clearly indicating its surviving the hydrolysis process.

It can be readily seen from Figure 4.20 B that the signals for the crosslinked units are present before hydrolysis, indicating the participation of the acrylate group in the copolymerization process. The reactivity of the α-carbonyl double bond towards cationic centers has been documented. Acrolein is reported to polymerize cationically through both the carbonyl and the carbon-carbon double bond. The cationic homo- and copolymerization of acrolein (43,44) occur primarily by carbonly addition; vinyl addition occurs to a lesser extent. For copolymerization with styrene, the styryl cation attacks acrolein at the carbonyl and vinyl groups in a ratio of approximately 92 to 8.

It is believed that glycidyl acrylate behaves in a similar manner, resulting in homo- and copolymers with pendant acrylate groups. Crosslinking of these copolymers results from attack by cationic centers on vinyl groups.

Based on NMR spectra and possible reactions of glycidyl acrylate, the structures of secondary units in the crosslinked structure are proposed. These structures are III, IV, V and VI.

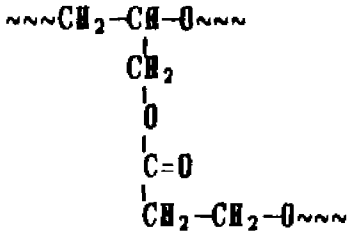

III

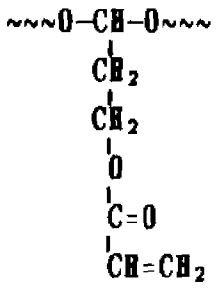

IV

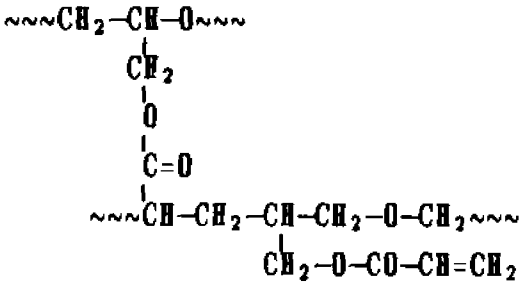

V

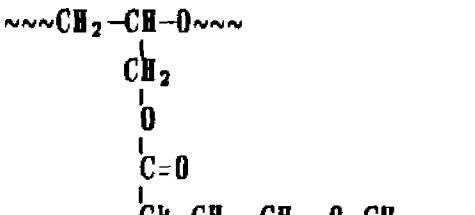

VI

Structure III could result from chain initiation by the acrylate group, i.e.:

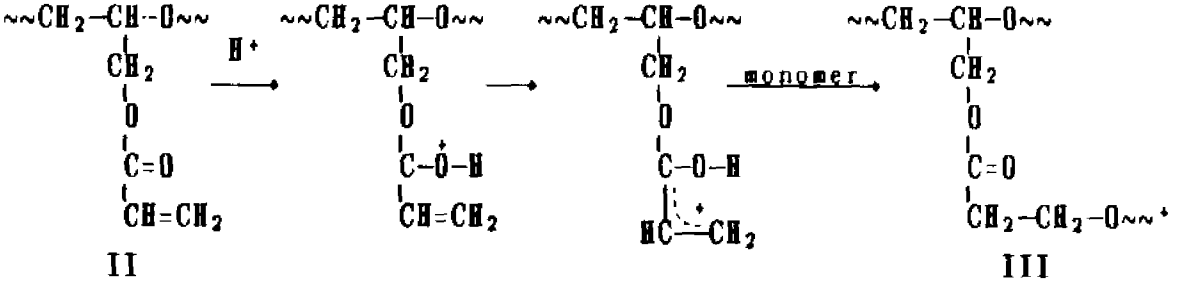

II III

A 1,2 carbon shift after ring of the oxirane yields (45):

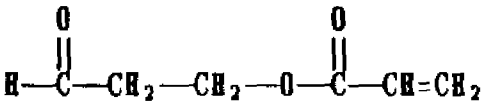

Incorporation of this unit during copolymerization gives structure IV, and accounts for carbon 7 in the spectra in Figure 4.20 B, C and D. Some absorptions due to this compound are observed in the spectra of unhydrolyzed homo- and copolymer (Figure 4.20 C and D). Signals at 193

and 135 ppm are assigned to the aldehyde and double bond carbons respectively.

Structures V and VI may result from reaction of the acrylate carbon-carbon double bond with cationic centers.

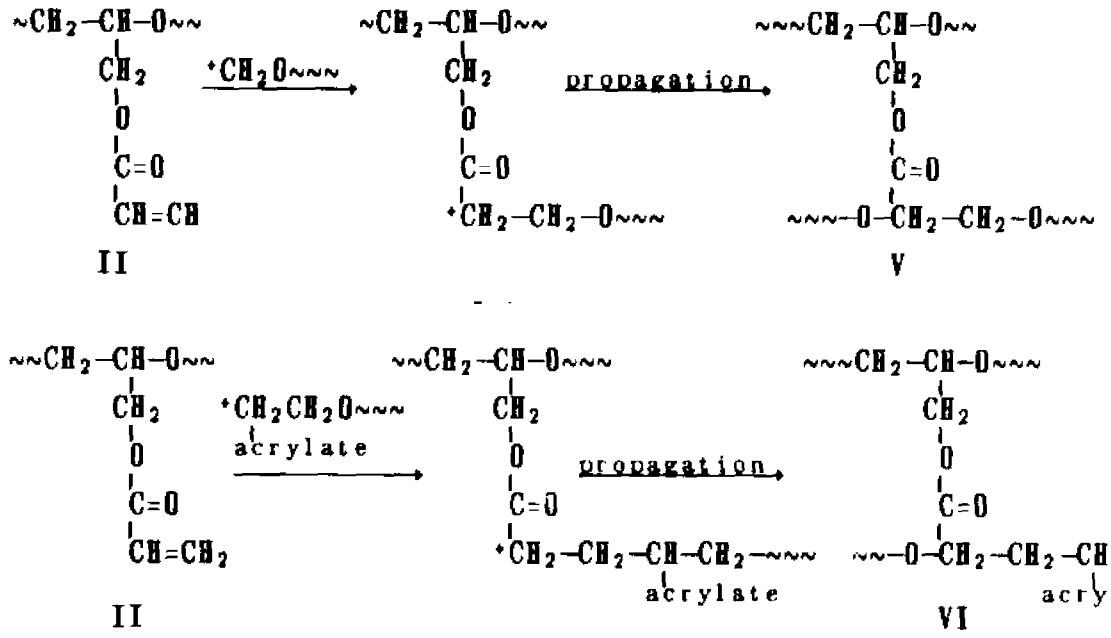

Signals from unit VI should be more obvious in the spectrum of the low conversion copolymer (Spectrum 4.20 D) than in either of the GA homopolymer spectra (Figure 4.20 B and C). This is readily confirmed (see carbon #11 in in Figure 4.20 D).

The presence of crosslinking units, evidenced by signals appearing in the range of 25 to 55 ppm in the ^{13}C NMR spectra in Figure 4.15 D, indicates that a significant degree of crosslinking occurs in the early stages of copolymerization. The gel, as the low conversion product, consists almost entirely of glycidyl acrylate units. Based on this observation, it was suspected that transacetalization would be inefficient and that a non-random distribution of comonomer units would

result. TGA analysis demonstrates that this in not the case, especially for samples with large comonomer feeds.

Figure 22 gives sample DSC thermograms for two trioxane-glycidyl acrylate copolymers (1.1 and 2.4 mole percent comonomer incorporation) and a trioxane-ethylene oxide copolymer (1.4 mole percent comonomer incorporation). The broad endotherm of the TX-GA copolymer with 2.4 mole percent incorporation has a much lower area than the TX-EO copolymer even though the sample mass is almost twice as great.

Data presented in Table 4.7 indicate that crystallinity of the TX-GA copolymers is much lower than one would expect for samples with

Table 4.7 : Heat of fusion and percent crystallinity of trioxane-glycidyl acrylate and trioxane ethylene oxide copolymers

Comonomer feed weight percent	ΔH_f (mcal/mg)	Percent crystallinity
3 (GA)	21	35
24 (GA)	7	11
2* (EO)	35	50
0‡	58.7	100

* 2 weight percent incorporation

‡ hypothetical 100% crystalline POM homopolymer

very long POM blocks. This suggests that although the copolymers are crosslinked, the transacetalization process still occurs, and a random distribution of GA is achieved. It is believed that 11% is the lowest reported value for crystallinity of well characterized acetal copolymer with low level comonomer incorporation.

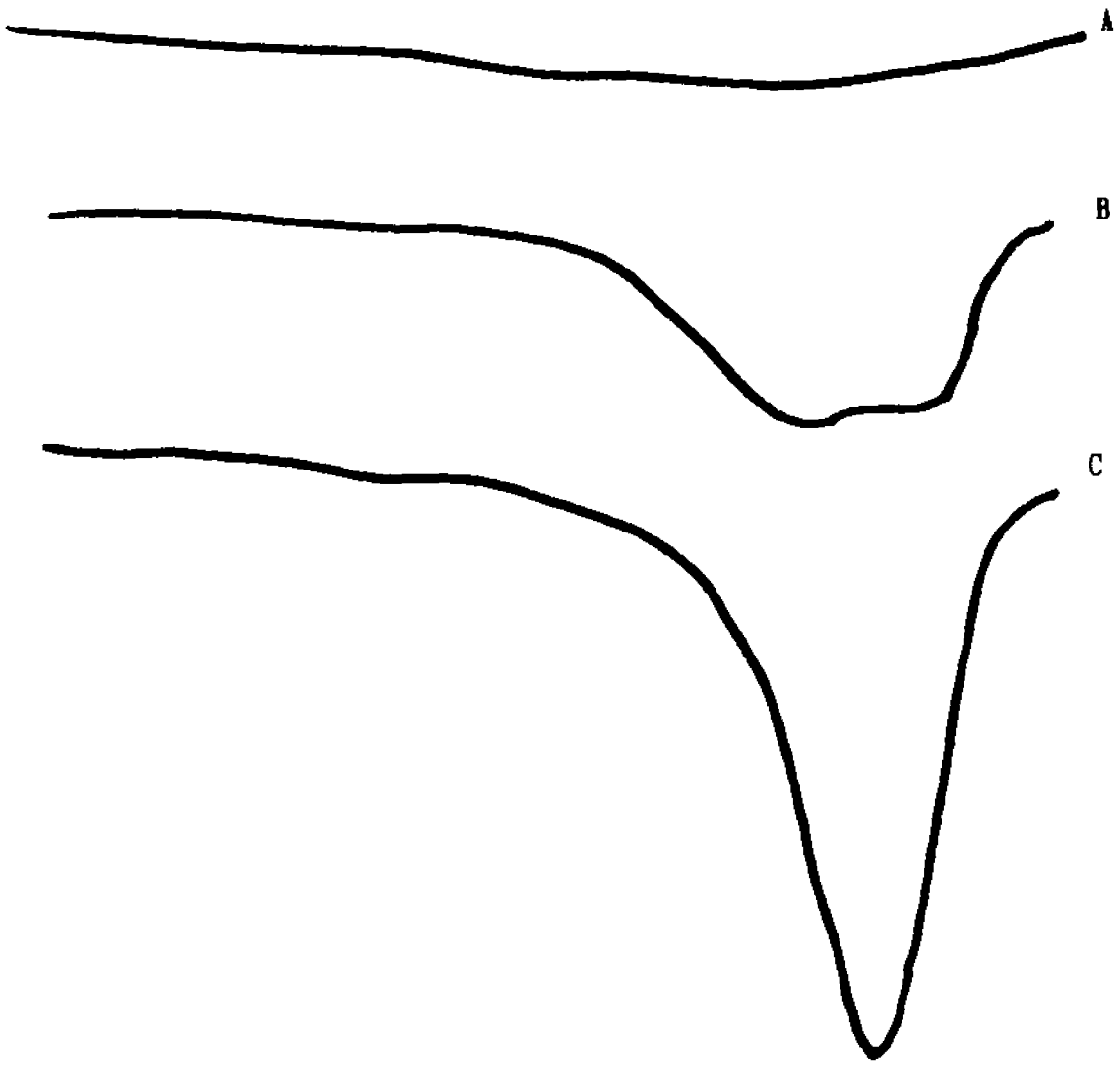

Figure 4.22

DSC thermograms of acetal copolymers

A. trioxane-glycidyl acrylate copolymer,
2.4 mole % comonomer incorporation (3.26 mg)

B. trioxane-glycidyl acrylate copolymer,
1.1 mole % comonomer incorporation (1.14 mg)

C. trioxane-ethylene oxide copolymer,
1.4 mole % comonomer incorporation (1.74 mg)

TGA thermograms indicate that the thermal stability of the trioxane-glycidyl acrylate copolymers is superior to a trioxane-ethylene oxide copolymer with a comparable level of comonomer incorporation (Figure 4.23). The thermal stability of the trioxane -glycidyl acrylate copolymer as compared to the glycidyl acrylate homopolymer (Figure 4.24) suggests that its stability is not due to glycidyl acrylate blocks, but rather to efficient stopper units as well as uniform crosslinking in the copolymer.

The thermal stability of the TX-GA copolymer can be attributed to the ability of the acrylate group to act as a free radical sink, a proton acceptor and a formaldehyde acceptor as well (46).

The retention of a significant level of the acrylate group in the crosslinked copolymer after hydrolysis is apparent from the NMR spectra presented (Figure 4.20 A and B, peaks 5 and 6). Thus the presence of the acrylate group stabilizes thw copolymer against both routes of degradation, i.e. acidolytic and radical (9). Furthermore, formaldehyde, the harmful common degradation product of both routes, is also removed. The impediment of chain mobility due to crosslinking contributes, of course, to the thermal stability of the system.

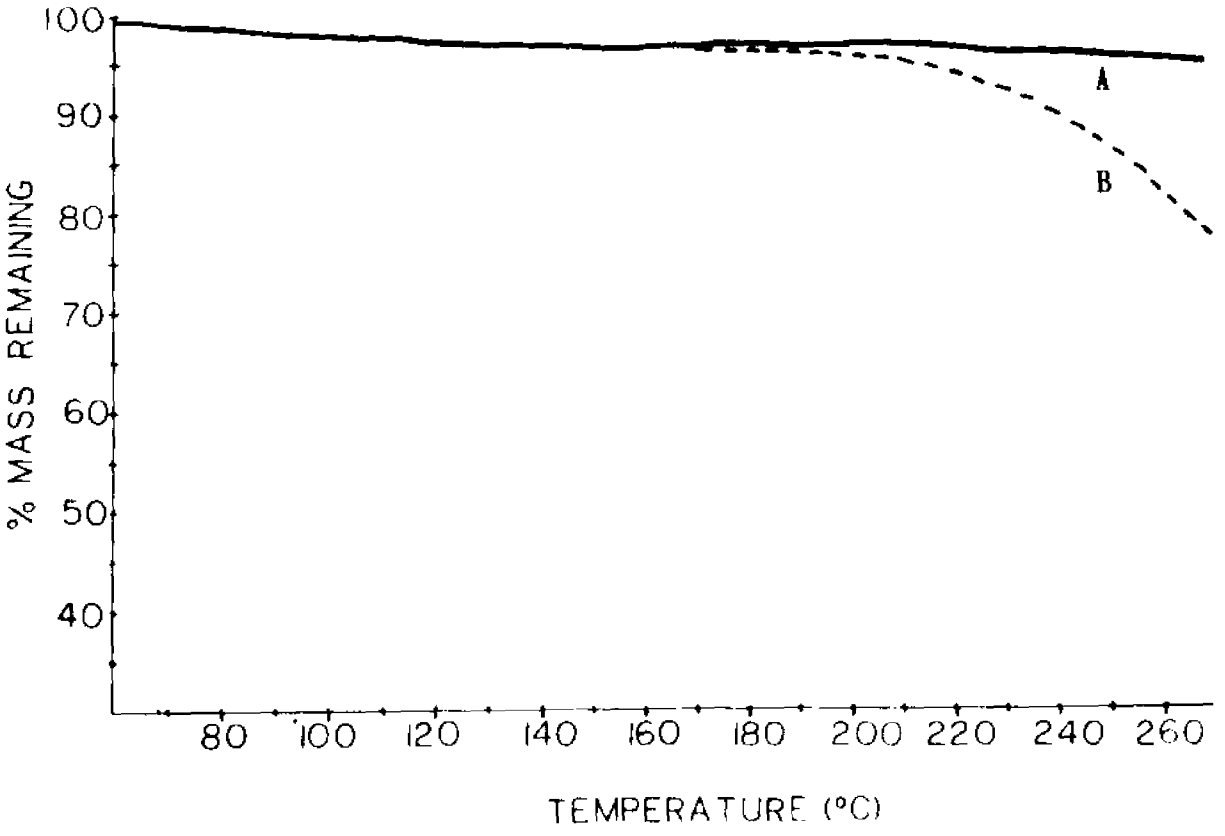

Figure 4.23

TGA thermograms of acetal copolymers (heating rate = 10°C/min)

A : trioxane-glycidyl acrylate copolymer
B : trioxane-ethylene oxide copolymer

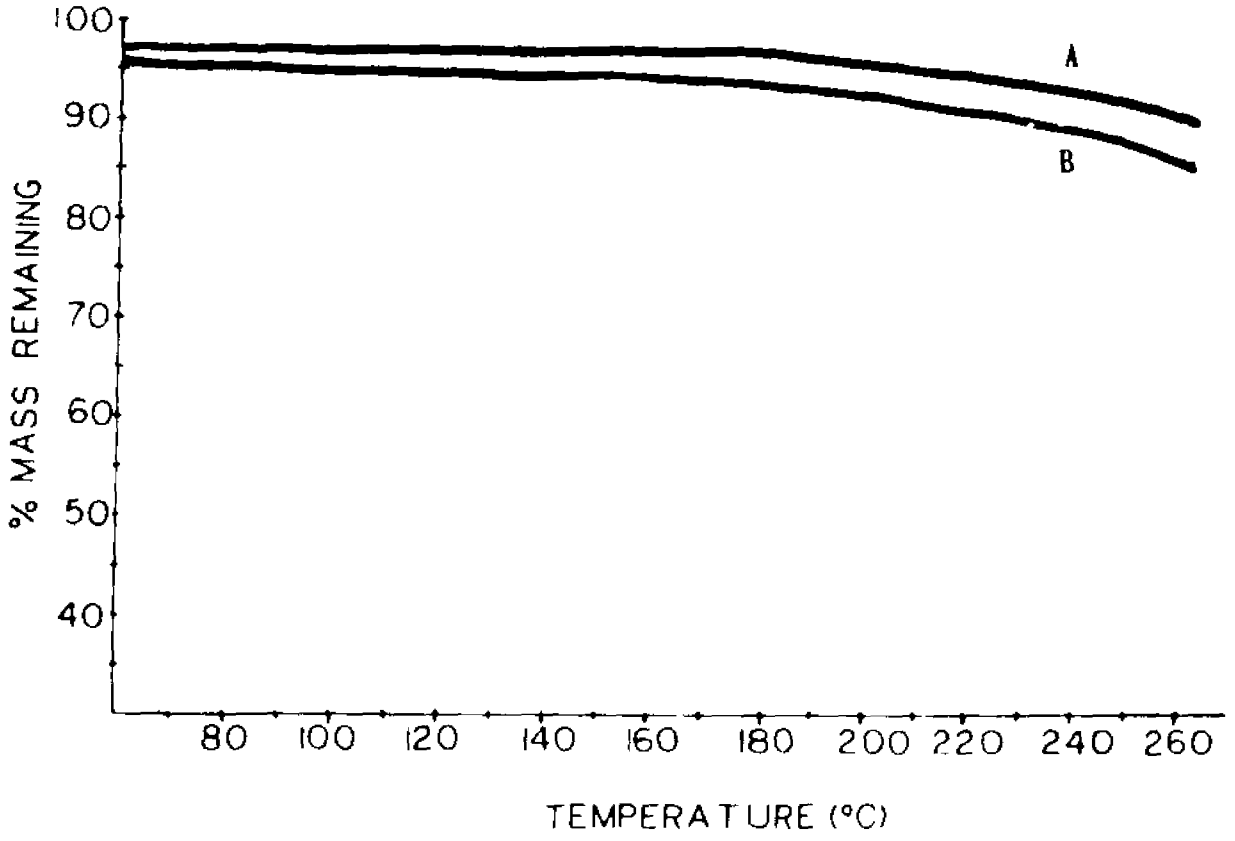

Figure 4.24

TGA thermogram of glycidyl acrylate homopolymer

A : glycidyl acrylate homopolymer (before hydrolysis)
B : glycidyl acrylate homopolymer (after hydrolysis)

5 CONCLUDING REMARKS

The ultimate goal of this investigation was to develop systems of polymer-bound stabilizers. Although this goal has not been completely achieved, some advances in the area of polyacetal stabilization have been made.

One of the most important developments towards polymer-bound stabilizers was the synthesis and characterization of three functionalized polyacetals. Copolymers possessing backbone *cis*-2-butene units have been found to have thermal stability and resistance to bromine degradation superior to trioxane-ethylene oxide acetal copolymers. This was achieved without the loss of crystallinity. Furthermore, it has been demonstrated that these unsaturated copolymers can be modified further, leading to other functionalities.

In addition to functional groups on the polymer backbone, pendant groups can also be attached. Two additional copolymers were synthesized and characterized to demonstrate this approach. It was expected that for pendant functionalities, the extent of modification could be better controlled. The new copolymers contain pendant hydroxy and methylol groups in one system and pendant acrylate groups in the other. Modification of these novel systems have not yet been attempted, but the potential for modification is clearly evidenced.

When considering polyacetal modification, one factor stands out.

That is that the very properties that make polyacetal so useful also render them difficult to modify. Because of the polymer's high degree of crystallinity and the nature of its chemical composition, polyacetals are not readily soluble at room temperature. The use of HFIP, the only known room-temperature solvent, restricts possible modification reactions to those using HFIP-soluble reagents. It is often the case that the presence of these reagents results in polymer insolubility. Modifications requiring acid or radical catalysis run the risk of extensive polymer degradation. The limited success of modifications reported in Section 4-1c is due only to the fact that modification was limited to the surface. For functional groups trapped within the crystal lattice, there was no opportunity for modification.

New copolymers containing pendant acrylate groups have been found to have significantly lower crystallinity than most acetal copolymers. Providing that crosslinking is not extensive, this system presents promising opportunities for modification because of increased access to units otherwise trapped within the crystal lattice. The potential applications of this system will likely be different from conventional acetal copolymers due to property changes resulting from decreased crystallinity.

Copolymers with pendant hydroxyl and methylol functional groups have, in general, found to be of relatively low molecular weight. This system may find use for applications requiring oligomers with reactive end groups as well pendant sites for further modification, e.g. stabilizer bonding.

A different, but related, approach taken with respect to polyacetal stabilization and degradation involved a study of the radical and acidolytic degradation of a model trioxane-ethylene oxide copolymer in solution. From this investigation it was learned that degradative unzipping is a much faster process than the back biting process that results in cyclic acetal degradation products. No significant differences in the relative proportion of these degradation products was observed between the radical and acid catalyzed degradation studies, supporting reports of the production of formic acid in systems degrading by radical speciesis.

The evaluation of a series of formaldehyde-accepting compounds for polyacetal stabilizers resulted in the development of a useful "screening" method for potential stabilizers.

The investigations presented here establish a number of potential avenues for the improvement of polyacetal stabilization. It is hoped that future work stemming from these exploratory results will lead to further advances.

6 REFERENCES

1. Butlerov, A.M. *Ann.* **1859**, *9*, 242.

2. Staudinger, H. *Die Hochmolecxlaren Organischen Verbingen*, Springer: Berlin, **1932**.

3. MacDonald, R.N. (to E.I. du Pont de Nemours & Co. Inc.) U.S. Patent 2 768 994, Oct. 30, 1956.

4. Walling, C.; Brown, F.; Bartz, K. (to Celanese Corp.) U.S. Patent 3 027 352, March 27, 1962.

5. Dolce, T.; McAndrew, F. "Acetal Copolymers, A Historical Perspective," in *High Performance Polymers : Origins and Development*, G. Kirshenbaum and R. Seymor Eds.; American Chemical Society : Washington, D.C., 1986, p 115.

6. Chen, C.S.H.; DiEdwardo, A. *Adv. Chem. Ser.*, **1969**, *91*, 359.

7. Chen, C.S.H.; DiEdwardo, *J. Macromol. Sci. Chem*, 1970, *4*, 349.

8. Collins, G.L.; Greene, R.K.; Berardinelli, F.M.; Ray, W.H. *J. Polym. Sci. Polym. Chem. Ed.* **1981**, *17*, 667.

9. Yang, N.L.; Patel, V.; Dolce T.; Auerbach, A. *Proceedings of the ACS Div.of Polym. Mater. Sci. & Eng.*, **1984**, *51*, 149.

10. Scott, G. in *Polymer Stabilization and Degradation*, Klemchuk, P.P., Ed.; ACS Symposium Series 280: American Chemical Society: Washington, DC, 1985, pp 173-196. Vogl, O.; Albertsson, A.C.; Janovic, Z. in in *Polymer Stabilization and Degradation*, Klemchuk, P.P., Ed.; ACS Symposium Series 280: American Chemical Society: Washington, DC, 1985, pp 173-196.

11. Penczek, S.; Kubisa, P.; Matyjaszwski, K. "Cationic Ring-Opening Poylmerization, Part II, Synthetic Applications," in *Adv. in Polym. Sci.*; Springer-Verlag: Berlin, 1985; Vol. 38, p 118.

12. Wissbrun, K.F. *Makromol. Chem.*, **1968**, *118* ,211.

13. Hermann, H.D.; Burg, K.H. *Angew. Makromol. Chem.*, **1971**, *15*, 219.

14. DeMejo, L.; MacKnight, W.J.; Vogl, O. *Polymer*, **1978**, *19*, 956.

15. DeMejo, L.; MacKnight, W.J.; Vogl, O. *Polymer*, **1979**, *11*, 15.

16. Mateva, R.S.; Sirashki, G. *J. Polym. Sci., Part A : Polym. Chem.*, **1988**, *26*(*2*), 511.

17. Bednar, B.; Chuchmas, F.; Zajic, Z.; Kalal, J.; Kralicek, J. *Sb. Vys. Sk. Chem.-Technol. Praze*, **1982**, *S7*, 255. *Chem. Abstr.* **1983**, *98*, 198800a.

18. Konsulov, V.; Grozeva, Z.; Stefanova, R. *Khim. Ind.*, **1986**, *58(6)*, 252. *Chem. Abstr.* **1986**, *104*, 69489z.

19. Pregaglia, G.; Roffia, P.; Zamboni, V. , French patent 1 512 216, 1968. *Chem. Abstr.* **1968**, *68*, P 13570q.

20. Hellerman, V.; Schulz, R.C.; *Makromol. Chem. Rapid Commun.*, **1981**, *2*, 585.

21. Schulz, R.C., *Makromol. Chem. Suppl.*, **1985**, *12*, 1.

22. Schulz, R.C., *Makromol. Chem. Suppl.*, **1985**, *13*, 123.

23. Fleischer, D.; Schulz, R.C. *Makromol. Chem.*, **1975**, *176*, 677.

24. Fleischer, D.; Schulz, R.C. *Makromol. Chem.*, **1972**, *152*, 311.

25. Martin, M.L.; Delpuech, J.J.; Martin G.J. *Practical NMR Spectroscopy*; Heydon and Sons: London, 1980, pp 153-155.

26. *Formaldehyde and Other Aldehydes*; Committee on Aldehydes, National Academy of Science. National Academy Press: Washington, DC, 1981, p 133.

27. Walker, J.F. *Formaldehyde*, 3rd ed.; Reinhold: New York, 1964, p 394.

28. Brydson, J.A. *Plastic Materials*, 4th ed.; Butterworths Scientific: London, 1982, pp 615 -616.

29. Bann, B.; Miller, S.A. *Chem. Rev.*, **1958**, *58*, 131.

30. Brannock,K.C.; Lappin, G.R. *J. Org. Chem.*, **1956**, *21*, 1366.

31. Pattison, D.B. *J. Org. Chem.*, **1957**, *22*, 662.

32. Tinsley, S.W.; MacPeek, D.L. US Patent 3 337 587, 1967.

33. Wittekind, R.R.; Rosenau, J.D.; Poos, G.I. *J. Organic Chem.*, **1961**, *26*, 444.

34. Berckenbach, L.; Linhard, M., *Ber.*, **1931**, *45*(2), 433.

35. Gebelein, C.G. *J. Macromol. Sci., Chem. Ed.*, **1971**, *A5(1)*, 433

36. Inoue, M. *J. Polym. Sci.*, **1963**, *A-1*, 2697.

37. Abraham, R.J. and Loftus, P., Proton and Carbon-13 NMR Spectroscopy, an Integrated Approach, Heydon and Sons Ltd., London, 1981 p.18.

38. Inoue, M.J. *J. Appl. Polym. Sci.*, **1964**, *8*, 2225.

39. Okatani, T.; Eguchi, T. Jap. Patent 7 021 951, 1970, *Chem. Abstr.* **1970**, *70*, P 69215m.

40. Brown, D.W. *J. Chem. Ed.*, **1985**, *62*, 209.

41. Schultz, M.; Tollens, B. *Ann.*, **1895**, *20*, 289.

42. Libert, H. *Z. Anal. Chem.*, **1973**, *265*, 328.

43. Toi, Y.; Huchihama, Y. *Bull. Chem. Soc. Jpn.*, **1964**, *37*, 662.

44. Kobayshi, K.; Sumitamo, H.; Furuya, K. *J. Polym. Sci., Polym. Chem. Ed.*, **1977**, *15*, 1503.

45. Lewars, E.G. in *Comprehensive Heterocyclic Chemistry*, W. Lwowski, Ed.; Pergammon Press: Oxford, 1984, Vol. 7, Part 5, Chap. 5 p 103.

46. Walker, J.F. *Formaldehyde*, 3rd ed.; Reinhold: New York, 1964, p 416.

47. Flory, P.J. *Trans. Faraday Soc.*, **1955**, *51*, 848.

48. Flory, P.J. *J. Chem. Phys.*, **1949**, *17*, 223.